SHARING

SELF-ORGANIZED HETEROGENEOUS ADVANCED RADIO NETWORKS GENERATION

D5.1 (Task T5.1)

Advanced Relays: innovative concepts and performance evaluation

Date of delivery	23/02/2015
Contractual date of delivery	31/12/2014
Project number	C2012/1-8
Editor(s)	Antonio Cipriano (TCS)
Author(s)	Dorin Panaitopol (TCS), Hicham Anouar (TCS), Antonio Cipriano (TCS), Jean-Marc Conrat (OLABS), Issam MAAZ (OLABS), Sylvie Mayrargue (CEA), Martina Cardone (Eurecom), Raymond Knopp (Eurecom)
Dissemination level	PU
Workpackage	5
Version	1.0
Total number of pages	80

Abstract:

This deliverable describes the different proposals related to relays which have been investigated in Task 5.1 "Advanced Relaying". A wide spectrum of issues about relaying are investigated in this document, ranging from propagation models for relay scenarios up to scheduling policies in presence of relays. A considerable effort was also spent on innovative coding strategies and on shedding lights on information theoretical problems concerning relay channels. Link level and MAC level simulations are used for performance evaluation. Progress is reported on theoretical boundaries, which help to monitor how far the expected performances are from the ideal scenario.

Keywords: LTE-Advanced relaying, relays for PMR, propagation, non-binary LDPC codes, collaborative relaying, degrees of freedom, collaborative scheduling, relay-aided broadcast, two-way relaying, multi-hop resource allocation, proportional fair scheduling, opportunistic scheduling

Document Revision History

Version	Date	Author	Summary of main changes
0.1	29/09/14	Antonio Cipriano (TCS)	Creation of the Table of Contents (ToC) and merge of content from IR5.1
0.2	30/10/14	Issam MAAZ (OLABS)	Introducing Propagation channel modeling (OLABS) "Section 3"
0.3	18/11/14	Martina Cardone (EURE)	LTE-Advanced collaborative relaying [EURE], "Section 5"
0.4	26/11/14	Hicham Anouar (TCS)	Merging of TCS contribution
0.5	19/12/14	Dorin Panaitopol (TCS), Antonio Cipriano (TCS)	Insertion of the second TCS contribution and main editing of the document. First draft for review.
1.0	11/02/2014	Antonio Cipriano (TCS)	Final editing after review rounds

TABLE OF CONTENTS

List of figures

EXECUTIVE SUMMARY

This deliverable describes the different proposals related to relays which have been investigated in Task 5.1 "Advanced Relaying". Link level and MAC level simulations are used for performance evaluation. Progress is reported on theoretical boundaries, which help to monitor how far the expected performances are from the ideal scenario.

As written in the Description of Work, SHARING pays considerable attention to the topic of relaying since the potential of this class of techniques still remain to be entirely revealed. For instance, there are open problems about fundamental limits of the system, like the evaluation of achievable rates. Little is known about the potential gain of relaying in a multi-user and dense heterogeneous environment (which is one of the main focus of SHARING) taking into account small cells density, backhaul constraints and environment-dependent parameters such as fading and shadowing. The ambition of the work presented here is to contribute to fill this gap.

Inserting a relay in a cellular network has a cost and operators are expecting benefits in terms of cell edge and average rates. Work on achievable rates in the context of LTE-Advanced relaying helps to shed lights on how to achieve relaying gains. Moreover, relaying is an important topic also in the context of Private Mobile Radio (PMR) networks supporting industrial, transportation and public safety communications. Recently, 3GPP has witnessed an important activity to support PMR services in LTE networks; actors are motivated by new possible business cases, for instance traditional network operators are certainly interested in becoming future PMR communication providers. In this market, especially for critical services, it makes sense to add relays not only for increasing throughput but also link robustness. The previous facts motivate the interest of SHARING T5.1 about relays for both traditional cellular network and PMR networks. Notice, that PMR networks have a large variety of deployments, including the traditional cellular one.

Cooperation between relays and the source, the Donor eNodeB (DeNB) in the cellular context, is fundamental for achieving interesting gains, hence cooperative strategies which enable to obtain significant capacity gains will be studied from theoretical and practical perspectives, by proposing precise coding strategies. Moreover, the impact of relaying on system performance can be realistically evaluated only if fine-tuned propagation models for realistic relay scenarios are used for evaluation. Finally, the introduction of relays has an impact also at MAC level, on scheduling and resource allocation algorithms. These issues are addressed in this document.

The first topic presented in the document is the study on path loss model for relays. The addition of relays in a standard deployment is one of the techniques considered for increasing the average and cell edge performance of the network. The gains of a given solution are typically evaluated at a first stage through system-level simulations based on path loss models to simulate propagation losses. Models that underestimate the path loss of the link between Base Station and relay and overestimate the path loss of the link between relay and a mobile user will not promote relay-based solution or microcell densification and can lead in general to wrong decision or inaccurate evaluations. Extensive measurement campaigns have been conducted in Belfort (France) in order to clarify the currently available path loss models for the relay case in a urban environment. The collected and processed data are used to compare the accuracy of existing models. The final recommendation of the study is that, for the propagation environment of a medium urban city, the ITU models defined for macrocell and microcell environment for Line-of-Sight (LOS) and Non-Line-of-Sight (NLOS) conditions give the best performance. The recent 3GPP 3-D UMi and Uma models defined for 3-D simulations may also be recommended. These ITU and 3GPP models are thus recommended for system-level simulations with relays in urban environment. Moreover, a new general equation of the path loss model was derived with an explicit dependence on the relay height for the relay-user link in NLOS conditions. In this case, in fact, the study pointed out an insufficient precision of the existing models with respect to the antenna height (sometimes path loss is underestimated, sometimes it is overestimated, depending on the model). Another interesting conclusion of this study is that the path loss models for the relay-user link (i.e. in microcell environment) depend on the relay close environment, for instance, the presence of vegetation of not. The general recommendations of this study are based on measurements collected in a medium-size European city and may change with large cities which include large avenues and high-rise buildings.

After having investigated propagation which is linked to physical phenomena, the document deals with PHY layers aspects related to coding. A cooperative coding scheme over multiple-relay fading channels is presented. The particularity of the presented approach is to rely on non-binary Low Density Parity Check (LDPC) codes at the source, coupled with non-binary repetition codes at the relays. When the number of

relays increases, the existing methods suffer from a large increase of decoding complexity, while the coding gain they present becomes increasingly less important. To overcome this drawback, we propose a simple joint decoding strategy, with a complexity comparable to a system without relays and independent on the number of relays. In other words, state of the art schemes show coding gains which become less important when the number of relays increases, while the present approach brings an effective coding gain such that the performance in terms packet error rate has a constant SNR degradation with respect to the optimal theoretical packet error probability (called outage probability), irrespective of the number of relays.

A consistent part of work deals with fundamental limits of transmission for relaying systems in the framework of LTE-Advanced. Two main groups of innovations are reported here for two distinct scenarios which provide interesting recommendations.

In the first scenario a Donor eNodeB (DeNB) communicates with a user across a Gaussian channel and is assisted by *N* relays operating in half-duplex mode. Currently only an outer bound on capacity is known in this case, without knowing if a specific coding strategy is able to reach that bound or not. The first important contribution is the proof of a precise coding strategy based on noisy network coding which gives a guaranteed capacity for this network. In other words, the proposed coding strategy is able to convey a rate which is lower than the optimal capacity of the system but this degradation is bounded by a value (called constant gap) which depends on the number of relays but otherwise it is independent of the actual values of the system parameters (e.g., channel gains, power constraints at the DeNB and at the relays, signal-to-noise ratio). The second part of the work focus on the Gaussian half-duplex single relay network, where the DeNB can potentially directly communicate with the user. In this case, a simple two-phase three-message transmission strategy by using practical codes is proposed. This scheme uses superposition encoding, decode-and-forward relaying and successive interference cancellation in order to send three messages in two time slots from a DeNB to a user with the help of a relay, which forwards one of the three messages. The previously mentioned transmission strategy was implemented on the OpenAirInterface LTE simulator which includes LTE constraints about coding rates and granularity. In a Gaussian channel, the gaps of a realistic implementation with respect to the theory are obtained; according to the simulations up to 90% of the theoretical maximum rate is achieved. Moreover, the proposed scheme shows a throughput increase going from 40% to 100% (and depending on the SNR and coding parameters) with respect to the current baseline relaying scheme without cooperation with the DeNB. This is a first important step towards the evaluation of the practical feasibility of these new relay-assisted coding strategies.

The second scenario is a Gaussian relay-aided broadcast channel, a system where a DeNB communicates with multiple users across a Gaussian channel with the help of a full duplex relay. The study of this system was motivated by the fact that it is applicable in practical heterogeneous deployments for 4G cellular networks in frequency flat channels. This scheme differs from the traditional broadcast channel in the presence of a relay helping the base station. The two transmitters could act as a virtual multiple-antenna transmitter, with antennas not co-localized but distributed over the base station and the relay. However, the performance of a virtual MIMO system, which is the highest ones in terms of throughput at high signal-to-noise rations, is not always achievable. This study sheds light on how strong the DeNB-relay link should be, such that the DeNB and the relay might behave as a single 'virtual' base station with 2 antennas. In other words, the results give interesting insights on how this link should be dimensioned in order that the system behaves like a multiple antenna broadcast channel with 2 transmit antennas and 2 single-antenna users at the reception. The study is then generalized to a generic number of users in the downlink. For this latter a more general scenario, namely a polynomial-time algorithm is proposed which selects at most the 2 'best' users, among the possible ones, to serve. The choice depends on the values of the channel parameters; understanding this dependence will give an insight on how to smartly manage and schedule the different available resources in the network.

The studies continue then with evaluations at MAC level, while the focus is shifted to clusterized mesh networks for PMR systems. In this context, in the particular case of fast deployable systems e.g. for crisis management, there can be absence of wired backhaul between the cells, called here clusters, and hence inter-cluster communications are taken in charge by some relay nodes called bridging mesh routers. Since the back-bone traffic is going through those relay nodes, and part of it may be bidirectional, a two-way relaying technique was investigated and compared to a more traditional decode-and-forward strategy. Results are presented for two main deployment scenarios. The first one corresponds to a small city for example with low roof-top height in which there is no need of extremely high throughput, while the second one corresponds, for example, to a more populated city with a higher roof-top height, predominant non-line-of-sight propagation and with more data rate to be offered. 3GPP and ITU parameters and system constraints have been also considered, for example, the 700 MHz band was considered for simulations since it is one of the main candidate bands for deployment of the future broadband PMR networks. In the two scenarios, two-way relaying (TWR) provides better throughput

than decode-and-forward (DF), for any possible position of the relay. TWR typically doubles the throughput at the best relay position. However, in the first scenario, TWR achieves significant throughput gains only for certain distances (typically the relay must be placed in between the served nodes). For more dense urban deployments like the second scenario, throughput gains of the TWR strategy are weakly sensitive to the relay position, which is a desired feature in rapidly deployable PMR systems. Hence, TWR is rather to be preferred in the latter scenario, in which the link qualities are good. DF is in fact more robust than TWR in terms of end-to-end packet error rate and it is to be preferred for long-distance communications, i.e. in case in which coverage is the required metric.

Finally, resource allocation is investigated for multi-hop communications inside a cell or cluster, for applications to PMR context. In PMR systems relaying and direct communications between users are features which are particularly appreciated by the customers since they are included by the legacy PMR standards. The study focus on efficient and fair opportunistic scheduling of delay tolerant traffics in clustered/cellular environment with dynamic relaying. A wide range of nowadays applications generate this type of traffic, i.e. email, internet browsing, asynchronous file transfer, etc. They are generally classed as requiring a best effort service and give more flexibility to the system to handle them. The work extends three scheduling policies to this new framework. In order to differentiate the impact of relaying on performance a comparison is made among the case when all the communications pass mandatorily through the base station (also named cluster head in mesh deployments), which is the traditional configuration, the case in which also direct communications between users are allowed, and finally the case in which any user can be a relay. The maximum proportional fair scheduler achieves the most interesting compromise between the aggregated rate over the cell and the fairness. Also, it was shown that allowing all the users being a relay brings an interesting diversity advantage which however can be exploited only if an additional complexity and signalling burden is accepted in the system. Finally, increasing the number of possible relays increases the spectral efficiency of the three schemes and helps also enhancing the fairness of the maximum and traditional proportional fair scheduling. The case in which only the base station can relay communications, but direct communications are allowed too, is an interesting compromise, because it allows to control the signaling burden and achieve at least a gain of 20% over the traditional scheduling approach without direct communications.

1 Introduction

This report presents the main innovations and performance evaluation of Task 5.1 "Advanced Relaying" inside WP5.

The document is split in 7 sections, in which a wide selection of topics related to relaying in next generation cellular and Private Mobile Radio (PMR) networks is dealt with. This deliverable covers a wide range of topics. Modelling of propagation environment for deployments with relays is fundamental for correct system performance evaluations. Then work is presented on coding for relaying techniques: a specific code is presented besides an investigation of fundamental theoretical limits of relaying. Finally, the impact of relaying in simple deployments is evaluated and new resource allocation algorithms at Medium-Access Control (MAC) level are proposed for exploiting the presence of relays.

Section 2 presents a study on path loss model for relays. The addition of relays in a standard deployment is one of the techniques considered for increasing the average and cell edge performance of the network. The gains of a given solution are typically evaluated at a first stage on system-level simulations which use path loss model to simulate propagation losses. Models that underestimate the path loss of the link between Base Station and relay and overestimate the path loss of the link between relay and a mobile user will not promote relay-based solution or microcell densification and can lead in general to wrong decision or inaccurate evaluations. The purpose of this work is hence to conduct an extensive measurement campaign in order to make a point on the currently available path loss models for the relay case in a urban environment. The collected and processed data are used to compare the accuracy of existing models, to propose corrections for the case in which no model is sufficiently precise and to draw general recommendations on the type of models to be used for system-level simulations in such conditions.

Section 3 presents a cooperative coding scheme to communicate efficiently over multiple-relay fading channels with applications to OFDM or narrowband communications. The particularity of the presented approach is to rely on non-binary Low Density Parity Check (LDPC) codes at the source, coupled with non-binary repetition codes at the relays. When the number of relays increases, the existing methods suffer from a large increase of decoding complexity, while the coding gain they present becomes increasingly less important. Here, the final goal is to avoid the previous drawbacks by proposing an effective yet computationally affordable relaying and coding / decoding strategy.

While the previous sections deal with proper modeling of the propagation channel and the impact of the use of specific coding schemes on relaying scenarios, Section 4 deals with more fundamental limits but taking at the same time a more systemic view in the framework of relay for LTE-A. Two main groups of innovations are reported here for two distinct scenarios.

In the first scenario a Donor eNodeB (DeNB) communicates with a UE across a Gaussian channel and is assisted by N relays operating in half-duplex mode. Channel knowledge is supposed to be available to all the nodes in the network. This is a scenario is sufficiently realistic to represent the main features of practical relays deployments. Currently only an outer bound on capacity is known in that case, without knowing if a specific coding strategy is able to reach that bound or not. The first important contribution is the proof of a precise coding strategy based on noisy network coding which guarantees that the capacity is achievable to within a constant number of bits. In fact, it is important also to understand the dependence if this result with respect to system parameters which can cover a quite large range of values in practical deployment. The main parameters have been integrated in the analysis framework. Then the work focus on a particular case of the previous scenario, namely when there is a single relay helping the DeNB and the channel is supposed Gaussian, meaning with a very strong line-of-sight component. In this specific case too, there is a lack of practical coding strategies in the open literature and the work done will shade light on that, proposing a solution which can be realistically implemented. The authors evaluate it on a LTE simulator based on OpenAirInterface and are thus able to show, under the LTE standard constraints in a Gaussian channel, the gaps of a realistic implementation with respect to the theory. This is a first important step towards the evaluation of the practical feasibility of these new relay-assisted coding strategies.

The second scenario is a Gaussian relay-aided broadcast channel, a system where a DeNB communicates with multiple users across a Gaussian channel with the help of a full duplex relay, under the assumption of the availability of full channel state information to all the nodes in the network. The study of this system was motivated by the fact that it is applicable in practical heterogeneous deployments for 4G cellular networks in frequency flat channels. This scheme differs from the traditional broadcast channel in the presence of a relay helping the base station. The two transmitters could act as a virtual multiple-antenna transmitter, with antennas not co-localized but distributed over the base station and the relay. However, the performance of a virtual MIMO system, which is the highest one in

terms of throughput at high signal-to-noise ratios, is not always achievable. This study sheds light on how strong the DeNB-relay link should be, such that the DeNB and the relay might behave as a single 'virtual' base station with 2 antennas. In other words, the results give interesting insights on how this link should be dimensioned in order that the system behaves like a multiple antenna broadcast channel with 2 transmit antennas and 2 single-antenna users at the reception. These results, which were not knows in the literature, are useful for assessing if such relay configuration has practical interest or not. The general case with a generic number of users in then tackled.

Section 5 focuses on clusterized mesh networks for PMR systems. In this context, in the particular case of fast deployable systems e.g. for crisis management, there can be absence of wired backhaul between the cells, called here clusters, and hence inter-cluster communications are taken in charge by some relay nodes called bridging mesh routers. Since the back-bone traffic is going through those relay nodes, and part of it may be bidirectional, a two-way relaying technique was investigated. Many works have been done in the open literature on the two-way relaying technique which promises interesting throughput gains. Here we are interested in comparing it to a more traditional decode-and-forward strategy in two main deployment scenarios, a small town with low buildings and a more populated city with higher buildings. The aim is to understand when it is worth considering using two-way relaying.

Section 6 deals with resource allocation for multi-hop communications inside a cell or cluster, for applications to PMR context. In PMR systems relaying and direct communications between users are features which are particularly appreciated by the customers since they are included by the legacy PMR standards. In this section a wireless communication system consisting in a single cluster having multiple users is considered. The study focus on efficient and fair opportunistic scheduling of delay tolerant traffics in clustered/cellular environment with dynamic relaying. A wide range of nowadays applications generate this type of traffic, i.e. email, internet browsing, asynchronous file transfer, etc. They are generally classed as requiring a best effort service and give more flexibility to the system to handle them. The work extends three traditional scheduling policies to this new framework. In order to differentiate the impact of relaying on performance a comparison is made among the case when all the communications pass mandatorily through the base station (also named cluster head in mesh deployments), which is the standard cellular configuration, the case in which also direct communications between users are allowed, and finally the case in which any user can be a relay.

The global conclusions of the document are summarized in Section 7.

2 Propagation channel modeling

2.1 Scenario: Path loss models for relay scenarios

This scenario considers a network densification with relays to increase the average or cell edge user throughput. The benefits of this solution are generally evaluated by system level simulations which define many simulation parameters such as path loss models. From a propagation point of view, the multiple links between relay, mobile and Base Station (BS) can be modeled by two propagation channel models (Figure 1). The first one is the model for a macrocell environment that applies for the macro link between a BS and a mobile or for the backhaul link that applies for the backhaul link between a BS and a relay. The difference between a relay or a mobile is given by the antenna height. The second one is the model for a microcell environment that applies for the access link between a relay and a mobile. Path loss models may significantly change simulation results. It explains why path loss models need to be realistic and well-balanced. Models that underestimate the path loss for the macro link and overestimate the path loss for the access link will not promote relay-based solution or microcell densification. For the previously explained reasons, a precise model of propagation loss for the relay case is fundamental, and hence a measurement campaign was performed in order to check the accuracy of the available path loss models.

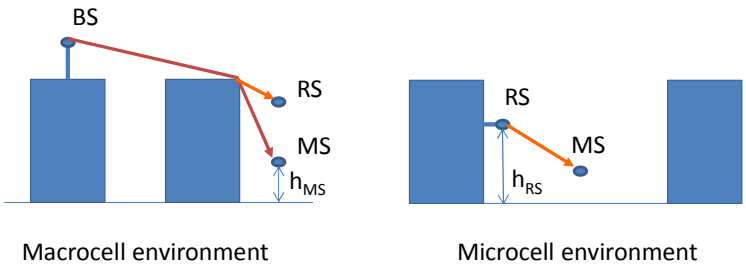

Figure 1: Propagation channel environments for relay scenario

As a first step, a measurement campaign was performed in an outdoor urban environment. Path loss models for the macro, backhaul and access links were calibrated with the collected data. The results were compared with well-known propagation channel models such as COST231-HATA, Winner, 3GPP or ITU channel models. The data analysis focused on the impact of the relay position (X-Y location and antenna height) on the path loss models.

2.2 Challenge: consistent channel modeling for relay networks

Long Term Evolution – Advanced (LTE-A) aims to offer higher data rate and higher capacity than the Universal Mobile Telecommunications System (UMTS) and LTE system currently employed. In these systems, the spectral efficiency at the cell edge is relatively limited due to the low Signal to Interference Noise Ratio (SINR). Many techniques have been proposed by LTE-A in order to solve this problem. One of these techniques is the relaying technique. Relay Station (RS) is an intermediate node between the Base Station (BS) and the Mobile Station (MS). It receives, processes and re-transmits the signal between the BS and the MS. Deploying RS in the cell may lead to increasing the cell capacity and extending its coverage area. This could be a solution to the cell edge problem [1], [2] and [3]. Evaluating the relay system performance requires relay channel propagation characteristics for three different links: BS-RS, RS-MS and BS-MS.

A number of propagation models have recently been suggested by 3rd Generation Partnership Project (3GPP) [4], the Wireless World Initiative New Radio (WINNER) project [5] and the International Telecommunication Union (ITU) [6]. However, parts of these models are either derived from previous work or validated with limited data sets. Therefore, their validation in various urban environments is yet to be fully examined. Besides, 3GPP, WINNER and ITU models do not define the relay antenna height as a parameter for their Path Loss (PL) predictions.

2.3 Description of the measurement campaign

The measurements were performed in the city of Belfort, France. The measurement environment is a typical medium urban city with 3-5 storey buildings. The average building height and the street width are about 15-20 meters and 7-12 meters, respectively. The BS was mounted on the roof of a 20-meter height building and transmitted a narrow band signal (one frequency tone) at 2147 MHz (Figure 2.a). It

was made of a sectorial antenna with a half power beam width of 90° in azimuth and 10° in elevation. The maximum antenna gain was 12 dBi and the transmitted power was set up at 43 dBm.

The measurement antenna, which represents the RS, was mounted on a van as shown in Figure 2.b. The RS antenna, with a gain of 2 dBi, was mounted at one end of a 1-meter-long pole. The other end of this pole was fixed on a mast. The antenna mast could be raised up. Thus, the antenna height can be varied from 4 meters to 13 meters.

In order to simulate the MS, a 2 dBi omnidirectional antenna was set on a car of 2 m height as shown in Figure 2.c. It allowed simultaneous measurements of the signal powers from the BS and RS.

The frequency band used in the measurement campaign is the UMTS band 2140-2155 MHz. The measurement campaign was performed in two phases. The first phase was dedicated to the BS-RS link. The transmitted frequency was fixed at 2147 MHz. The received power was measured when the RS antenna mast was set at three different heights corresponding to 4.7 m, 8.8 m and 12.7 m. These heights were below the rooftops of the surrounding buildings. Thus, the BS-RS link was always in Non-Line Of Sight (NLOS) conditions at all RS positions. The measurements were performed at a total number of 78 RS locations (red and green dots) distributed over 2 areas named herein the Train Station area Figure 3.a and the Old city area Figure 3.b.

In the second measurement phase, the received power of the transmitted signal from the BS and the RS were simultaneously measured at the MS. The RS transmitted frequency was fixed at 2148 MHz. The measurements were performed at ten RS locations (green dots). Five RS locations (RS1, RS2, RS3, RS4, RS5) were distributed in the Train Station area and five RS locations (RS6, RS7, RS8, RS9, RS10) were located in the Old City area. These locations were chosen among the 78 locations taken in phase I. The RS positions were chosen in a way to get a general idea about the RS environment effect on the PL model. During the measurement campaign, the received power of the transmitted signal from the RS or BS was measured at the MS while it was moving along a predefined measurement route. The measurement route lengths of the Train Station and the Old City were 17 Km and 9 Km, respectively. The measurements were carried out when the relay antenna was set at 4.7m, 8.8m and 12.7m. The RS positions of the two areas with the measurement routes of the Train Station and the Old City area are depicted in Figure 3.left and Figure 3.right, respectively.

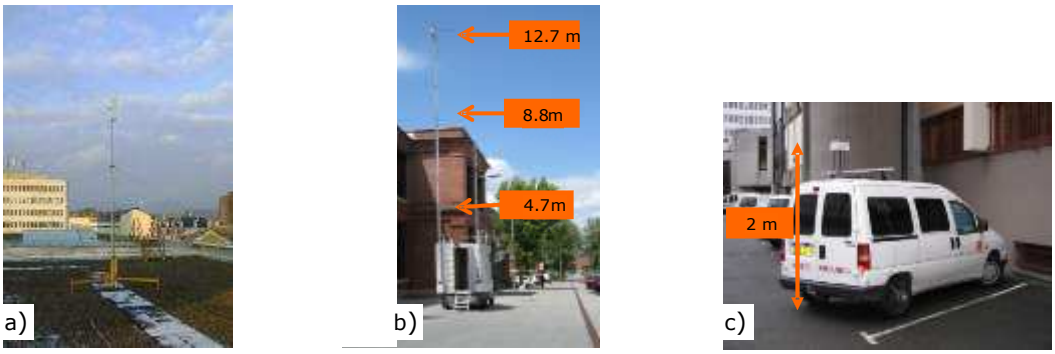

Figure 2: a) Photo of BS, b) Measurement van with 3 antenna heights, c) Measurement car

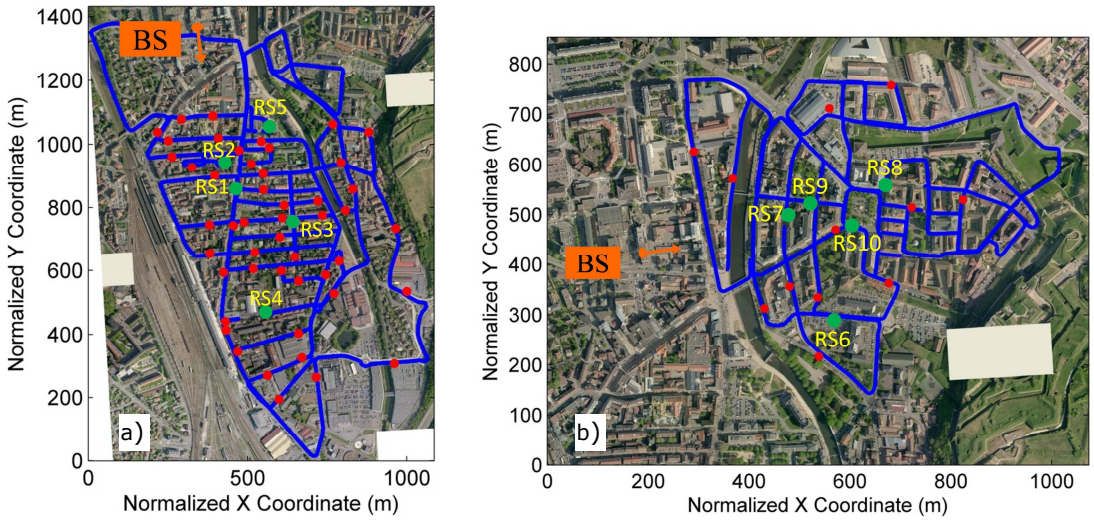

Figure 3: Static RS locations at 4.7m, 8.8m and 12.7m (red and green dots) and measurement routes (blue line) for the two measurement areas left (Train Station), right (Old City)

Before analyzing the collected data, measurements were processed. For the first phase measurement (BS-RS link), the RS positions were defined in a geo-referential map. At each RS location the mean received power was obtained by averaging all the measurement samples taken when the antenna was rotating around its vertical axis. The nearest locations from the measurements route, in the second phase, enclosed within a circle of 10 meter radius around the relay location were selected for each relay location. Mean powers corresponding to the selected locations were averaged. The average value gives the mean power at 2 meters.

For the second phase (BS-MS and RS-MS links), several steps have been followed in the data processing [7]:

- Measurement route localization: The objective of this step is to assign a Lambert coordinate (X,Y) to each measurement point and to localize the measurement route on a geographical map. The measurement route was divided into several sections and the collected measurement for each section was saved into the computer. The starting and the ending point of each section were street corners in order to ease the measurement point's localization on the geographical map. After the localization of the starting and the ending point of each section, the measurement route was manually drawn and the measurement points acquired on each section were then automatically distributed every 2 cm. This method is not accurate as the GPS but it avoids the erroneous positions in severe urban conditions. After completing the localization procedure, each measurement point was assigned with its Lambert coordinate.
- Data averaging: After measurement, the received signal consists of fast fading and slow fading components. Before analysis, the data need to be averaged in order to obtain the local mean power by smoothing out the fast fading part. The averaging process was done by the shifting window method. This method is defined by two parameters W and T where W defines the averaging distance expressed by the number of raw measurement points. T represents the shifting distance between two successive groups of W. According to [7], the optimal values of W and T, valid for this measurement campaign, are $20\,\lambda$ and $10\,\lambda$ respectively.
- Measurement route synchronization: measurements were carried out for 5 relay locations at 3 different relay antenna heights in each area. Thus, a total of 15 measurement routes are performed in each measurement area. The measurement routes are similar but not identical. Each measurement route starts and finishes at different positions which are generally close together but not exactly the same. Furthermore, the number of measurement points of the different routes is not the same. Consequently, a straightforward point-to-point comparison is impossible and the measurement routes should be synchronized. The synchronization is composed of 4 main steps: erroneous section removal, pairing, new position calculation and results [7].
- Line Of Sight (LOS) / NLOS classification was performed for the RS-MS link. For more information about the classification see [8]. For BS-RS link, the classification was not performed due to the lack of LOS measurement for this link.

2.4 Description of PL models

The models that can be applied for the relaying technique are presented below.

The parameters used for the model descriptions are given as follows:

- d [m] is the ground distance between Tx and Rx
- d_{3D} [m] is the real distance between the Tx and Rx.
- h_{MS} [m] is the MS antenna height
- h_{BS} [m] is the BS antenna height
- f [GHz] is the central frequency
- W [m] and h [m] represent the street width and the average buildings height, respectively.
- Δh_{MS} [m] represents the difference between the rooftop level h_{roof} and the h_{MS}.

Models applied to the BS-RS link:

Table 1 presents the PL models which can be applied to the BS-RS link with the shadow fading standard deviation (σ) for NLOS conditions. The 3GPP BS-RS [4] and WINNER B5F [5] models were proposed for

relaying technique. RS antenna height is not taken into account in these models. ITU UMa [6] and 3GPP UMa 3D [9] models were dedicated to macro cell scenario. These models take into account the mobile antenna height as a correction factor and can be applied to the BS-RS link. The 3GPP UMa 3D model is similar to the ITU UMa model where the mobile antenna height correction factor is introduced in this model. For a 2 m mobile antenna height, this factor is null.

Due to the complexity of the COST231 WI [10], this model is presented at a frequency of 2.1 GHz in a simplified numerical form adapted to Belfort city environment by assuming a street width of 10 m, an average rooftop level of 15 m, a building separation of 20 m and an h_{BS} of 20m.

Table 1: Model description for BS-RS link

Organisation	*Model type*	*PL equation*	σ *(dB)*
3GPP	***BS-RS [4]*** ***10m < d < 5 km***	$PL = 16.3 + 36.3\log_{10}(d)$	10
	BS-MS [4] h_{MS} = 1.5m 10m < d < 5 km	$PL = 2.7 + 42.8\log_{10}(d)$	10
	NLOS 3-D UMa [9] 1.5m < h_{MS} < 22.5m *10m < h_{BS} < 150 m*	$PL = 161.04 - 7.1\log_{10}(W) + 7.5\log_{10}(h) - \left(24.37 - 3.7\left(h/h_{BS}\right)^2\right)\log_{10}(h_{BS})$ $+ (43.42 - 3.1\log_{10}(h_{BS}))(\log_{10}(d_{3D}) - 3) + 20\log_{10}(f) - \left(3.2(\log_{10}(17.625))^2 - 4.97\right)$ $- 0.6(h_{MS} - 1.5)$	6
WINNER	***B5f*** h_{MS} = 15m 30m < *d* < 1.5 km	$PL = 42.5 + 20\log_{10}\left(f/5\right) + 23.5\log_{10}(d)$	8
	C2 h_{MS} = 1.5m 50m < *d* < 5km	$PL = (44.9 - 6.55\log_{10}(h_{BS}))\log_{10}(d) + 34.46$ $+ 5.83\log_{10}(h_{BS}) + 23\log_{10}\left(f/5\right)$	8
ITU [6]	***UMa*** 1m < h_{MS} < 10m 10m < *d* < 5 km	$PL = 161.04 - 7.1\log_{10}(W) + 7.5\log_{10}(h) - \left(24.37 - 3.7\left(h/h_{BS}\right)^2\right)\log_{10}(h_{BS})$ $+ (43.42 - 3.1\log_{10}(h_{BS}))(\log_{10}(d) - 3) + 20\log_{10}(f) - \left(3.2(\log_{10}(11.75h_{MS}))^2 - 4.97\right)$	6
COST231 [10]	***WI*** 1m < h_{MS} < 10m 20m < *d* < 5km	$PL = 31.6 + 38\log_{10}(d) - [22.6 - 20\log_{10}(\Delta h_{MS})]$	4-8
	HATA 1m < h_{MS} < 10m 1km < *d* < 20 km	$PL = 46.3 + 33.9\log(10^3 f) - 13.82\log_{10}(h_{BS}) - (1.1\log_{10}(10^3 f) - 0.7)h_{MS}$ $+ (1.56\log_{10}(10^3 f) - 0.8) + (44.9 - 6.55\log_{10}(h_{BS}))\log_{10}(10^{-3} d) + 3$	NA

Models applied to the RS-MS link:

In the microcell deployment, the BS antenna is under the rooftops of the surrounding buildings. The relay antenna will be deployed under the rooftops (it is proposed to install relays on street lamps). Thus, the PL models proposed for microcell deployment can be applied to the RS-MS link. PL models can be classified into two types depending on the measurement environment. The first type is the PL for Manhattan grid layout [4], [5] and [6]. In this scenario, the streets are laid out in a Manhattan-like grid. The streets are classified as the main street where the BS and MS are in LOS. Streets that intersect the main one are referred to as perpendicular streets and those that are parallel to it are referred to as parallel streets. The attenuation depends on the distances d_1 and d_2 which represent the distance in the main street and in the intersection street, respectively, as shown in Figure 4.

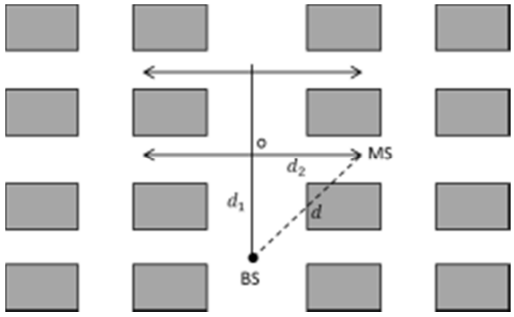

Figure 4: Manhattan grid layout

The second type is the PL for the hexagonal layouts. For such a type, the models are based on one single distance which is the ground or 3-D distance between the transmitter and the receiver. This type of models can be easily implemented in the system level simulators which do not define a Manhattan grid and they do not assume an urban structure. Thus, these models are more generic and can be used for various urban environments.
As a conclusion, we focus only on the PL models that can be applied to the hexagonal layouts. Therefore, the models presented by WINNER, 3GPP and ITU for Manhattan-layout scenarios are not considered in this work.
Table 2 presents the PL models for the RS-MS link with the shadow fading standard deviation (σ).

Table 2: Model description for RS-MS link

Organisation	*Model type*	*PL equation*	*σ (dB)*
3GPP	***LOS RS-MS***	$PL = 41 + 20.9\log_{10}(d)$	NA
	NLOS RS-MS	$PL = 32.9 + 37.5\log_{10}(d)$	NA
	NLOS 3-D UMi h_{BS} = 10m h_{MS} = 1.5-22.5m	$PL = 36.7\log_{10}(d) + 22.7 + 26\log_{10}(f) - 0.3(h_{MS} - 1.5)$	4
ITU (UMi)	***LOS BS-MS***	$PL = 22\log_{10}(d) + 28 + 20\log_{10}(f)$	3
	NLOS BS-MS h_{BS} = 10m h_{MS} = 1-2.5m	$PL = 36.7\log_{10}(d) + 22.7 + 26\log_{10}(f)$	4
WINNER+ (UMi B1)	***LOS BS-MS*** h_{BS} = 10m h_{MS} = 1.5m	$PL(d) = 22.7\log_{10}(d[m]) + 27 + 20\log_{10}(f)$	3
	NLOS BS-MS h_{BS} = 10m h_{MS} = 1.5m	$PL(d) = (44.9 - 6.55\log_{10}(h_{BS}))\log_{10}(d) + 5.83\log_{10}(h_{BS}) + 18.38 + 23\log_{10}(f)$	4
COST231 WI	***NLOS BS-MS*** h_{BS} = 4-50m h_{MS} = 1-3m f = 800-2000 MHz	$PL = \begin{cases} 160 + (53 - h_{BS})(\log_{10}(d) - 3) - 0.0016(h_{BS} - 15)d & d < 500m \\ 172 + (53 - h_{BS})(\log_{10}(d) - 3) - 0.8h_{BS} & d \geq 500m \end{cases}$	4-8

3GPP 3-D UMi for NLOS is the same as ITU UMi with introducing the mobile antenna height as a correction factor. For 2 m mobile antenna height, the correction factor becomes zero.

2.5 Comparison of PL models with measurements

BS-RS and BS-MS PL Models Vs. Measurement:
From propagation point of view, BS-MS and BS-RS links are the same in terms of PL models (macrocell). The only difference is the height of the terminal (MS or RS). For this reason, in this section we compare the PL models for BS-MS and BS-RS.

Figure 5 compares the measured path losses with those predicted by the different models presented in Table 1. For each measurement point, the model error is defined as the difference between the measured path loss and the path loss predicted by the model. Table 3 summarizes the mean error for all antenna heights and models. The error standard deviation is around 6 dB which is in accordance with the shadow fading values reported in Table 1.

At street level, the COST231 Hata, ITU UMa, COST231 WI and WINNER C2 channel models are consistent with our measurement and can be considered as realistic PL models, even though the difference between the ITU UMa and COST231 WI is around 6 dB. They correspond to various density degrees of urbanization.

The 3GPP BS-MS is not realistic as it approximately underestimates the PL by 10 dB. The WINNER B5f scenario assumes that relay antennas are situated some meters either over or below the rooftop. As reported in [12], the B5f model is more appropriate to a mixed condition between LOS and NLOS rather than a complete NLOS condition as in the measurement environment presented in this study. Therefore, the WINNER B5f underestimates the measured path loss according to its definition. The 3GPP BS-RS model underestimates the path loss too but it is specified for a RS antenna height at 5 meters in an urban environment. The mean error between the 3GPP BS-MS model and the measurement at 5 meters

is more than 10 dB. Thus, the WINNER B5f model and the 3GPP BS-RS model must be considered as the lower limit for the PL prediction when the relay is in NLOS condition.

The COST231 Hata proposes a simple linear Antenna Height Correction Factor (*AHCF*) but exhibits poor performance at high RS antenna heights. For instance, it under-predicts the PL by 15 dB at 8.8 m above the street level. At 12 meters, its performance is not given as it predicts values below the free space level. The COST231 WI or ITU UMa model gives better results and may be used to coherently predict the path loss for the links BS-RS and BS-MS.

A more detailed analysis about the effect of the relay antenna height on the PL model, based on this measurement campaign is presented in [13]. The PL decreases with the increase of the relay antenna height by a factor of 0.9 dB/m. This factor is in agreement with the *AHCF* given by the COST231 WI model.

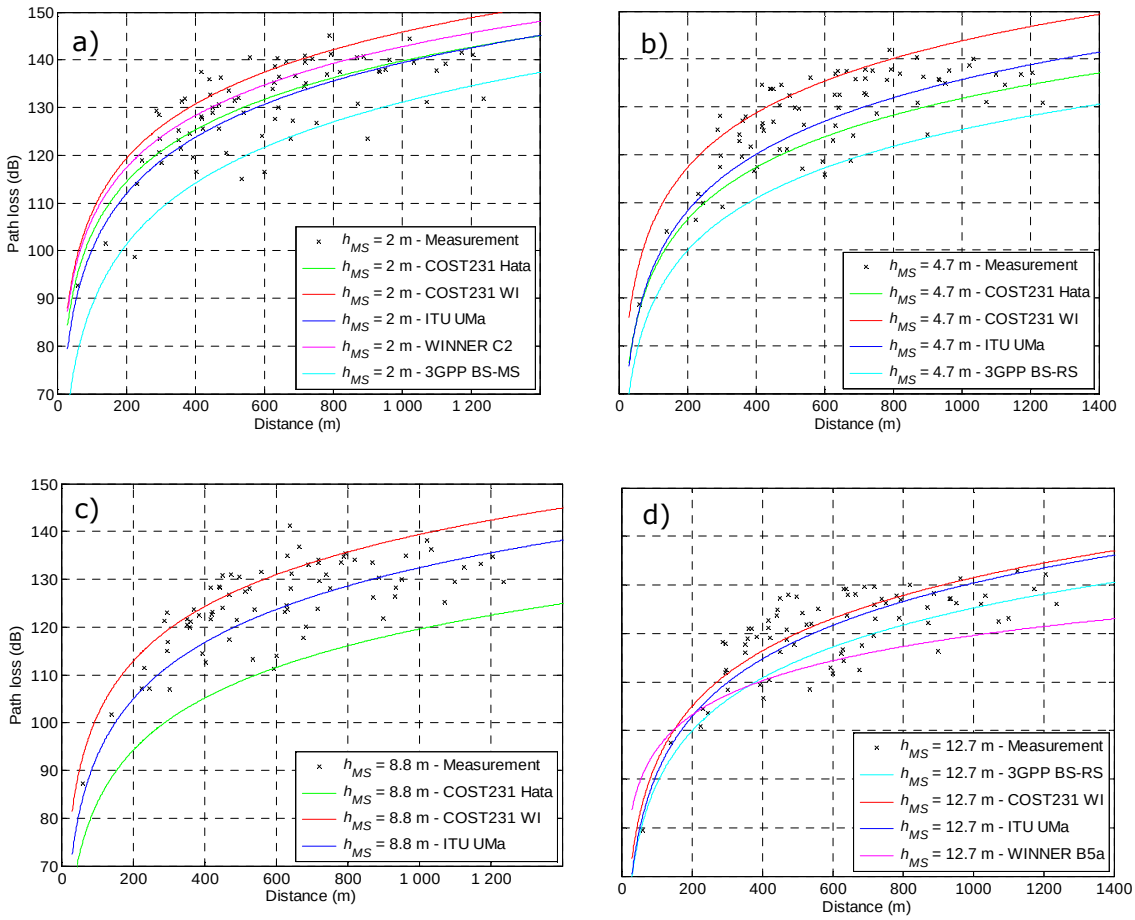

Figure 5: Comparison between PL models and measured points at different relay antenna height

Table 3: Mean error (dB)

PL model	h_{MS} = 2m	h_{RS} = 4.7m	h_{RS} = 8.8m	h_{RS} = 12.7m
3 GPP BS-RS	14.5	12.3	9.1	4.5
3 GPP BS-MS	10.3	8.1	4.9	0.3
WINNER B5f	16.8	14.6	11.4	6.8
WINNER C2	-3	-5.2	-8.4	-13
ITU-UMa	1.1	2.7	2.7	0.2
COST-WI	-5.2	-5.3	-4.1	-0.8
COST-Hata	0	5.8	14.7	NA

RS-MS PL Models Vs. Measurements

For the RS-MS link, the comparison is achieved for LOS and NLOS conditions as follows:

LOS Conditions:

Figure 6 compares the PL models presented in Table 2 to the LOS measurements. Table 4 presents the mean error. The error standard deviation is about 6 dB. WINNER+ UMi and ITU UMi propose PL models close to the Free Space PL (FS PL) with a mean error of about -1dB). 3GPP RS-MS proposes a PL model higher than the FS PL model with a mean error of 3 dB.

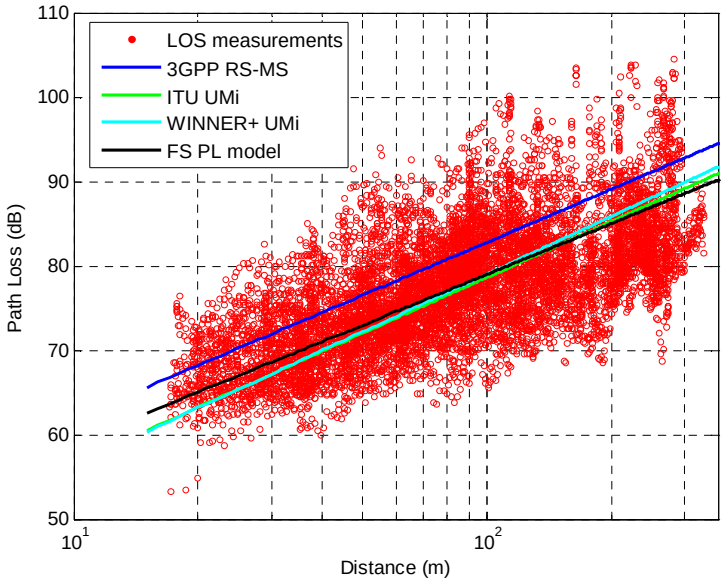

Figure 6: LOS PL models in comparison with the measurement

Table 4: Mean error for LOS RS-MS link (dB)

PL model	mean (dB)
WINNER+ UMi	-0.9
3GPP RS-MS	3
ITU UMi	-1.2

A detailed analysis in [8] based on this measurement campaign shows that the PL model depends on the RS position. In the position where vegetation exists, the PL can be higher than the FS PL up to 5 dB while in the places where street canyon can exist the PL is lower than the FS PL model down to 5 dB. Thus, 3GPP RS-MS PL model can be applied for an environment with a high vegetation density while ITU UMi and WINNER+ UMi models can be applied for an environment with a low vegetation density.

NLOS Conditions:

Figure 7.a, 7.b and 7.c compare the PL models presented in Table 2 to the measurements for h_{RS} = 4.7m, 8.8m and 12.7m, respectively. Table 5 presents the mean error. The error standard deviation varies between 8 and 10 dB. The error standard deviation values can be considered high compared to the shadow fading standard deviation values presented in Table 2. A detailed analysis about the standard deviation values can be found in [14]. [14] shows that the shadow fading standard deviation, in the locations where street canyon phenomenon exists, can be higher than the shadow fading standard deviation related to the diffraction over rooftops

COST231 WI extremely overestimates the PL prediction for the different relay antenna heights. COST231 WI considers only the diffraction over rooftop phenomenon and it neglects the street canyon effect. These reasons may explain the poor performance of this model in the microcell scenario (h_{BS} < h_{roof}).

WINNER+ UMi overestimates the PL. WINNER+ UMi is a modified version of COST 231 Hata model [10]. Moreover, the proposed model by WINNER+ for microcell scenario is the same as the one proposed for macro cellular scenario.

ITU UMi and 3GPP for relaying scenario models are more consistent to the measurement data. However, the PL exponent proposed by 3GPP and ITU are considered low compared to those extracted from the measurements. For a low PL exponent, the model overestimates the measured PL over short distances and underestimates it over long distances. Their performance depends on the antenna height as well.

Basically, the ITU UMi and 3GPP RS-MS PL models are independent of the transmitter antenna height. 3GPP RS-MS PL model does not define the antenna height application range. Therefore, it is difficult to comment its performance. ITU UMi PL model is proposed for a BS of 10 m antenna height. The absolute mean error of ITU UMi model (error < 2dB) can be considered low compared to other mean error values. As a conclusion, ITU UMi model agrees our measurements.

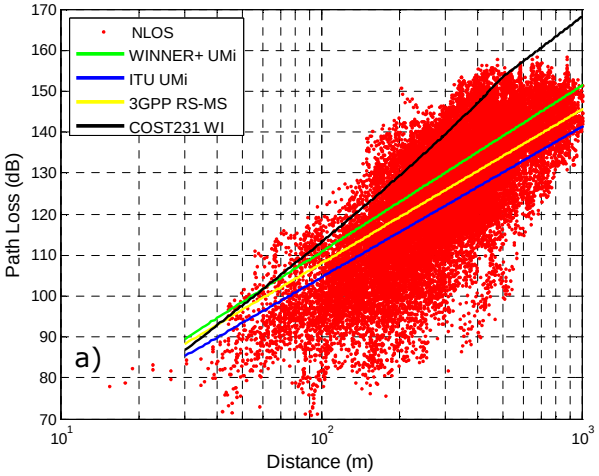

Measurement data for h_{RS} = 4.7 m

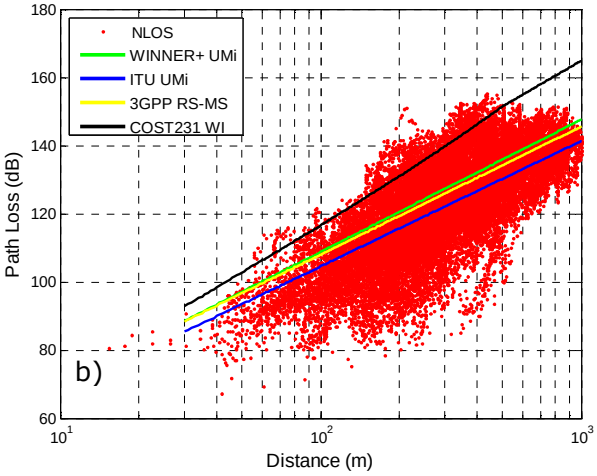

Measurement data for h_{RS} = 8.8 m

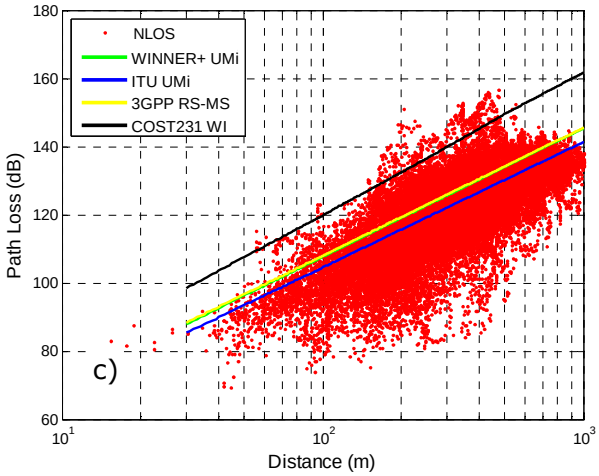

Measurement data for h_{RS} = 12.7 m

Figure 7: PL models in comparison to NLOS measurements

Table 5: Mean error for NLOS RS-MS link (dB)

PL model	h_{RS} = 4.7m	h_{RS} = 8.8m	h_{RS} = 12.7m
WINNER+ UMi	4.7	4	5.6
3GPP RS-MS	0.5	2.6	5.6
ITU UMi	-3.4	-1.3	1.7
COST231 WI	15	17	20

A more detailed analysis about the effect of the relay antenna height and the environment that is around it on the PL model, based on this measurement campaign is presented in [15]. The PL model depends on the building blockage in azimuth and elevation at the relay station. The difference between the minimal and the maximal PL models is about 17 dB. An average gain of about 5 dB is achieved by increasing the relay antenna height from 4m to 12 m. The general equation of the PL model according to [15] is given as follows:

$$PL(dB) = 46\log_{10}(d) + 14.2 - 0.6h_{RS} + SF$$

where h_{RS} is the relay antenna height and SF is a Gaussian variable with a standard deviation of 9.6 dB.

2.6 Discussion and conclusion

The existing PL models that can be applied for relaying technique were reviewed and compared to the measurement data. Some intermediate conclusions were given for each individual link (BS-RS, BS-MS, RS-MS). When cross checking all separate conclusions, a final recommendation can be drawn. According to the measurements, the ITU [6] models defined for macrocell and microcell environment for LOS and NLOS conditions give the best performance. The recent 3GPP 3-D UMi and Uma models [9] defined for 3-D simulations may also be recommended as they are based on the ITU UMi and Uma [6] models, respectively. We want to emphasize that the PL models in microcell environment depends on the environment that is around the relay. The general recommendations are based on measurements collected in a medium-size European city and may change with large cities which include large avenues and high-rise buildings.

3 Non-binary LDPC code design for multi-relay scenarios

In this section, we propose a cooperative coding scheme to communicate efficiently over multiple-relay fading channels. The particularity of our approach is to rely on non-binary Low Density Parity Check (LDPC) codes at the source, coupled with non-binary repetition codes at the relays. A simple joint decoding strategy is used at the receiver end, so that the decoding complexity is not increased compared to a system without relays, while preserving the coding gain brought by re-encoding the signal at the relays. We show by simulations that the proposed scheme allows maintaining a constant gap to the outage probability of the cooperative system, irrespective of the number of relays.

3.1 Scenario and challenge

Cooperative diversity techniques over wireless relay channels [16] [17], allow exploiting the broadcast nature and the inherent spatial diversity of wireless communications. A relay channel is a multi-node network consisting of a source, a destination, and a collection of relays that might be of different nature. The source broadcasts a message to both relays and destination, while the relays forward the message or modified versions of it to the destination. Subsequently, different cooperation protocols have been proposed, which can be classified into three major categories, namely the amplify-and-forward (AF), the compress-and-forward (CF), and finally the decode-and-forward (DF) protocol [18], [19]. The DF protocol allows each relay to decode the received signal, re-encode it, and forward it to the destination. The forwarded message can either be identical to, or part of the initial transmission [20] (repetition coding), or it can be obtained by using a dedicated coding scheme at the relays. The destination uses the global knowledge of the cooperative coding scheme to jointly decode the received signals both from the source and the relays. Distributed coding using parallel turbo-codes [21] or binary LDPC codes ([22],[23], [24], [25], [26], [27]), has already been proposed in the literature. The existing approaches are either based on serial or parallel code concatenation, meaning that the graph of the LDPC code broadcasted from the source is a subgraph of the destination decoding graph, or based on punctured rate-compatible LDPC codes. A different approach was proposed in [28], where the relay generates extra parity-bits by splitting parity-checks of the LDPC code broadcasted by the source. When the number of relays increases, these methods suffer from a large increase of decoding complexity, while the coding gain they present becomes increasingly less important.

In this deliverable, we propose a new approach to the problem of cooperative coding in the case of multiple relays. The approach is based on non-binary LDPC (NB-LDPC) codes and the recently introduced technique of multiplicative non-binary coding [29], which will be referred to as non-binary repetition coding. In our setting, the source broadcasts a NB-LDPC codeword to the destination and the relays. When the relays successfully decode the received word, extra parity symbols are computed at the relays through optimized non-binary repetition codes, which are then sent to the destination. The receiver collects the original received word from the source and the non-binary extra symbols from the relays and combines them before the iterative decoding. The iterative decoding complexity is the same in presence or absence of relays, while combining the codeword and the additional non-binary repetition symbols brings an effective coding gain.

Our contribution is organized as follows. In Section 3.2, we describe the proposed cooperative coding scheme and discuss its advantages. The joint optimization of both NB-LDPC and non-binary repetition codes is presented in Section 3.3. The performance of the proposed coding scheme over block-fading multi-relay channels is evaluated in Section 3.4. Finally, Section 3.5 concludes this work and discuss future works.

3.2 Innovation: Proposed Cooperative Coding Scheme

3.2.1 Non-Binary LDPC Codes and Decoding

We denote by GF(q) the Galois field with q elements. A NB-LDPC code is defined by a sparse parity-check matrix H, with M rows and N columns, whose entries are taken from GF(q). We shall assume that H is full rank, hence the coding rate is $R = K/N$, where $K = N - M$ is the number of source symbols. A NB-LDPC code can be advantageously represented by a bipartite (Tanner) graph containing N symbol-nodes and M constraint-nodes, associated respectively with the N columns and M rows of H. A symbol-node and a constraint-node are connected by an edge if and only if the corresponding entry of H is non-zero. Each edge of the graph is further assumed to be "labeled" by the corresponding non-zero entry.

The Belief-Propagation (BP) decoding passes messages along the edges of the graph, in both directions, which are iteratively updated by Bayesian rules. In the non-binary case, each message is a probability distribution vector on GF(q), which gives the probabilities of the incident symbol-node being equal to

each of its possible values. These probability distributions are iteratively updated until a codeword has been found or a maximum number of iterations has been reached. We shall not present the BP decoding here, but merely refer to [30] for details. We also note that the BP decoding can be efficiently implemented by using binary Fourier transforms [31]. Moreover, at the cost of a small performance degradation, several low-complexity decoding algorithms, which operate in the Log Likelihood Ratio (LLR) domain, have been proposed in the literature [32][33].

3.2.2 Cooperative System Description

Throughout this contribution, we will assume that the source broadcasts a NB-LDPC codeword to the destination and a given number N_r of relays. Parameters of the different links in the system will be indicated by using subscripts SD, SR_i, and R_iD, with obvious meaning. We assume QAM signaling constellations of order M_{SD}, M_{SR_i}, and M_{R_iD}. Since relays and destination receive the same modulated signal broadcasted by the source, we have by construction $M_{SD} = M_{SR_i}$, $\forall i = 1,\ldots,N_r$.

Our cooperative coding scheme, depicted in Figure 8 in the case of two relays, can be described as follows:

[S] The source encodes the packet of information bits, generating a NB-LDPC codeword c (red filled circles in Figure 8). It modulates c with the M_{SD}-QAM constellation and broadcasts the modulated symbols x to both relays and destination.

[R_i] Each relay R_i decodes the received signal, so that to correct the transmission errors on *c*. If decoding fails (e.g. using a CRC check or with syndrome check inside the LDPC decoder), the relay does not transmit any information to the destination. Otherwise, it generates a new sequence $c^{(i)}$ of non-binary symbols using the *non-binary repetition* coding (blue or green filled circles in Figure 8). Vector $c^{(i)}$ needs not be of the same size as the original codeword c, since the coding rates for the links relay-destination are typically higher. The vector $c^{(i)}$ is modulated using the M_{R_iD}-QAM constellation, and the modulated symbols $x^{(i)}$ are then sent to the destination.

[D] The destination receives noisy versions of x and $x^{(i)}$ (from both source and relays), and performs a joint iterative decoding using only the parity check matrix *H* of the NB-LDPC code broadcasted by the source.

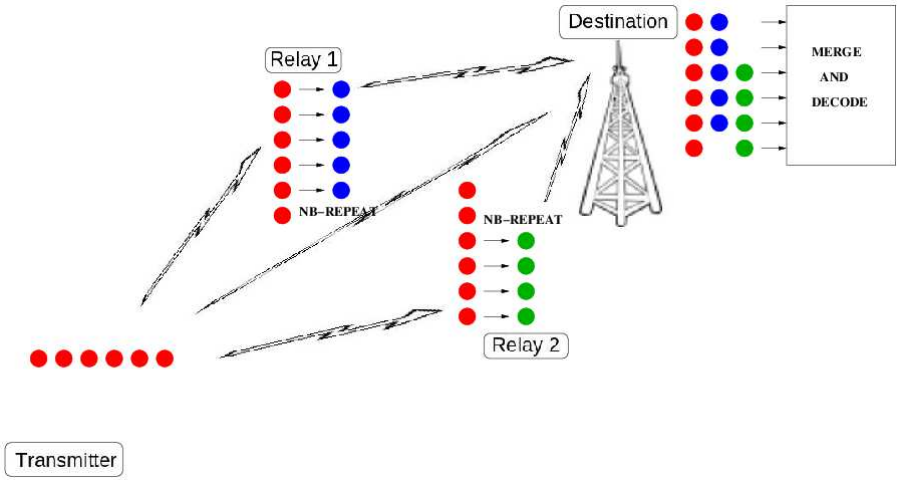

Figure 8 : Cooperative coding using non-binary repetition coding. Circles: symbols transmitted by the source or the relays; Red: symbols of the source; Blue: symbols of the first relay (NB-repetition versions of all or part of the red symbols); Green: as above, but for the second relay.

The next section explains in details how non-binary repetition symbols are generated, and how the joint decoding is performed at the destination.

3.2.3 Non-Binary Repetition coding and Joint Decoding

We assume that the parameters of the transmission system, namely the constellation orders $\{M_{\mathrm{SD}}, M_{\mathrm{R}_i\mathrm{D}}\}$ and the coding rates $\{R_{\mathrm{SD}}, R_{\mathrm{R}_i\mathrm{D}}\}$ are fixed *a priori*. When the *i*-th relay successfully decodes the codeword c broadcasted by the source, it generates $N_i = N\frac{R_{\mathrm{SD}}}{R_{\mathrm{R}_i\mathrm{D}}}$ non-binary repetition symbols as follows:

- Select N_i symbols $\{c_{k_l^{(i)}}\}_{l=1,\ldots,N_i}$ among the *N* symbols of c.
- Generate new symbols $c_l^{(i)} = h_l^{(i)} c_{k_l^{(i)}}$, where $h_l^{(i)} \in GF(q)$ are predetermined non-zero values, corresponding to the local NB-repetition code.

The vector $c^{(i)}$ is then modulated and sent to the destination. As a particular case, choosing $h_l^{(i)} = 1, \forall l$, reduces to classical repetition coding. In our case, with a very limited extra complexity, we allow the use of non-binary repetitions with $h_l^{(i)} \neq 1$, which provides a non-negligible coding gain, as explained in Section 3.3.2.

We discuss now the joint decoding at the destination. To simplify the notation, we drop the index of the symbol within the codeword, and consider a particular code symbol $c \in \mathrm{GF}(q)$. We denote by x the QAM symbols built from c and transmitted by the source. Similarly, we denote by $x^{(i)}$ the QAM symbols corresponding to the non-binary repetitions of c transmitted by the relays. The destination receives channel values, denoted by $\{ y^{(0)}, y_l^{(1)}, \ldots, y_l^{(I)}\}$, from the source and I active relays, according to one row in Figure 8. These values are used to compute the joint-probability vector $P = \{P(a)\}_{a \in GF(q)}$, where $P(a) = \Pr[c = a \mid y^{(0)} \ldots y^{(I)}]$, which merges the sufficient statistics of all active links. Using the fact that the SD and $\mathrm{R}_i\mathrm{D}$ channels are conditionally independent, we can write:

$$P(a) = \prod_{i=0}^{I} \Pr[c = a \mid y^{(i)}] = \prod_{i=0}^{I} \Pr[c^{(i)} = h^{(i)} a \mid y^{(i)}],$$

where $h^{(i)}$ is the non-zero value used for the non-binary repetition encoding of symbol c at relay i, and $h^{(0)} = 1$. Consequently, the main transmission and the relay transmissions are combined into one joint-probability vector per code symbol, which is fed to the BP decoder.

The process is depicted in Figure 9, which shows the factor graph used for the joint decoding of the NB-LDPC code from the source and the repetition codes from the relays. We considered in this figure the case of 3 relays, each of them sending $N_i = 2N/3$ extra repetition symbols, such that the destination receives 3 probability measures for each coded symbol: one from the source, and two from the relays. Coded symbols broadcasted by the source are represented by red filled circles, while extra repetition symbols are represented by yellow, green or blue filled circles. Constaint-nodes are represented by black filled squares.

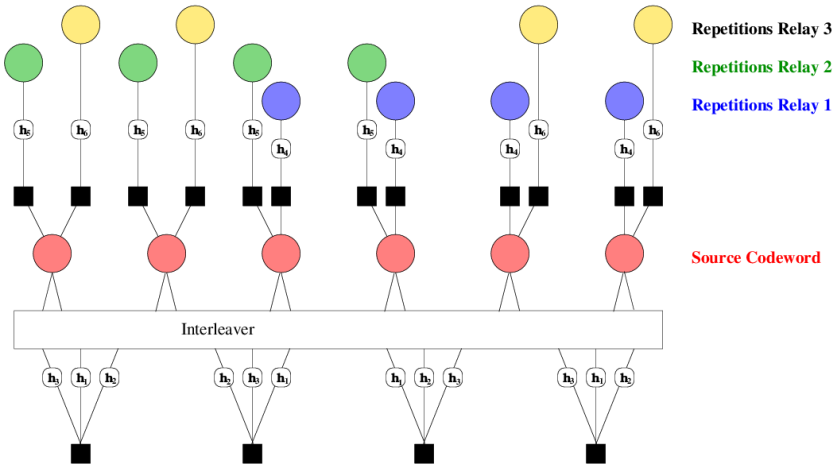

Figure 9 : Tanner graph of the joint-receiver at the destination

3.3 Optimization of the Proposed Cooperative Coding Scheme

3.3.1 NB-LDPC code Optimization at the Transmitter

For codes defined over GF(q), it has been shown in [34] that selecting carefully the non-binary entries of the parity-check matrix H can improve the overall performance of the code. The approach proposed in *loc. cit.* consists in choosing the non-zero entries of H such that the binary image of each non-binary check-node has the maximum *minimum Hamming distance* $D_{\min}$, together with the minimum multiplicity of codewords with Hamming weight $D_{\min}$. Although locally optimal, this strategy is not optimal when used in a message passing iterative decoder, where extrinsic vector messages are propagated along graph's edges.

We propose here a new selection criterion for the non-zero entries of H. In the sequel, we should also refer to a non-binary parity check as a *component code*; it is thus determined by the non-zero entries within a row of H. We consider non-binary codes defined by regular Tanner graphs, with all symbol-nodes of degree d_v, and all check-nodes of degree d_c. Our strategy is to optimize the balance between sub-codes of the component code, which is especially efficient when the code is an ultra-sparse code with $d_v = 2$. Since the message-passing decoder will propagate d_c extrinsic messages computed from the incoming message at each iteration, it is better to build extrinsic messages which statistically behave equally. In other words, the extrinsic messages should have their quantity of mutual information as close as possible to their average. Our optimization criterion for component code selection is described in Algorithm 1 below. This algorithm ensures that all the sub-codes of the component code have good and equally distributed error correction capabilities. This new optimization criterion is indeed interesting since we saw slight improvement in the waterfall region compared to codes that use non-optimized sets of non-zero values. The best sets of $d_c = 4$ values for GF(64) and GF(256) that have been optimized with the new criterion are given in Table 6. GF(q) elements are denoted by $\{0, \alpha^0, \alpha^1, \ldots, \alpha^{(q-2)}\}$, where α is a primitive element of the field. Four sets of values were found to have exactly the same performance with respect to the criterion of the optimization algorithm.

Algorithm 1: Component Code Optimization

1. Consider a non-binary parity check of degree d_c with non-zero values $\{h_1 \ldots h_{d_c}\}$
2. Let $S_{cc}(k)$ be the binary code determined by the binary images of $d_c - 1$ values in the set $\{h_1 \ldots h_{d_c}\}$ except h_k.
3. Choose for $\{h_1 \ldots h_{d_c}\}$ the field values in GF(q) such that:

$$\{h_1 \ldots h_{d_c}\} = \operatorname{argmax}_{\{h_1 \ldots h_{d_c}\}} \left(\sum_{k=1}^{d_c} D_{\min}(S_{cc}(k)) \right),$$

constrained to $\left| D_{min}(S_{cc}(k)) - D_{min}(S_{cc}(k')) \right| \leq 1$

Table 6 : Best rows with d_c = 4, for GF(64) and GF(256)

GF(64)	$(\alpha^0, \alpha^9, \alpha^{26}, \alpha^{46})$	$(\alpha^0, \alpha^{17}, \alpha^{26}, \alpha^{43})$	$(\alpha^0, \alpha^{17}, \alpha^{37}, \alpha^{54})$	$(\alpha^0, \alpha^{20}, \alpha^{37}, \alpha^{46})$
GF(256)	$(\alpha^0, \alpha^8, \alpha^{173}, \alpha^{183})$	$(\alpha^0, \alpha^{10}, \alpha^{82}, \alpha^{90})$	$(\alpha^0, \alpha^{72}, \alpha^{80}, \alpha^{245})$	$(\alpha^0, \alpha^{165}, \alpha^{175}, \alpha^{247})$

3.3.2 Repetition code Optimization at the Relays

We now discuss the impact of the non-binary repetition symbols built by the relays and used in the joint-probability computation at the destination. Let us first concentrate on the case of a single repetition. Let c be the symbol to be repeated and $h^{(i)}c$ be the repeated Galois field value. The destination receives noisy values on both c and $h^{(i)}c$, corresponding to the same code symbol. It follows that the demodulation actually acts as a maximum-a-posteriori decoder of the code built from the concatenation of the two Galois field values $[1, h^{(i)}]$. Now the coding gain is increasing with the minimum distance of the binary image of $[1, h^{(i)}]$. In case of simple a copy, *i.e.* $h^{(i)} = 1$, the binary minimum distance is $D_{\min} = 2$ and no coding gain can be achieved, while for non-binary repetitions, this minimum distance is typically larger $D_{\min} \geq 3$ when the field size q is sufficiently large. Additionally, the non-zero repetition values $h_l^{(i)}$ need to be optimized with the knowledge of the non-zero values which have been used in the source NB-LDPC code. Indeed, during the iterative decoding algorithm, the extrinsic vector messages will be computed using the joint-probabilities, that is, with the modified parity-check nodes including the repetition nodes as well. The modified parity-check nodes act then as the new *component codes* of the joint coding scheme.

The optimization criterion for non-binary repetition code selection is described in Algorithm 2. We advise in particular to use the same non-zero value $h^{(i)}$ for all the repeated symbols at the relay i. The optimization algorithm stops when the maximum number of potential relays I has been reached. Table 7 shows the optimized repetition values for NB-LDPC codes over GF(64) and GF(256), with d_c = 4. The non-zero entries of the NB-LDPC parity check are defined according to any of the four sets of best rows presented in Table 6.

Algorithm 2: Non-Binary Repetition Code Optimization

1. Let a parity-check equation have fixed non-zero values given by the set $\{h_1, h_2, \ldots, h_{d_c}\}$. Let H_0 be the binary image of the equivalent code. Set $i = 1$.
2. Consider the modified binary code H_i, build from H_{i-1} and the repetition codes with the same $h^{(i)}$ on all the d_c symbols,
3. Choose $h^{(i)} \in$ GF(q) such that the minimum distance of H_i is maximum. If several values $h^{(i)}$ have the same minimum distance, choose the one with minimum multiplicity,
4. $i = i + 1$, goto step 2).

Table 7 : Optimum values used at the relays for repetition coding

Relay #	1	2	3	4	5	6	7	8

$GF(64)$	α^{26}	α^{41}	α^{52}	α^{6}	α^{56}	α^{17}	α^{50}	α^{11}
$D_{\min}$	8	14	20	25	31	37	43	49
$GF(256)$	α^{15}	α^{165}	α^{71}	α^{150}	α^{128}	α^{122}	α^{113}	α^{104}
$D_{\min}$	10	17	24	32	39	46	54	62

3.4 Performance Evaluation

3.4.1 Cooperation scenario

The performance of the proposed cooperative coding scheme has been assessed by Monte-Carlo simulations under the following scenario. The source broadcasts a NB-LDPC code with $N = 2K$ (rate $K = 1/2$). Each relay decodes the received signal, then computes an exact number of K non-binary repetition symbols, which are sent to the destination. Whether the relays operate in the half-duplex or in the full-duplex mode is out of the scope of this work, however we mention that in our cooperation scenario both modes are possible. We consider that the source and the relays use multicarrier modulation with Orthogonal Frequency-Division Multiplexing (OFDM), and that the different signals, from the source and the relays, can be separated at the destination. This can be done by using different multiple access methods, in which the source and the relays are separated either in time, in frequency, or by using spatial diversity. Finally, we shall further assume that the signals transmitted by the source and the relays use the same QAM modulation, hence $M_{\mathrm{SD}} = M_{\mathrm{R}_i\mathrm{D}}$, and the transmission of the N coded symbols at the source and of the K non-binary repetition symbols at the relays takes the same period of time. Therefore, we assume that the source transmits on two frequency Physical Resource Blocks (PRBs), while each relay transmits on one separate frequency PRB (as a side note, notice that the number of relays is limited by the number of PRBs). In case of Spatial Division Multiple Access (SDMA), relays can transmit in any of the frequency PRB allocated to the source, which ensures an efficient use of the frequency spectrum.

According to the above scenario, the wireless channels can be modeled as block-fading channels, with flat Rayleigh fading, constant on each block and i.i.d. on different blocks [35]. The N coded symbols broadcasted by the source span two fading blocks, while the K repetition symbols transmitted by each relay span exactly one fading-block. Consequently, the number of fading blocks is given by $n_f = 2 + N_r$. For each fading block $j = 1, \ldots, n_f$, the baseband equivalent channel model is given by:

$$y_i^{(j)} = \sqrt{\rho^{(j)}}\, f^{(j)} x_i^{(j)} + z_i^{(j)},$$

where $x_i^{(j)}$ and $y_i^{(j)}$ denote the i^{th} QAM symbol transmitted in block j and the corresponding received symbol, $f^{(j)}$ is the fading coefficient of block j, and $z_i^{(j)} \approx CN(0,1)$ is the i.i.d. circular complex Gaussian noise. We assume that the QAM-constellation has unit energy and that the fading is normalized on each block, *i.e.* $\mathrm{E}\left[\, |f^{(j)}|^2 \right] = 1$. It follows that $\rho^{(j)}$ is the average received SNR on block j, thus, $\rho^{(1)} = \rho^{(2)} = \mathrm{SNR}_{\mathrm{SD}}$ and $\rho^{(2+i)} = \mathrm{SNR}_{\mathrm{R}_i\mathrm{D}}$. We shall assume that $\rho^{(j)}$ and $f^{(j)}$ are perfectly known at the receiver.

For a given set of SNR values $\boldsymbol{\rho} = (\rho^{(1)}, \ldots, \rho^{(n_f)})$, we denote by $I_{\boldsymbol{\rho}}(\mathbf{f})$ the mutual information between channel input and output, assuming that the fading coefficients are given by $\mathbf{f} = (f^{(1)}, \ldots, f^{(n_f)})$ and that the channel input is uniformly distributed over the complex QAM constellation. Hence, $I_{\boldsymbol{\rho}}(\mathbf{f})$ takes values in $[0, m]$, where $m = \log_2(M_{\mathrm{SD}}) = \log_2(M_{\mathrm{R}_i\mathrm{D}})$ is the number of bits per QAM symbol. Let R_d be the *overall coding rate* of the cooperative system, defined as the ratio between the number of information symbols K and the number of non-binary symbols received at the destination both from the source and the relays. According to the previous settings $R_d = 1/n_f$. The *outage probability*, given by:

$$P_{out}(\boldsymbol{\rho}, R_d) = \Pr\left(I_{\boldsymbol{\rho}}(\mathbf{f}) < mR_d \right)$$

is the probability of the instantaneous mutual information $I_{\boldsymbol{\rho}}(\mathbf{f})$ being less than the information rate value mR_d. Since this probability is non-zero, it follows that the Shannon capacity of the channel is 0. As a consequence, the performance of a code over the block fading channel is usually evaluated in terms of the SNR gap to the outage probability [35]. If this gap is maintained constant for arbitrarily large SNR values, the code is said to be *full-diversity*.

3.4.2 Simulation Results

A class of full-diversity LDPC codes over block-fading channels, referred to as *root-LDPC* codes, was proposed in [36]. Since the *N* coded symbols transmitted by the source span two fading blocks, for the NB-LDPC code at the source we chose a rate 1/2 root-NB-LDPC code with (d_v = 2, d_c = 2), defined over GF(64). Namely, the bipartite graph of the NB-LDPC code was designed according to the approach proposed in [36], while the non-zero entries on each row of the parity-check matrix were randomly selected among the four sets of "best rows" given in Table 6. The code has *K* = 50 information symbols, corresponding to 300 information bits.

We consider here the case of 4 relays: R_1, …, R_4. The non-binary symbols transmitted by both the source and the relays are modulated using QPSK modulation. The Frame Error Rate (FER) performance of the root-NB-LDPC code broadcasted by the source is shown in Figure 10, and corresponds to the case when no relay is activated (the right-most curve). Consequently, we shall assume that $\mathrm{SNR}_{\mathrm{SR}_i} > 24$ dB, for each relay R_i, such that the probability that the relay fails decoding the signal broadcasted by the source is less than 10^{-4}.

Moreover, we consider that the links between relays and destination are assumed to be better that the "direct" link (source-to-destination):

$$SNR_{R_1D} = SNR_{SD} + 6 \text{ dB}, \quad SNR_{R_2D} = SNR_{SD} + 4 \text{ dB, and} \quad SNR_{R_3D} = SNR_{R_4D} = SNR_{SD} + 2 \text{ dB.}$$

The *K* symbols transmitted by R_1 and R_3 are non-binary repeated versions of the *K* information symbols, while the *K* symbols transmitted by R_2 and R_4 are non-binary repeated versions of the *K* parity symbols. The non-zero field values used at the relays for repetition coding are chosen according to Table 7. Specifically, R_1 and R_2 use $h^{(1)} = \alpha^{26}$ (together, they send to the destination a first repeated version of the *N* coded symbols), while R_3 and R_4 use $h^{(2)} = \alpha^{41}$ (they send to the destination a second repeated version of the *N* coded symbols).

Figure 10 shows the FER performance of the proposed cooperative coding scheme in case that 1, 2 or 4 relays are activated. For each case, we plotted the corresponding outage probability (dotted curves, asterisk markers) and the FER of the proposed cooperative coding scheme with optimized non-binary repetition coefficients (solid curves, full markers). For comparison purposes, we have also plotted the FER of the proposed cooperative coding scheme with classical repetition coding (same *optimized* NB-LDPC code at the source, but $h^{(1)} = h^{(2)} = 1$ dotted curves, empty markers). It can be seen that the proposed coding scheme achieves full-diversity in every case, hence fully exploiting the spatial diversity brought by the existence of relays. When no relay is activated, the gap between the FER of the NB-LDPC code used at the source and the outage probability is about 1 dB. More important, the non-binary repetition coding proves to be strong enough to maintain the same gap to the outage probability, irrespective of the number of activated relays.

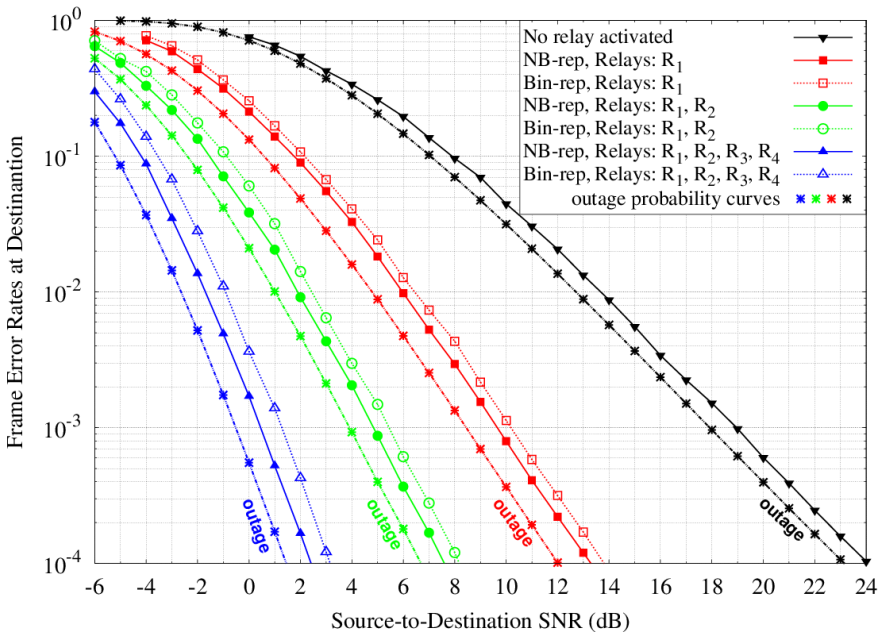

Figure 10 : FER performance of the proposed cooperative coding scheme

3.5 Discussion and Conclusion

We have introduced and optimized a new cooperative coding scheme based on NB-LDPC coding at the source and NB-repetition coding at the relays. For cooperative systems with block-fading wireless channels, we showed that the proposed scheme achieves full diversity, with constant gap to the outage probability of the system, irrespective of the number of relays. Additionally, our scheme is independent of the channel model or of the order of the modulation used for each link in the system, which allows preserving all the advantages shown in this contribution with advanced link-adaptation and channel estimation techniques.

As future work, we will investigate the use of Network-Coding (NC) at the relays, in case that two or more users use the same relays to communicate with the final destination. The use of NC is mainly aimed at reducing the traffic load on the relay-to-destination links, while providing the users with significant diversity gain brought by the use of several relays.

4 LTE-Advanced collaborative relaying

4.1 Scenario: LTE-Advanced collaborative relaying

The use of relay stations in today's and future cellular networks has been proposed as a promising solution to enhance the performance of wireless systems in terms of coverage, throughput, network generalized Degrees-of-Freedom (gDoF) and robustness / diversity.

We consider two collaborative relaying topologies as depicted in Figure 11 and Figure 12, which allow for extensions to LTE-Advanced relaying.

The first scenario in Figure 11 corresponds to the case where two Relay Nodes (RNs) attached to the same Donor eNB (DeNB) can collaborate to cover User Equipments (UEs). We consider Half-Duplex (HD) mode of operation at the RNs, i.e., at any time / frequency instant they cannot simultaneously transmit and receive. Although high performances would be attained by employing Full-Duplex (FD) relays, the HD modeling assumption is at present more practical. This is so because practical restrictions arise when a node can simultaneously transmit and receive, such as for example how well the self-interference can be canceled, making the implementation of FD relays challenging.

The second scenario in Figure 12 is the so-called relay-aided broadcast channel and aims to use a RN in cases where multiple UEs are covered by both the DeNB and the RN. We consider deployment scenarios where the DeNB→RN link operates on the same carrier frequency as the DeNB→UEs links in FD (Inband Relay type 1b). This mode of operation could be made possible by the combination of sophisticated self-interference cancellation techniques and sufficient antenna spacing at the RN between the DeNB→RN receive antenna and RN→UEs transmit antenna.

The key difference between 4G network topologies and this proposal is that in 4G, the RN is constrained to operate in a decode-and-forward fashion without physical-layer cooperation with the DeNB. In our work, we consider deployment scenarios where the RN can operate using decode-and-forward, however with cooperation in the form of joint channel coding through superposition and potentially distributed (virtual) Multiple Input Multiple Output (MIMO) techniques. The second main difference is that in the receivers of RN and UEs we consider sophisticated interference-mitigation techniques which exploit knowledge of the codebooks used at both DeNB and the transmitter of RN.

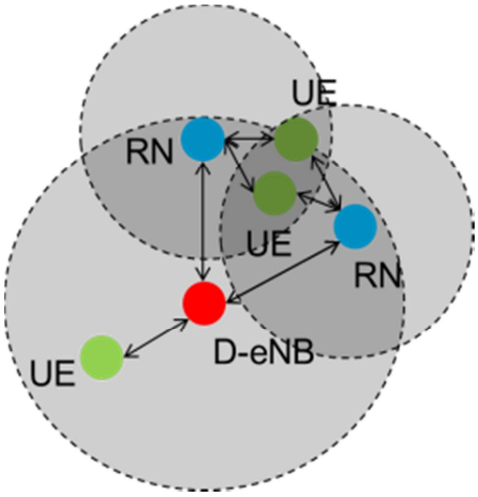

Figure 11: Multiple RN Collaboration Topology.

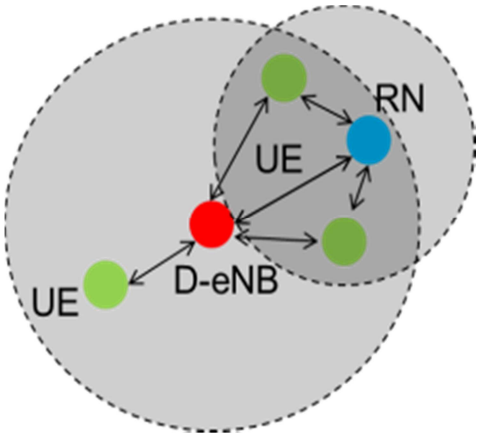

Figure 12: Relay-aided Broadcast Topology.

4.2 Challenges

Regarding the challenges for the LTE-Advanced collaborative-relaying scenario, the main issue is to show the provision of spatial-multiplexing (gDoF [37]) through the use of relays in addition to improved coverage. The latter can be achieved with existing Rel-10/11 relaying techniques. To obtain spatial-multiplexing (gDoF gains), we must make use of physical-layer relaying techniques to perform signal-

level combining at the UE when receiving from either multiple RN (first topology) or jointly from the DeNB and the RN (second topology).

In the first topology in Figure 11, the parallel use of multiple relays should allow for distributed MIMO on the downlink, provided that the DeNB-RN links are of sufficiently high quality. On the uplink, similar distributed spatial-multiplexing should be achievable. It will clearly be more difficult to achieve, however, since the weak links are those between the UEs and the RNs. This would call for techniques where final processing is only performed at the DeNB. For the scenario in Figure 11 we focus on the downlink transmission (from the DeNB to the UEs through the use of RNs). We first propose and evaluate the performance of several relaying schemes, which are proved to be gDoF-optimal and to achieve the network capacity to within a constant gap, universally over all channel gains. We then focus on the relays' schedule, i.e., how much time each relay should spend to listen to the channel and show that HD multi-relay networks have intrinsic properties that allow for simplification of the optimal relay scheduling policy. We finally provide a practical LTE-based implementation of a three-message relay strategy for the case where a single HD RN assists the communication between the DeNB and one UE by also exploiting physical cooperation between the DeNB and the RN to convey information to the UE (the UE is not shadowed from the DeNB).

In the second topology in Figure 12, the RN provides additional spatial-streams in a causal fashion (i.e. in subframes after those where it received the DeNB's signal) and aims to increase the level of spatial-multiplexing (gDoF) offered by the DeNB through multiple transmissions. As for the first scenario, also for this system we focus on the downlink transmission. This type of causal MIMO scenario firstly requires a partial redesign of the MIMO transmission strategy since it is distributed (the DeNB and the RN forms a virtual base station with two antennas provided that the DeNB→RN is of sufficient good quality), and secondly requires more sophisticated UE receivers to optimally combine transmissions from the DeNB and RN corresponding to the same transport block but arriving in different subframes. For the wireless system in Figure 12 we design schemes by combining features of both the relay and broadcast channels.

Using this analysis we are able to study the different regimes of operation of such a network and, in particular, those where distributed spatial multiplexing can occur and those where it cannot.

4.3 Innovation: Coding and collaborative scheduling for multiple-relays

In this section we provide an overview of the relaying schemes designed for the scenario in Figure 11, where HD RNs assist the communication between the DeNB and the UE. The key techniques that should be implemented in such a scenario are the use of distributed spatial-multiplexing and collaborative-scheduling at the RNs. In particular, the framework presented here holds for general HD multi-relay networks where there are $\mathrm{N} \geq 1$ RNs which can exchange information among themselves and where the UE can receive information directly from the DeNB. We refer to this system as a fully-connected HD multi-relay network. The scenario in Figure 11 is a particular case of this more general framework where the $\mathrm{N} = 2$ RNs cannot exchange information among themselves and where the DeNB→UE link is absent. We consider the practically relevant Gaussian noise channel, and we assume Gaussian codebooks at the transmitters of the DeNB and RNs.

For the general HD network with $\mathrm{N} \geq 1$ relay, we conduct a theoretical study, by determining its absolute performance limits (e.g., capacity) through the use of information theoretical tools. The capacity of the HD multi-relay network, i.e., how much information (measured in bits per channel use) can be reliably transmitted from the DeNB to the UE, is not known in general. The currently-known tightest outer bound on the capacity of this system is the max-flow min-cut outer bound, or cut-set for short. With outer bound we refer to a bound which we know to be greater than the actual capacity of the network, but not shown to be achievable through a transmission strategy. Our first main contribution is to show that, no matter the actual values of the channel parameters, the cut-set outer bound is achievable to within a constant gap, i.e., we design a transmission strategy whose achievable rate approximates the capacity (i.e., it is a constant number of bits apart from the cut-set bound universally over all channel gains). The transmission strategy considered is Noisy-Network-Coding (NNC), which is a network generalization of Compress-and-Forward (CF). The main feature of CF is that, differently from Decode-and-Forward (DF), the RN does not attempt to recover the DeNB message, but it just compresses the received signal and then sends it to the UE. The transmission takes place in B time blocks and a block Markov coding scheme is used at the RN, i.e., at the end of each time block the RN outputs a reconstruction of the message sent by the DeNB and sends it to the UE.

In such a network, since each RN can either listen or transmit (each RN operates in HD mode), there are 2^{N} possible listen / transmit configuration states. Thus, if one aims to characterize the capacity of this network, an optimization over all these 2^{N} states has to be performed, in order to find the capacity-achieving one. As N increases, this optimization becomes prohibitively complex. It becomes therefore critical to identify structural properties of HD multi-relay networks for efficient numerical evaluations.

Our second main contribution is to show, through the use of well-known properties on the sub-modularity and linear programming fields, that HD multi-relay networks have indeed intrinsic structural properties which allow for the design of reduced complexity / simple relaying policies.

We finally focus on the Gaussian noise single RN case, i.e., the scenario depicted in Figure 11 with $\mathrm{N} = 1$, where the DeNB can directly communicate with the UE without passing through the RN, i.e., the DeNB→UE link is not absent. For this scenario our contribution is two-fold. We first conduct an information theoretic study by showing that a simple two-phase three-message scheme (which we shall discuss later) as well as more sophisticated coding strategies such as CF and DF, approximately (to within a constant gap) achieve the cut-set outer bound. Two-way coding strategies may also be studied in the same spirit as those for the mesh topology in Section 5. We then provide a practical LTE-based implementation of the simple two-phase three-message strategy, based on Turbo code superposition encoding and interference-aware Successive Interference Cancellation (SIC). The impact of finite block-length and discrete input constellations on the Block Error Rate (BLER) performance is evaluated through extensive simulations on an LTE simulation test bench and compared to the theoretical performance of asymptotically large block-length Gaussian codes. We next describe, see also Figure 13, the two-phase three-message scheme and key functional units of the simulation testbed.

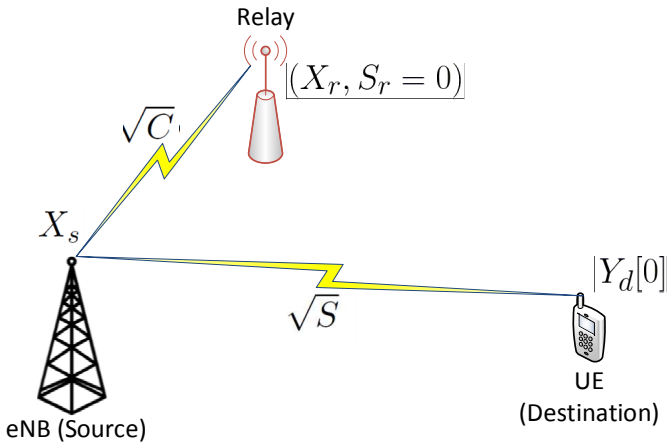

(a) Phase I

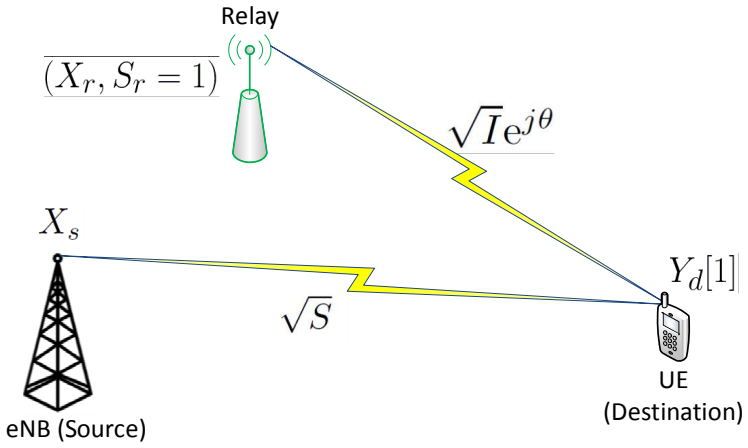

(b) Phase II

Figure 13: Two-phase relay system mode.

The input/output relationship of the channel in Figure 13 is

$$Y_r = \sqrt{C}(1 - S_r)X_s + Z_r \in \mathbb{C},$$
$$Y_d = \sqrt{S}X_s + e^{j\vartheta}\sqrt{I}\,X_r S_r + Z_d \in \mathbb{C},$$

where the channel parameters $(\mathrm{S}, \mathrm{C}, \mathrm{I}, \vartheta)$ are fixed and known to all nodes (full Channel State Information (CSI)), the inputs X_s at the DeNB and X_r at the RN are subject to unitary power constraints, $\mathrm{S_r}$ is the

switch random binary variable which indicates the state of the RN, i.e., when $\mathrm{S_r} = 0$ the RN is listening to the channel while when $\mathrm{S_r} = 1$ the RN is transmitting, and the noises Z_r and Z_d form independent white Gaussian noise processes with zero-mean and unit-variance. We focus here on $\mathrm{C} \geq \mathrm{I} \geq \mathrm{S}$ which, as we shall see later, implies that the RN is able to successfully decode whatever the receiver of the UE decodes. We study a two-phase scheme with four codebooks to transmit three messages. The codes are

$$\mathrm{C}_{a1} = \{X_{a1}^{N_1}(w) : w \in [1 : M_0]\},$$
$$\mathrm{C}_{a2} = \{X_{a2}^{N_2}(w) : w \in [1 : M_0]\},$$
$$\mathrm{C}_{b} = \{X_{b}^{N_1}(w) : w \in [1 : M_1]\},$$
$$\mathrm{C}_{c} = \{X_{c}^{N_2}(w) : w \in [1 : M_2]\}.$$

We focus on the case $\mathrm{N_1} = \mathrm{N_2} = \mathrm{N}$, i.e., we assume an equal resource allocation during the two phases. The two-phase three-message scheme, employs superposition encoding at the transmitter of the DeNB, SIC both at the receivers of the RN and of the UE, and DF at the RN. We now describe the two phases (each of duration N) of the proposed transmission strategy.

Phase 1: During this phase the RN is listening, i.e., $S_r = 0$, and the transmitted signals are

$$X_s^N[1] = \sqrt{1-\delta}\,X_b^N(w_1) + \sqrt{\delta}\,X_{a1}^N(w_0),$$
$$X_r^N[1] = 0^N,$$

where $\delta \in [0,1]$ is a scaling parameter that allows for superposition, and the received signals are

$$Y_d^N[1] = \sqrt{S(1-\delta)}\,X_b^N(w_1) + \sqrt{S\delta}\,X_{a1}^N(w_0) + Z_d^N[1],$$
$$Y_r^N[1] = \sqrt{C(1-\delta)}\,X_b^N(w_1) + \sqrt{C\delta}\,X_{a1}^N(w_0) + Z_r^N[1].$$

The RN first decodes $\mathrm{w_1}$ from $\mathrm{Y_r^N}[1]$ and outputs the estimate $\widehat{\mathrm{w}}_1^{(\mathrm{r})} \in [1 : \mathrm{M_1}]$. The RN then decodes $\mathrm{w_0}$ from $\mathrm{Y_r^N}[1] - \sqrt{\mathrm{C}(1-\delta)}\,\mathrm{X_b^N}\left(\widehat{\mathrm{w}}_1^{(\mathrm{r})}\right)$ and outputs the estimate $\widehat{\mathrm{w}}_0^{(\mathrm{r})} \in [1 : \mathrm{M_0}]$. The UE decodes $\mathrm{w_1}$ from $\mathrm{Y_d^N}[1]$ and outputs the estimate $\widehat{\mathrm{w}}_1^{(\mathrm{d})} \in [1 : \mathrm{M_1}]$.

Phase 2: During this phase the RN is transmitting, i.e., $S_r = 1$, and the transmitted signals are

$$X_s^N[2] = X_c^N(w_2),$$
$$X_r^N[2] = X_{a2}^N\left(\widehat{w}_0^{(r)}\right),$$

where X_{a2}^N is a different redundancy version of X_{a1}^N transmitted by the DeNB in Phase I. The received signals are

$$Y_d^N[2] = \sqrt{S}X_c^N(w_2) + \sqrt{I}\,e^{j\vartheta}\,X_{a2}^N\left(\widehat{w}_0^{(r)}\right) + Z_d^N[2],$$

The UE forms the aggregate received signal

$$Y_d^{2N} = \begin{bmatrix} Y_d^N[1] - \sqrt{S(1-\delta)}\,X_b^N\left(\widehat{w}_1^{(d)}\right) \\ Y_d^N[2] \end{bmatrix}$$

and first decodes w_0 from Y_d^{2N} by assuming that all decoding operations in Phase I were successful and outputs the estimate $\widehat{w}_0^{(d)} \in [1 : M_0]$ (note that both observations in Y_d^{2N} are used to output the estimate $\widehat{w}_0^{(d)}$). We assume that a perfect error detection mechanism, such as the Cyclic Redundancy Check (CRC), is employed at the decoders. The UE finally decodes w_2 from $Y_d^N[2] - \sqrt{I}\,e^{j\vartheta}\,X_{a2}^N\left(\widehat{w}_0^{(r)}\right)$ and outputs the estimate $\widehat{w}_2^{(d)} \in [1 : M_2]$.

Error analysis: Since we assume $C \geq I \geq S$, we focus now on the error analysis at the receiver of the UE, by assuming that all the decoding operations at the RN in Phase I were successful. Since we are exploiting SIC in the decoding operation, we need to understand the performance of codes C_{a1}, C_{a2} and C_b in non-Gaussian noise (C_b in the first decoding step in Phase I and C_{a1}, C_{a2} in the first decoding step in Phase II) and the performance of code C_c in Gaussian noise (second decoding operation in Phase II when no error propagation). In the decoding stages where a message is treated as noise, we develop a decoder that specially accounts for the fact that the overall noise is non-Gaussian. We will consider different choices for the codebooks (C_{a1}, C_{a2}, C_b, C_c). For each choice, we make sure that in all the decoding stages we have a BLER below a given threshold.

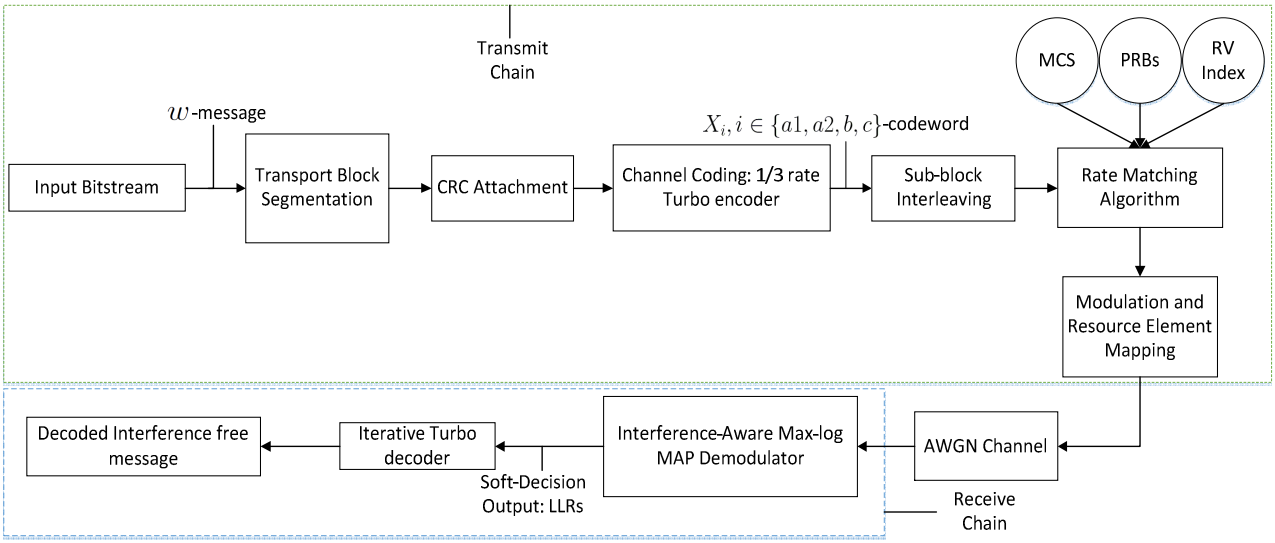

Figure 14: Overall simulation block diagram.

In order to evaluate the performance of the above two-phase three-message strategy with practical codes, we develop a simulation testbed using the OpenAirInterface (OAI) [38](a platform for wireless communication experimentation) software libraries. The software platform is based on 3GPP's evolving standard of LTE that is closely aligned with the standards in commercially deployed networks. The simulations were carried out on the Downlink Shared Channel (DL-SCH), which is the primary channel for transmitting user-data (or control information) from the DeNB to the UE. The data messages are transported in units known as Transport Blocks (TBs) to convey the messages w_0, w_1 and w_2. The TB Size (TBS) depends on the choice of the Modulation and Coding Scheme (MCS), which describes the modulation order and the coding rate of a particular transmission. The key functional units of our system are shown in Figure 14, which we now describe in details.

1) **TB Processing**. The TBs undergo a series of processing stages prior to modulation before the codeword can be mapped onto the Resource Elements (REs) in the Physical DL-SC (PDSCH). The different stages involved to obtain the desired codeword are shown in Figure 14. Error detection at the receiver is enabled by appending 24 CRC bits to the TB. The subsequent bit sequence is then fed into the 1/3 rate Turbo encoder.

2) **Channel Coding**. The channel coding scheme is composed of a 1/3 rate Turbo encoder, which follows the structure of a parallel concatenated convolutional code with two 8-state constituent encoders, and one Turbo code internal interleaver. A single set of systematic bits and two sets of parity bits are produced at the output of the encoder. The systematic bits and the two sets of parity bits are passed through separate block interleavers.

3) **Rate Matching**. The rate matching component ensures, through puncturing or repetition of the bits, that the output bits from the Turbo encoder match the available physical resources using the MCS, the Redundancy Version (RV) index [39] and the Physical Resource Blocks (PRBs). For the numerical evaluations, an equal bandwidth allocation is chosen between the two phases of the relay strategy, i.e., the number of PRBs allocated in the first (RN listening) and second (RN transmitting) phases is the same. The message w_0, transmitted by the DeNB and the RN over the two phases, corresponds to two different RVs with equal resource allocations. The Circular Buffer (CB) generates puncturing patterns depending on the allocated resources, and the sub-block interleaver facilitates the puncturing of the three outputs of the encoder. Furthermore, the code block is concatenated if segmentation was required prior to channel coding.

4) **Modulation and REs Mapping**. During this stage, complex-valued symbols are generated according to the chosen modulation scheme supported in LTE. However, in this study we only use QPSK as it is assumed that the channel quality between the RN and the UE is not much better than that of the DeNB→UE link. Note that when the RN-UE link is significantly stronger than the DeNB→UE link, a better performance / higher spectral efficiency may be attained with higher modulation schemes at the RN. The complex-valued symbols are then mapped to the antenna ports for transmission on the PDSCH.

5) **Demodulator**. The demodulator is composed of an interference-aware (of the finite constellation) receiver designed to be a low-complexity version of the max-log MAP detector.

The main idea is to decouple the real and imaginary components through a simplified bit-metric using the Matched Filter (MF) output and thus reduce the search space by one complex dimension [40]. As a result, it is possible to decode the required codeword in the presence of an interfering codeword of the same (or different) modulation scheme. Thereafter, it is possible to strip out the decoded signal from the received signal and then decode the remaining signal (in an interference-free channel in case of no error propagation). The generated Log-Likelihood Ratios (LLRs) are soft-combined in decoding w_0 at the destination at the end of Phase II.

4.4 Results for the collaborative relaying strategy

This section aims to highlight and describe our main results on the Gaussian HD multi-relay network, a wireless system where a DeNB can communicate with a UE through N RNs, which operate in Time Division Duplexing (TDD), i.e., at each time instant a RN can either be listening to the channel or transmitting. The information theory based proofs are here omitted and can be found in [41]-[47].

Our first main result gives a capacity guarantee for this network, namely it states that, no matter the actual values of the system parameters (e.g., channel gains, power constraints at the DeNB and at the RNs), the capacity is achievable to within a constant number of bits. More formally, let C (measured in bits per channel use) be the capacity of the Gaussian HD multi-relay network, whose knowledge is still an open problem. If we can find an outer bound R^{out} (measured in bits per channel use) on C (i.e., such that $C \leq R^{out}$ always holds) and a transmission scheme, which achieves a rate R^{in} (measured in bits per channel use), and if we can show that $R^{out} - R^{in} \leq GAP$ bits, where GAP is a constant which might depend on the number of RNs N, but not on the values of the channel parameters, then we can claim we know the capacity C of the network to within GAP bits, universally over all possible system parameters. The following theorem states our main result, whose formal proof can be found in [42].

Theorem 1. The cut-set outer bound R^{out} for the Gaussian HD relay network with N RNs is achievable by Noisy Network Coding (NNC) – a network generalization of CF – to within $GAP \leq 1.96\,(N+2)$ bits, uniformly over all channel gains.

It is worth noting that our gap result in Theorem 1 improves on previously gap results available in the literature, like for example the one in [50] of $8(N+2)$ bits. However, while giving a capacity guarantee that is valid universally, the gap result in Theorem 1 is linear in the number of RNs (N), i.e., as the number of RNs increases the gap might become too big. Designing transmission strategies seeking to reduce the gap, for example from linear in N to logarithmic in N, is an important open problem which is object of our current investigation.

In general, finding the capacity of a Gaussian HD-multi-relay network is a combinatorial problem since the cut-set outer bound (shown to be achievable to within a constant gap in Theorem 1) is the minimum between 2^N bounds (one for each possible cut in the network), each of which is a linear combination of 2^N RN states (since each RN can either listen or transmit). Consider for example the case of $N = 2$; in this setting, in order to evaluate the cut-set outer bound, we have to consider $2^2 = 4$ possible cuts of the network (both RNs are in the cut of the DeNB, both RNs are in the cut of the UE and one RN is in the cut of the DeNB and the other in the cut of the UE (here we have 2 possibilities)), each of which is a linear combination of $2^2 = 4$ possible listen / transmit configuration states (both RNs are transmitting, both RNs are listening and one RN is listening while the other is transmitting (here we have two possibilities)). Thus, as the number of RNs (N) increases, optimizing the cut-set outer bound becomes prohibitively complex. Identifying structural properties of the cut-set upper bound is therefore critical for efficient numerical evaluations and might have important practical consequences for the design of reduced complexity / simple relaying policies**. Our second main result**, whose formal proof can be found in [47], shows that Gaussian HD multi-relay networks have indeed intrinsic structural properties which allow for simplification in the design. In particular, we first numerically observed the result in Figure 15. In the following we refer to active states as those, among the 2^N possible ones, which have a strictly positive probability to occur. Again, consider the case of $N = 2$; if, for example, we are able to prove that the state when both RNs are always listening never occurs (i.e., it has a zero probability) without loss of optimality (i.e., the result in Theorem 1 still holds), then we can assert that there are only 3, out of the possible $2^2 = 4$, active states (with a strictly positive probability).

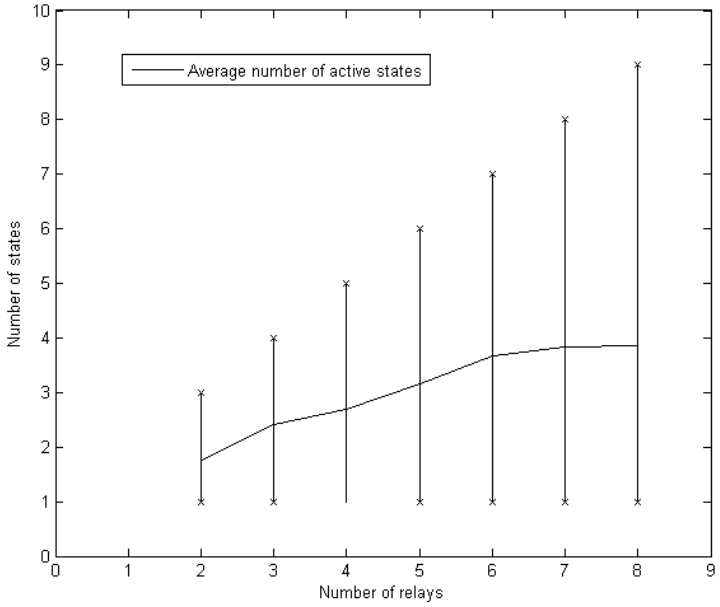

Figure 15: Average, minimum and maximum number of active states to characterize the capacity of a Gaussian HD multi-relay network.

Figure 15 shows the number of active states (y-axis) versus the number of RNs N (x-axis), for $2 \leq N \leq 8$ (the details of how the extensive numerical evaluation was run can be found in [41] and [42]). From Figure 15 we observe a nice result, i.e., the maximum number of active states, out of the possible 2^N, is always $N+1$. Motivated by the encouraging numerical result in Figure 15 (namely at most $N+1$, out of the possible 2^N, appear to have a strictly positive probability to occur), we seek to prove that this result is indeed true without loss of optimality for any value of N. Our main result, whose formal proof can be found in [47], is stated in the following theorem, where with schedule we refer to the vector containing the probability with which each of the 2^N possible states occurs.

Theorem 2. For Gaussian HD wireless networks with N RNs, the approximately optimal schedule (i.e., for which the result in Theorem 1 still holds) has at most $N+1$ non-zero entries / active states.

The key idea to prove the result in Theorem 2 is to use the Lovász extension [49] and the greedy algorithm for submodular polyhedra to highlight structural properties of the minimum of a submodular function. Then, by using the saddle-point property of min-max problems and the existence of optimal basic feasible solutions for linear programs, an (approximately) optimal relay policy with the claimed number of active states can be shown. The result in Theorem 2 is really encouraging since it implies a reduction of the complexity of a combinatorial problem (i.e., from exponential complexity in N to linear complexity in N). In other words, the reduction of the number of active states from exponential to linear, as stated in Theorem 2, offers a simpler and more amenable way to design the network, while still achieving a performance guarantee (i.e., capacity to within a constant gap in Theorem 1) and shows that Gaussian HD multi-relay networks have intrinsic structural properties irrespectively of their topology.

We now focus on the Gaussian HD single (i.e., $N=1$) relay network, where the communication from the DeNB to the UE is assisted by one HD RN. We consider the case where the DeNB can potentially directly communicate with the UE, without exploiting the RN, i.e., we exploit physical cooperation between the DeNB and the RN. We start by giving some information theoretical results and then we evaluate a simple two-phase three-message transmission strategy by using practical codes. The following theorem states our main result, whose formal proof can be found in [45].

Theorem 3. The cut-set outer bound R^{out} for the Gaussian HD relay channel is achievable to within:

1) $\mathrm{GAP}^{\mathrm{PD\&F}} \leq 1$ bit, by using Partial DF (PD&F) as transmission strategy; the PD&F strategy requires that the RN, at each time instant, decodes part of the information sent by the DeNB, re-encodes it and sends it to the UE in the next time slot;
2) $\mathrm{GAP}^{\mathrm{CF}} \leq 1.61$ bits, by using CF as transmission strategy;
3) $\mathrm{GAP}^{\mathrm{LDA}} \leq 3$ bits, by using the two-phase three-message scheme described in Section 4.3.

It is worth noting that $GAP^{\mathrm{CF}} \leq 1.61$ bits is smaller than the gap result in Theorem 1 of 5.88 bits (i.e., $1.96 \cdot 3$). As already highlighted before, NNC is a network generalization of CF, and in the single RN case

the two transmission strategies coincide. The smaller gap result is due to the fact that the bounding steps in the special case of $N = 1$ are tighter than those we used to prove Theorem 1 for a general Gaussian HD network with N RNs. The result in Theorem 3 gives also a capacity guarantee for the Gaussian HD relay channel when PD&F is employed at the RN. The reason why we evaluated also the performance of this strategy is that it is well-known that under certain channel conditions PD&F outperforms CF. In particular, CF achievable rate outperforms the one achieved by DF when the DeNB→RN link is weaker than the DeNB→UE link or when the RN→UE link is sufficiently strong. In other regimes PD&F outperforms CF. Moreover, in addition to CF and PD&F, we also designed a simple two-phase three-message transmission strategy, which is described in Section 4.3. We now point out some important features of this latter scheme which make it appealing for practical implementation:

1) The proposed scheme is not the classical block Markov encoding scheme with backward decoding; in particular, the receiver of the UE uses sliding window decoding, which simplifies the decoding procedure and incurs no delay.

2) The receiver of the UE uses successive decoding, which is simpler than joint decoding.

3) No power allocation is applied at the transmitters of the DeNB and of the RN across the two phases; this simplifies the encoding procedure and can be used for time-varying channels as well. The transmitter of DeNB uses superposition coding, i.e., power split, only to 'route' part of its data through the RN.

It is clear from the above comments that the two-phase three-message proposed scheme is simpler with respect to DF and CF strategies both in the encoding and decoding procedures. Note in fact that in the original DF and CF strategies, the receiver performs backward decoding, i.e., decoding at the receiver is done backwards after all blocks are received, which is more complex than SIC. However, as can be observed from the result in Theorem 3, the gap attained by this scheme is larger than that of PD&F and CF, thereby pointing to an interesting practical tradeoff between gap to capacity and complexity.

In [45], we also numerically evaluated and compared the performance of these three transmission strategies under two different RN's switching policies, namely the case of *deterministic* / fixed switch and the case of *random* switch. We refer to *deterministic* switch, when each node in the network (i.e., the DeNB and the UE) is aware of the activity (either listening or transmitting) of the RN. On the other hand, we refer to *random* switch, when the DeNB and the UE are unaware of the activity of the RN. In this case, from an information theory point of view, further information can be conveyed from the RN to the UE through the random switch. In particular, since when $N = 1$, we have $2^1 = 2$ possible listen / transmission configuration states at the RN, the maximum amount of information that can be conveyed from the RN to the UE through the random switch is of $\log_2 2 = 1$ bit per channel use (note that, in a practical system, this operation requires a signal detector for each channel use). In other words, a transmission strategy (e.g., PD&F) employed with random switch can outperform the same strategy implemented with deterministic switch for at most 1 bit per channel use. It is clear that there exist channel conditions for which a random switch does not bring gains compared to deterministic switch. Imagine for example a scenario where the RN is not exploited to route the information from the DeNB to the UE, i.e., the DeNB directly conveys the message to the UE. In such a system, since the RN is not used, the consequent achievable point-to-point rate is independent on the switch. However, in practical scenarios, the RN is placed in a way to experience high-quality transmission from the DeNB, in order to bring gains with respect to point-to-point transmission between the DeNB and the UE. Thus, it becomes critical to understand how to properly exploit the randomness that lies inside the switch in order to achieve higher (at most 1 bit per channel use) rates. The investigation of such a problem is open and it is object of our ongoing research.

Seen the appealing low-complexity, both in the encoding and decoding procedures, of the two-phase three-message strategy described in Section 4.3, we now numerically access its performance by using practical codes. We remark that the results presented in what follows consider single-antenna nodes in order to compare the practical results with the theoretical ones, but they can be straightforwardly extended to multi-antenna nodes, as supported by the LTE standard. We assume that the transmission bandwidth is of 5 MHz (25 PRBs). For all the decoding operations in Phases I and II (described in Section 4.3), the BLER performance at the UE is evaluated for different values of S (i.e., strength of the DeNB→UE link). For Phase I, the BLER performance of $\mathbf{w_1}$ is shown in Figure 16(a) for MCS values ranging in the interval $[0{:}9]$ (QPSK). For Phase II, the BLER performance of $\mathbf{w_0}$ is shown in Figure 16(b) and Figure 16(c), by using the LLRs of the two phases. Two ratios of I/S are examined, namely 0 dB in Figure 16(b) and 5 dB in Figure 16(c). It is worth noting that in our model, the RN→UE link is assumed to be stronger than the DeNB→UE link so that using the RN indeed boosts the rate performance with respect to direct transmission and, at the same time, motivates our choice of same (QPSK) modulation both at the DeNB and at the RN. We remark here that, for larger I/S ratios, it could be advantageous to

use a higher modulation scheme (such as 16 QAM) at the RN in order to fully exploit the higher quality of the RN→UE link. Finally, Figure 16(d) shows the BLER performance of $\mathbf{w_2}$ at the end of Phase II.

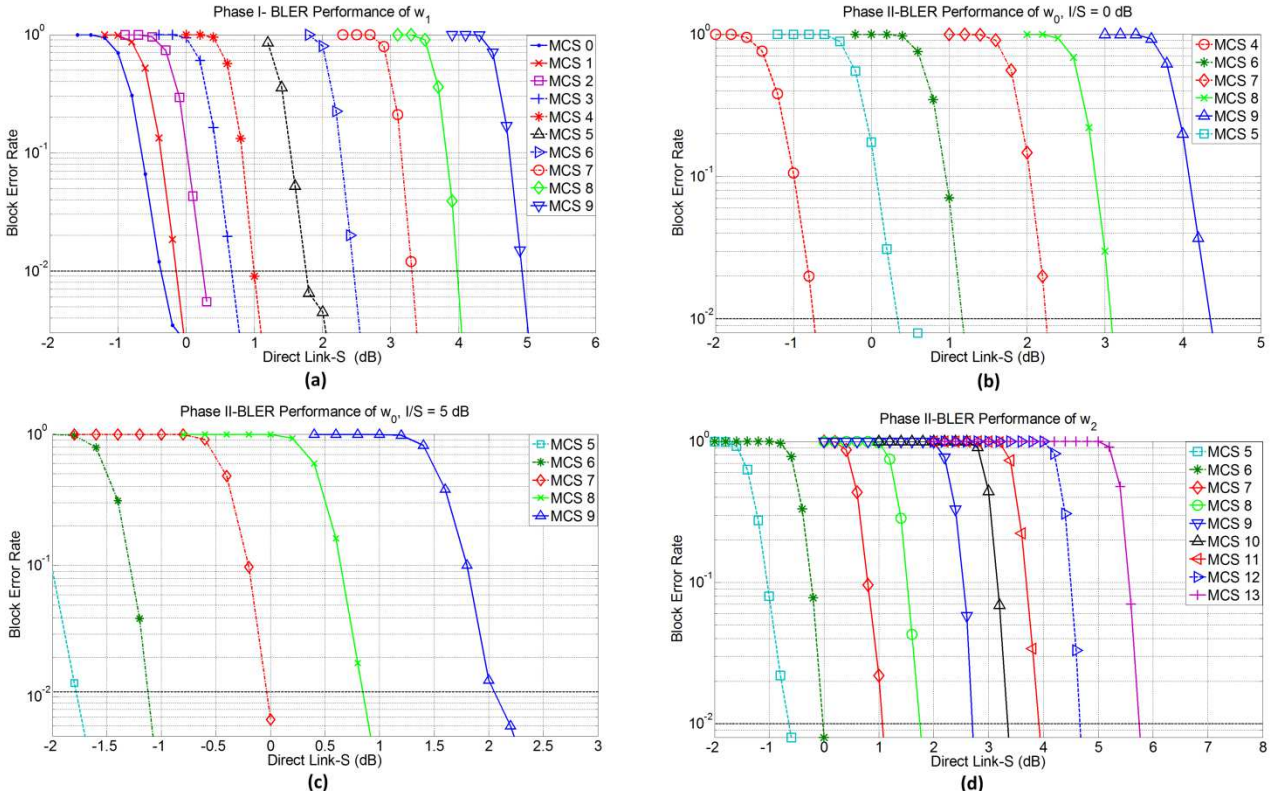

Figure 16: BLER performances of $\boldsymbol{w_0}$, $\boldsymbol{w_1}$ and $\boldsymbol{w_2}$ versus different strengths of the DeNB→UE link.

The results in Figure 16, Table 8 ($\mathrm{I/S} = 0$ dB) and Table 9 ($\mathrm{I/S} = 5$ dB) were generated as follows. From Figure 16(a), we considered a BLER = 10^{-2} and, for each value of the MCS of $\mathrm{X_b}$ (first column of Table 8 and Table 9), we selected the corresponding value of S (second column of Table 8 and Table 9). Thereafter, for each value of the ratio $\mathrm{I/S}$, we selected the MCS of $(\mathrm{X_{a1}}, \mathrm{X_{a2}})$ which, for each value of S (second column of Table 8 and Table 9), allowed to achieve a BLER$\leq 10^{-2}$. These MCS values are reported in the fourth column of Table 8 and Table 9. Similarly, we proceeded for selecting the MCS of $\mathrm{X_c}$ (sixth column of Table 8 and Table 9). The TBSs of each MCS (at the DeNB and at the RN), based on the LTE standard, are also reported in Table 8 and Table 9. In order to compare the achieved spectral efficiency with the theoretical rate (eighth column of Table 8 and Table 9), we firstly computed the value of C (strength of the DeNB-RN link), by reversing eq.(42) in [45] with $\gamma = 0.5$. Note that $\gamma \in [0,1]$ represents the fraction of time (normalized to one without loss of generality) the RN listens to the channel; thus if $\gamma = 0$, then the RN is always listening and if $\gamma = 1$, the RN is always transmitting. Since we assume an equal resource allocation during the two phases (i.e., listen and transmit), we set $\gamma = 0.5$. Finally, we used the values of $(\mathrm{S}, \mathrm{I}, \mathrm{C})$ and computed eq.(37) in [45]. The total rate R (ninth column of Table 8 and Table 9) was determined by using only the number of soft-bits (G-useful information bits), and ignoring the overhead bits, such as pilots used for channel estimation, as follows:

$$R = \frac{TBS\,(X_b) + TBS\,(X_{a1}, X_{a2}) + TBS\,(X_c)}{\left(\frac{G_1}{Q_{mod1}} + \frac{G_2}{Q_{mod2}}\right)},$$

where $\mathrm{G_1}$ is the number of soft-bits utilized to decode $(\mathrm{X_b}, \mathrm{X_{a1}})$ and $\mathrm{G_2}$ to decode $(\mathrm{X_{a2}}, \mathrm{X_c})$, and where $\mathrm{Q_{mod1}}$ and $\mathrm{Q_{mod2}}$ are the corresponding modulation orders (here equal to 2 since we use QPSK both at the DeNB and at the RN). Although here not presented, it can be easily checked that the BLER performance of $\mathrm{w_0}$ and $\mathrm{w_1}$ at the RN is always less than 10^{-2}, implying that the RN capabilities are superior than those of the UE (since we are assuming $\mathrm{C} \geq \mathrm{I} \geq \mathrm{S}$). Finally, for comparisons, we also considered a Baseline Scheme (last two columns of Table 8 and Table 9), which mimics relay models used in today's networks, where the UE does not have a direct connection with the DeNB, i.e., the DeNB -UE link is absent and the DeNB can communicate with the UE only through the RN.

From Table 8 and Table 9, the maximum difference between the theoretical rate in [45] and the achieved rate by the proposed scheme is of 0.458 bits/dim when $\mathrm{I/S} = 0$ dB and of 0.681 bits/dim when

5 dB. The rate gap between theory and practice can be mostly attributed to two key factors: (i) the TBs used are of finite length (see Table 8 and Table 9), differently from the theoretical assumption of infinite block length and (ii) the channel inputs are drawn from a discrete constellation (QPSK), rather than from Gaussian codebooks as assumed in the theoretical analysis. Furthermore, the fact that the difference is higher when $I/S = 5$ dB than when $I/S = 0$ dB is due to the fact that when the ratio I/S increases it becomes more critical to choose higher MCS values for the RN in order to fully exploit the strength of the RN→UE link. We also remark that the difference between theoretical and practical rates might be decreased by tuning the parameters δ (superposition factor) and γ (fraction of time the RN listens to the channel) in the interval [0,1], instead of considering them as fixed values.

From Table 8 and Table 9, we also notice that the maximum difference between the practical and the baseline scheme rates is of 1.33 bits/dim (factor of 2) and of 0.667 bits/dim (factor of 1.2), respectively. The fact that the difference is higher when $I/S = 0$ dB than when $I/S = 5$ dB is due to the fact that when the ratio I/S is small, the presence of the DeNB→UE link plays a significant role in the rate performance.

Table 8: MCS Relay matting for each decoding operation with I/S = 0 dB

Phase I - X_b			**Phase II - (X_{a1}, X_{a2})**		**Phase II - X_c**		**Theoretical**	**Practical**	**Theoretical BLS**	**Practical BLS**
MCS	S [dB]	TBS [bits]	MCS	TBS [bits]	MCS	TBS [bits]	Rate [bits/dim]	Rate [bits/dim]	Rate [bits/dim]	Rate [bits/dim]
0	-0.370	680	4	1800	5	2216	1.222	0.764	0.607	0.351
1	-0.145	904	4	1800	6	2600	1.265	0.862	0.629	0.413
2	0.242	1096	5	2216	6	2600	1.326	0.961	0.669	0.413
3	0.665	1416	5	2216	7	3112	1.425	1.100	0.714	0.494
4	0.992	1800	6	2600	7	3112	1.494	1.220	0.750	0.494
5	1.7588	2216	6	2600	8	3496	1.661	1.350	0.838	0.555
6	2.4535	2600	7	3112	9	4008	1.820	1.580	0.922	0.636
7	3.3115	3112	8	3496	10	4392	2.028	1.790	1.033	0.697
8	3.9743	3496	9	4008	11	4968	2.195	2.030	1.122	0.789
9	4.930	4008	9	4008	12	5736	2.446	2.240	1.254	0.910

Table 9: MCS Relay matting for each decoding operation with I/S = 5 dB

Phase I - X_b			**Phase II - (X_{a1}, X_{a2})**		**Phase II - X_c**		**Theoretical**	**Practical**	**Theoretical BLS**	**Practical BLS**
MCS	S [dB]	TBS [bits]	MCS	TBS [bits]	MCS	TBS [bits]	Rate [bits/dim]	Rate [bits/dim]	Rate [bits/dim]	Rate [bits/dim]
0	-0.370	680	7	3112	5	2216	1.605	0.98	1.125	0.788
1	-0.145	904	7	3112	6	2600	1.653	1.08	1.157	0.910
2	0.242	1096	7	3112	6	2600	1.737	1.11	1.211	0.910
3	0.665	1416	8	3496	7	3112	1.832	1.30	1.273	1.025
4	0.992	1800	8	3496	7	3112	1.907	1.37	1.321	1.025
5	1.7588	2216	9	4008	8	3496	2.088	1.58	1.435	1.147
6	2.4535	2600	9	4008	9	4008	2.261	1.73	1.541	1.228
7	3.3115	3112	9	4008	10	4392	2.482	1.87	1.676	1.267
8	3.9743	3496	9	4008	11	4968	2.658	2.03	1.780	1.451
9	4.930	4008	9	4008	12	5736	2.921	2.24	1.933	1.573

4.5 Discussion and conclusion

We analyzed a wireless network where a DeNB communicates with a UE across a Gaussian channel and is assisted by N RNs operating in HD mode. The capacity of this network was characterized to within a constant gap (uniformly over all possible choices of channel gains) by using NNC as achievable scheme. For such networks, the capacity achieving scheme must be optimized over the 2^N possible listen/transmit configurations. It was formally proved that the approximately optimal (achieving the cut-set outer bound to within a constant gap) schedule has at most $N+1$ active states (i.e., with a strictly positive probability).

We then consider the particular case of $N = 1$, by showing three schemes, namely PD&F, CF and a two-phase three-message strategy, that achieve the cut-set upper bound on the capacity to within a constant finite gap, uniformly for all channel parameters and by pointing out an interesting practical tradeoff between the coding scheme complexity and the gap, with lower gaps for more complex schemes. We discussed both the case of deterministic and random switch at the RN, by showing that, in general, random switch increases the achievable rate at the expense of more complex coding and decoding schemes.

We finally evaluated the two-phase three-message strategy by using codes as in the LTE standard and by running simulations on an LTE test bench. This scheme uses superposition encoding, DF relaying and SIC in order to send three messages in two time slots from a DeNB to a UE with the help of a RN (which forwards one of the three messages). Comparisons between the theoretical achievable rate with (point-to-point capacity achieving) Gaussian codes and the rate achieved in a practical scenario were provided for a BLER of 10^{-2}. In addition, a baseline scheme was also considered where the DeNB-UE link is absent. The rate performance of this scheme, which mimics the one implemented in today's wireless networks, was shown to be inferior to that of the proposed scheme, implying that physical layer cooperation brings throughput gains.

4.6 Innovation: Collaborative Coding for relay-aided broadcast

In this section we provide an overview of our approach and of the relaying schemes used to analyze the performance of the scenario in Figure 12. Our approach is to investigate the ultimate information theoretical performance of this wireless system, by leveraging features and schemes of both the broadcast and relay channels.

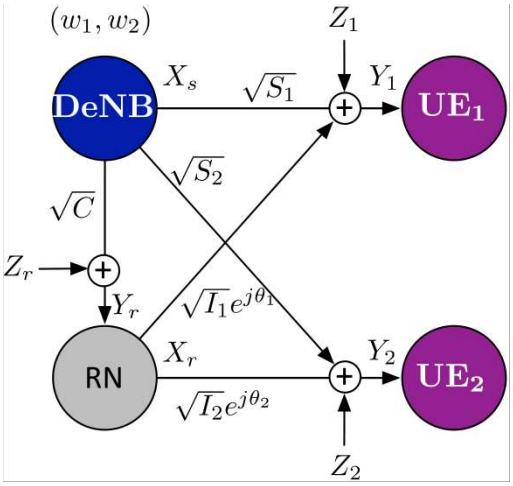

Figure 17: The relay-aided broadcast channel

We will first analyze the wireless scenario in Figure 17, where a DeNB aims to convey a different message to each UE, i.e., w_1 to UE1 and w_2 to UE2, through a Gaussian noise channel. The information arrives at the DeNB for all UEj, with $j \in \{1,2\}$, and the RN is used in a causal fashion to assist the transmission to the UEs. All the nodes are assumed to be equipped with a single antenna. Deployment scenarios where the RN operates in FD mode are considered. The focus will be on the sum-capacity / throughput of this network. The sum-capacity is defined as $R_\Sigma = \{\max(\sum_{j=1}^{2} R_j)\}$, where the maximization is intended over all possible achievable rate pairs (R_1, R_2).

The input/output relationship of the channel in Figure 17 reads

$$\begin{bmatrix} Y_1 \\ Y_2 \\ Y_r \end{bmatrix} = \begin{bmatrix} \sqrt{S_1} & \sqrt{I_1}e^{j\vartheta_1} \\ \sqrt{S_2} & \sqrt{I_2}e^{j\vartheta_2} \\ \sqrt{C} & \star \end{bmatrix} \begin{bmatrix} X_s \\ X_r \end{bmatrix} + \begin{bmatrix} Z_1 \\ Z_2 \\ Z_r \end{bmatrix},$$

where: the channel inputs are subject, without loss of generality, to the average power constraint $\mathbb{E}\left[|X_j|^2\right] \leq 1,\ j \in \{r,s\}$ (i.e., non-unitary power constraints can be incorporated into the channel gains), a $\star$ in the channel transfer matrix indicates the channel gain that does not affect the capacity region (because the RN can remove X_r from Y_r), the channel parameters $(C, S_1, S_2, I_1, I_2, \vartheta_1, \vartheta_2)$ are fixed and therefore known to all nodes, and the noises are independent proper-complex Gaussian random variables with, without loss of generality, zero-mean and unit variance. Some of the channel gains can be taken to be real-valued and non-negative because a node can compensate for the phase of one of its channel gains.

An often adopted figure of merit for the Gaussian channel is the gDoF, or "sum-capacity pre-log" which, is an asymptotic performance measure in the high-SNR regime and refines the classical DoF metric since it captures the fact that, in wireless networks, the channel gains can differ by several orders of

magnitude. The gDoF is defined as follows. For some $\mathrm{SNR} \geq 0$ and for some non-negative $(\delta, \alpha_i, \beta_i)$ with $i \in \{1,2\}$, consider the channel parameterization

$$S_i = \mathrm{SNR}^{\alpha_i},\ I_i = \mathrm{SNR}^{\beta_i}, C = \mathrm{SNR}^{\delta},$$

where α_1 and α_2 measure the strength of the direct links powers in dB, β_1 and β_2 measure the strength of the cross links powers in dB and δ measures the strength of the cooperation link power in dB. The gDoF is defined as [37]

$$d := \lim_{\mathrm{SNR}\to\infty} \frac{R_\Sigma}{\log(1+\mathrm{SNR})}.$$

With the above parameterization, in the next section, we will analyze the different operating regimes depending on the values of $(\alpha_i, \beta_i, \delta), i \in \{1,2\}$, by highlighting the regimes in which the use of the RN brings gDoF gains compared to the classical broadcast channel (where the DeNB directly transmits the messages to the UEs without the use of the RN) and the regimes where serving just one UE is (approximately) optimal for maximizing the throughput. This study will shed light on how strong the DeNB→RN should be, such that the DeNB and the RN might behave as a single 'virtual' base station with 2 antennas. In other words, this study will give interesting insights on how this link should be dimensioned in order that the system behaves like a MIMO broadcast channel with 2 transmit antennas and 2 single-antenna UEs.

Based on the above parameterization, we will then analyze a more general channel, where a number K of UEs (notice that in Figure 17 we have $K = 2$) has to be served by the DeNB, with the help of the RN. In this case the k-th, $k \in [1:K]$, UE has output

$$Y_k = \sqrt{SNR^{\alpha_k}} X_s + \sqrt{SNR^{\beta_k}} e^{j\vartheta_k} X_r + Z_k,$$

and the RN has output

$$Y_r = \sqrt{SNR^{\delta}} X_s + Z_r.$$

For this scenario, we will propose a polynomial-time algorithm which selects at most the 2 'best' UEs, among the K possible ones, to serve. In the next section, we will clearly define which are the 'best' 2 UEs to serve in order to attain the gDoF. We will see that this choice depends on the values of the channel parameters; understanding this dependence will shed light on how to smartly manage and schedule the different available resources in the network.

4.7 Results

This section aims to describe our main results on the relay-aided broadcast channel where the communication between a DeNB and a number *K* of UEs is assisted by one RN, which operates in FD mode. Our first main result, stated in the theorem below, derives the gDoF in closed-form for the scenario in Figure 17, where $K = 2$. The details of the proof of Theorem 4 can be found in [42].

Theorem 4. The gDoF, d^{R-BC}, of the Gaussian relay-aided broadcast channel in Figure 17 is

$$d^{R-BC} = \min\{max\{\alpha_1 + \beta_2, \alpha_2 + \beta_1\}, \max\{\alpha_1, \alpha_2, \delta\}\}.$$

Figure 18 shows the gDoF d^{R-BC} in Theorem 4 for the Gaussian relay-aided broadcast channel with $K = 2$. The whole set of parameters has been partitioned into multiple sub-regions depending upon the RN→UEs links strength (β_1 and β_2) compared to the strength of the DeNB→RN link (δ). Moreover, for each sub-region, again the whole set of parameters has been partitioned into multiple sub-regions depending upon the DeNB→UEs links strength (α_1 and α_2) compared to the strength of the DeNB→RN link (δ). Now, we compare d^{R-BC} in Theorem 4 with the gDoF of three well known scenarios:

1) The classical broadcast channel, i.e., a wireless system where there is not the presence of the RN, i.e., the DeNB directly transmits the information to the UEs, in which case we have
$$d^{BC} = \max\{\alpha_1, \alpha_2\}.$$
The broadcast channel represents a lower bound for the relay-aided broadcast channel, in the sense that any achievable rate for the broadcast channel is also achievable for the relay-aided broadcast channel. In other words, a gDoF optimal scheme consists in having the DeNB that conveys the information only to the best user (i.e., the one with the greatest SNR-exponent α) without exploiting the RN.
2) The classical relay channel, i.e., a system where the DeNB and the RN convey the information only to one UE (the best), in which case we have
$$d^{RC} = \max\{d^{BC}, min\{\beta_1, \delta\}, min\{\beta_2, \delta\}\}.$$

As the broadcast channel, also the relay channel represents a lower bound for the relay-aided broadcast channel, in the sense that any achievable rate for the relay channel is also achievable for the relay-aided broadcast channel.

3) The MIMO broadcast channel, in which case we have
$$d^{MIMO} = \max\{\alpha_1 + \beta_2, \alpha_2 + \beta_1\}.$$
The MIMO channel represents an outer bound for the relay-aided broadcast channel since it assumes that the RN a priori knows the two messages w_1 and w_2 and so can create a virtual multi-antenna base station with the DeNB.

From the analysis above, we can now highlight under which channel conditions d^{R-BC} in Theorem 4 is as d^{BC}, as d^{RC} and as d^{MIMO}. The cases that may arise can be summarized as follows:

1) If either $max\{\beta_1, \beta_2\} \geq \delta$ or if $max\{\beta_1, \beta_2\} < \delta$ and $\delta < max\{\alpha_1, \alpha_2\}$, we have
$$d^{R-BC} = \max\{\alpha_1, \alpha_2, \delta\} = d^{RC}.$$
Thus, in this regime, the gDoF optimal strategy is to serve the best UE, i.e., the RN and the DeNB allocate all their resources just to convey information to the best UE. This regime is the one depicted in yellow in Figure 18. Notice also that if $\delta < min\{\alpha_1, \alpha_2\}$, then $d^{R-BC} = d^{BC}$, the RN is not exploited for the transmission and the DeNB just serves the best UE.

2) If $\delta > max\{\alpha_1 + \beta_2, \alpha_2 + \beta_1\}$, we have
$$d^{R-BC} = max\{\alpha_1 + \beta_2, \alpha_2 + \beta_1\} = d^{MIMO}.$$
Thus, in this case, the ultimate performance predicted by MIMO is attained thanks to the strength of the DeNB→RN link with respect the other links. This regime is the one depicted in green in Figure 18.

The two cases above cover the all-region of parameters, except the one where either $\delta - \beta_2 < \alpha_1 \leq \delta$ or $\delta - \beta_1 < \alpha_2 \leq \delta$, in which case we have
$$d^{R-BC} = \delta \longrightarrow d^{RC} < d^{R-BC} < d^{MIMO}.$$
Thus, in this case: (i) the system achieves a larger gDoF of the classical relay channel, i.e., serving the best UE is not anymore gDoF optimal, (ii) the DeNB→RN link is not yet strong enough to achieve the MIMO performance. This region is depicted in orange in Figure 18.

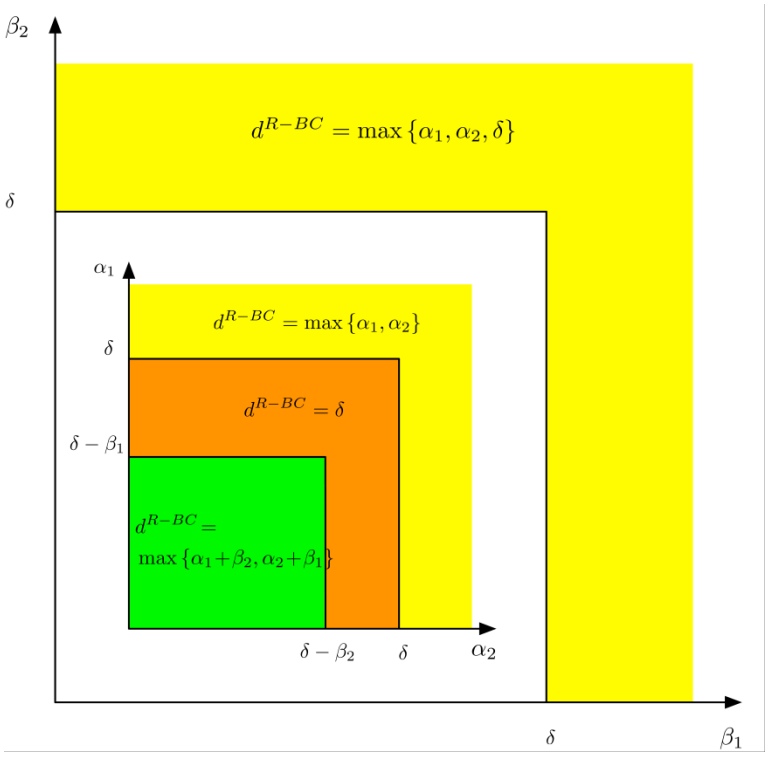

Figure 18: Optimal gDoF for the relay-aided broadcast channel in Figure 17.

From the analysis above we can draw an interesting practical conclusion: in order to obtain the gDoF gains of a MIMO broadcast channel with 2 transmit antennas at the base station and with 2 single antenna UEs, the strength of the DeNB→RN link should be of
$$C \geq \max\{S_1 \cdot I_2, S_2 \cdot I_1\}.$$

If the above condition holds, the DeNB→RN is of sufficient strength to allow the DeNB and the RN in Figure 17 to form a distributed / virtual base station with 2 transmit antennas (i.e., the gDoF in the green region in Figure 18 does not depend on β).

We now consider a more general wireless scenario than the one in Figure 17, where the DeNB has to convey independent messages to K UEs with the help of one RN. Without loss of generality, we let

$$\alpha_1 = max_{k\in[1:K]}\{\alpha_i\},$$

i.e., UE_1 has the strongest link from the DeNB. Our main result (see [42] and [48] for more details) is stated in the following theorem.

Theorem 5. The gDoF of the K UEs relay-aided broadcast channel is given by

$$d^{R-BC} = min\left\{max_{k\in[2:K]}\{\alpha_1+\beta_k, \alpha_k+\beta_1\}, max\{\alpha_1, \delta\}\right\}.$$

The closed-form expression for the gDoF in Theorem 5 sheds light into approximately optimal achievable schemes: if $\delta \leq \alpha_1$ the gDoF is as for the broadcast channel without a RN, i.e., in practical wireless broadcast networks it might not be worth using a RN if the DeNB→RN is weaker than the strongest DeNB→UE link, while if $\alpha_1 < \delta$ it is gDoF optimal to serve at most one extra UE in addition to UE1.

We would like to end this section, by describing, from a high-level point of view, how the result in Theorem 5 was derived. Actually, in order to find the gDoF in closed-form we proved an interesting connection between information theory and graph theory, namely the problem of finding the gDoF for the Gaussian K-UEs relay aided broadcast channel is equivalent to solve two (one for each cut in the network) assignment problems (a.k.a. Maximum Weighted Bipartite Matching (MWBM) problems).

The first MWBM problem, which considers the RN to be in the cut of the DeNB and which allows to find the first term in the minimum in $\mathrm{d}^{\mathrm{R-BC}}$, considers two sets: the first set, say Δ_1, consists of K nodes (number of UEs) and the second set, say Δ_2, consists of 2 nodes (1 DeNB + 1 RN). Roughly speaking, the MWBM problem assigns each node in Δ_2 to a different node in Δ_1 and outputs the set of the 2, among the K possible ones, best UEs to serve. In particular it is simple to understand which 2 UEs have to be served: UE1, i.e., the UE who has the strongest link from the DeNB, has to be always served and the second best UE is the one defined as

$$k^{\star} \coloneqq \arg\max_{k\in[2:K]}\{\alpha_1+\beta_k, \alpha_k+\beta_1\}.$$

The second MWBM problem, which considers the RN to be in the cut of the UEs and which allows to find the second term in the minimum in $\mathrm{d}^{\mathrm{R-BC}}$, considers two sets: the first set, say Δ_3, consists of $\mathrm{K}+1$ nodes (number of UEs + 1 RN) and the second set, say Δ_4, consists of 1 node (the DeN). Roughly speaking, the MWBM problem assigns the node in Δ_4 to one node in Δ_2 and outputs 1 node (among the possible $\mathrm{K}+1$) that has to be served by the DeNB, namely either the RN or UE1 (since it has the strongest link from the DeNB).

One of the most appealing features of the proposed algorithm to derive the gDoF for a Gaussian K-UEs relay-aided broadcast channel is its low complexity since polynomial-time routines exist to solve a MWBM problem. Although presented here for the single-relay case, the above algorithm can be straightforwardly extended to a general number N of RNs (by considering the practical assumption $\mathrm{N} < \mathrm{K}$, i.e., there are fewer UEs than RNs). In this case, the approximately optimal strategy would be to serve at most $\mathrm{N}+1$ (1DeNB + number of RNs) UEs. In particular, in this case 2^{N} (one for each possible cut of the network) MWBM problems should be solved and the gDoF result would be given by the minimum among the 2^{N} outputs of the MWBM problems.

4.8 Discussion and conclusion

We considered the Gaussian relay-aided broadcast channel, a system where a DeNB communicates with K UEs across a Gaussian channel with the help of a FD RN. The study of this system was motivated by the fact that it is applicable in practical heterogeneous deployments for 4G cellular networks.

We first focused on the case $\mathrm{K}=2$ and we derived the gDoF, or "sum-capacity pre-log", in closed-form. We then identified the set of parameters where the system achieves the same gDoF of the classical relay and broadcast channels. We finally highlighted under which channel conditions the gDoF attained by the system is the same as that of a MIMO system with two transmit antennas and two single-antenna UEs, i.e., when the DeNB and the RN create a virtual or distributed MIMO system. In particular, we discussed how the DeNB→RN link should be dimensioned in order to attain the gDoF predicted by MIMO.

We then considered a general number K of UEs and proved that serving at most 2 UEs (among the K possible ones) is gDoF-optimal. This choice was shown to depend on the values of the channel parameters. An interesting connection between information theory and graph theory, namely "the problem of finding the gDoF is equivalent to solve 2 MWBM problems and take the minimum among the

2 solutions", was also shown. This represents the most appealing feature of our scheduling algorithm, since a MWBM problem can be solved in polynomial-time.

5 Two-way relaying for clusterized mesh networks

5.1 Scenario: Clustered wireless mesh networks based on LTE

This activity refers to wireless mesh network based on LTE for public safety applications. As explained in SHARING D2.2, the scenario is focused on a clustered wireless mesh network: the network is divided in clusters, mapping (or equivalent) to LTE macro cells (or micro cells, depending on the available transmit power, type of equipment, etc.). The mesh networks will be further defined in Section 6, followed-up by a complete description in Subsection 6.1. As seen further in Figure 47 but also in Figure 19 and Figure 20 below, a mesh network has no longer a centralized structure such as for classic mobile communication networks, and can be easily deployable in an infrastructure-less environment. For those reasons, in Section 5 we extend the LTE network to a more general concept as mesh networks which are better adapted for public safety applications. In this context, each user is controlled by a ClusterHead (CH) which is acting as a 3GPP eNodeB. Mesh Routers (MR) which may be found in mesh networks in between two cells are acting as 3GPP relays, and inherit relay and User Equipment (UE) procedures from LTE. Some MRs, connected to 2 or 3 clusters, are called bridging MRs and allow communications between the clusters. Common bridging MRs between the clusters can cooperate for improving performance (robustness, throughput, latency). Edge MRs are possibly present, if the wireless mesh network is not independent but is linked to other networks via other technologies.

Wireless mesh networks can come in different flavors. They can be used as a mesh extension of a traditional wired network, as shown in Figure 19. Red links show infrastructure links, meaning that traffic among clusters is transferred over these links.

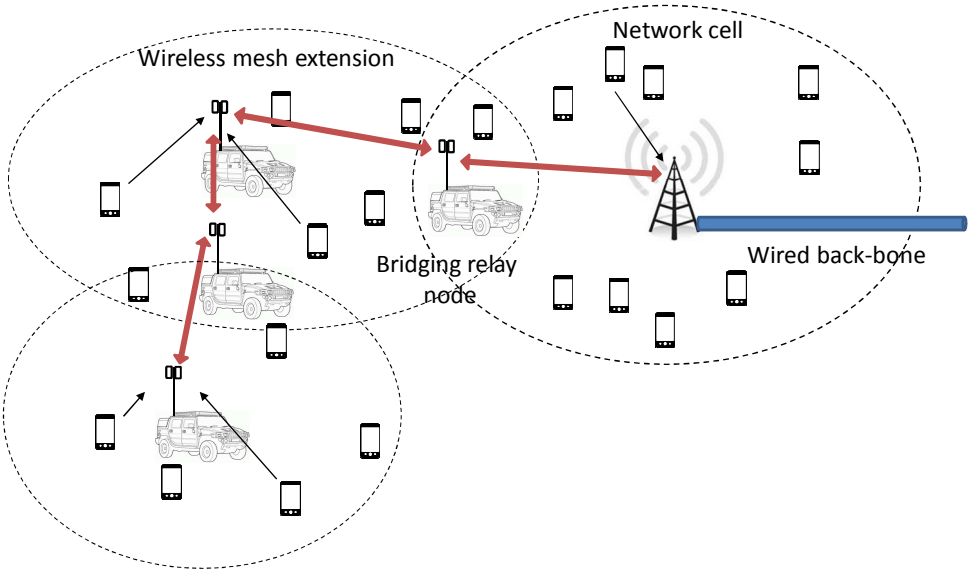

Figure 19: Wireless mesh extension

In crisis scenarios, it can be required to deploy a temporary wireless network quickly. Such a network is illustrated in Figure 20. In this configuration it can also be interesting to support connectivity while bridging nodes are still on-the-move at low vehicular speeds. Moreover, it would be interesting that isolated clusters (or cells) can be reached by relaying of UEs (see e.g. in Figure 20). This situation can happen, for example, when the relay is badly placed, in case of fast and unorganized deployment which can be required in certain situations. Therefore, as opposed to Figure 19, Figure 20 also defines a scenario where the function of the Mesh Router can be taken by mobile UEs.

In general, in such a network, a vehicular node can dispose of more power than a hand-held terminal. However, there is an interest also in having robust and interchangeable equipment. For instance if a CH is damaged or is out of service, it would be interesting that another node could take over its role.

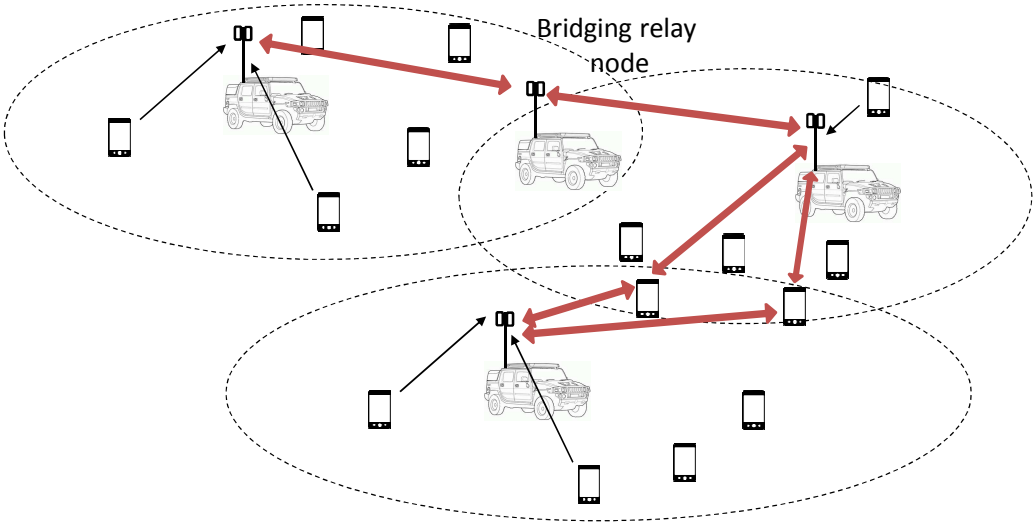

Figure 20: Quickly deployable mesh network

Notice that a very interesting point here, among others, is the inter-cluster communications which are indicated with red arrows. Similarly to Figure 19, inter-cluster links will enable communications between clusters, but the relays can also be UEs and not only relay nodes. These scenarios are also interesting for application in the Public Protection and Disaster Relief (PPDR) area. In the US, LTE has been identified as the technology for building up next generation of broadband radio system for PPDR applications, and 3GPP has already started working on adding features for implementing specific requirements linked to Private Mobile Radio (PMR), see for instance [69].

5.2 Challenges

A wireless mesh network built on top of LTE sets a number of challenges, which will be summarized here. There are challenges at the architecture level, since wireless mesh extensions or wireless mesh networks are not yet under standardization in 3GPP. 3GPP is actively working on introducing features for supporting PMR requirements like group call, direct communications between users in coverage or out of coverage of the cellular networks, definition of new UE classes, etc. However the scenario described in Section 5.1 is not yet in the focus of 3GPP, at least up to our knowledge, even if it may be a desirable feature for future broadband PMR based on LTE. For instance, radio bearer establishment and support, mobility support, etc. must be defined. Moreover, bridging MRs, which are under coverage of two CHs, must be able to synchronize and attach to both of them, as well as to decode control information in the two clusters. An additional difficulty is that the bridging MRs may be, in certain scenarios, moving too. Even if some initial work is available in the deliverables of the ICT project LOLA (Achieving Low-Latency for Wireless Communications) [70], a significant number of issues are still open.

Challenges are also present at Medium Access Control (MAC) and general Layer 2 level, for instance for management of bridging MRs, allocation of resources, scheduling. There are of course challenges also at the PHY layer. For instance, a bridging MR may not be able to follow the time advance procedure of both CHs in the Uplink (UL) and hence may generate interference at the CH. In the DL too, if the bridging MR is receiving signals from both CHs at the same time, the signals will arrive with delay equal to the difference of the propagation delay. These considerations may need the choice of extended CP depending on the coverage of the network, or advanced techniques at the receiver / transmitter for mitigating the possibly generated interference. Another example of challenges at PHY level is the definition of relaying strategy for bridging MRs.

5.3 Innovation: Relaying for inter-cluster communications

In an ideal situation with perfect channels, it is known that Two-Way Relaying (TWR) outperforms Decode-and-Forward (DF). This can be seen on top of Figure 21 where both schemes are represented. For TWR: 1) two users U1 and U2 are transmitting and are received at the same time (during reception phase) by the MR and 2) an eXclusive OR (XOR) operation is performed by MR on received data and retransmitted to both users U1 and U2 at the same time (during the broadcast phase). Compared to DF scheme, TWR uses 2 slots instead of 4 to transmit from U1 to U2 through MR and from U2 to U1 through the same MR.

In addition, in the bottom part of Figure 21, a real situation when some packets are not received is introduced. The main difference between the Simple TWR and Adaptive TWR is the following:

1. For simple TWR scheme, if one of the packets is not received, the MR discards the other packet since it cannot perform a XOR operation.
2. For adaptive TWR scheme, if one of the packets is not received, the MR forwards anyway the other packet (without performing XOR operation).

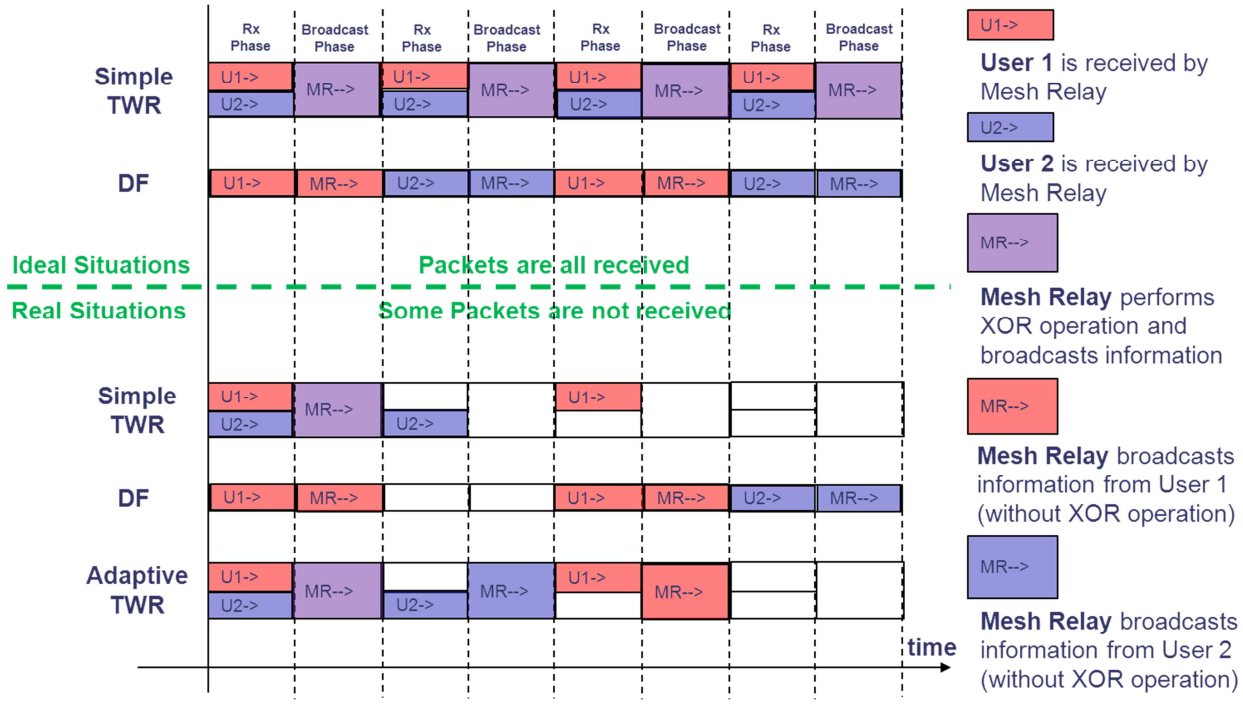

Figure 21: System Description of Simple Two-Way-Relaying Scheme, Decode-and-Forward Scheme, and Adaptive Two-Way-Relaying Scheme for Ideal and Real Situations

Adaptive TWR is better than simple TWR in terms of spectral efficiency. However, the advantage with respect to DF is not very clear since during the first slot, in TWR two users are simultaneously transmitting resulting in interference at MR level. Therefore, TWR theoretically can achieve higher throughput but in terms of PER (Packet Error Rate) DF may be better. The goal of the next sections is therefore to evaluate and compare these two schemes in terms of throughput and PER.

For this purpose, in Figure 22 we have represented the Key Performance Indicators (KPIs) and the system assumptions. At user level we are therefore interested to evaluate End-to-End throughput and End-to-End PER, while at relay level we are interested to evaluate total throughput and mean PER. The total distance between two users is considered to be equal to ISD (inter-site distance) or other. The distance between the first user (U1) and MR is *d*, and the distance between the second user (U2) and MR is ISD – *d*. A user uses 1 antenna in reception mode and 1 antenna in transmission mode but a MR uses 2 antennas in reception mode (in order to separate simultaneous transmission from the two users at the same time) and 1 antenna in transmission mode. For separating the two users several techniques can be employed, including Space-Division Multiple Access (SDMA), Successive Interference Cancellation (SIC) techniques or even linear equalization. In this deliverable we employ a linear space-time MMSE equalization technique implemented in frequency domain [71].

Another goal of this study is to evaluate the impact of MR position with respect to the position of users in terms of achievable throughput and PER for TWR and DF schemes. This would serve to evaluate for example which is the best position for a MR in order to satisfy Quality of Service (QoS) criteria and which is the maximum achievable distance for different channel models.

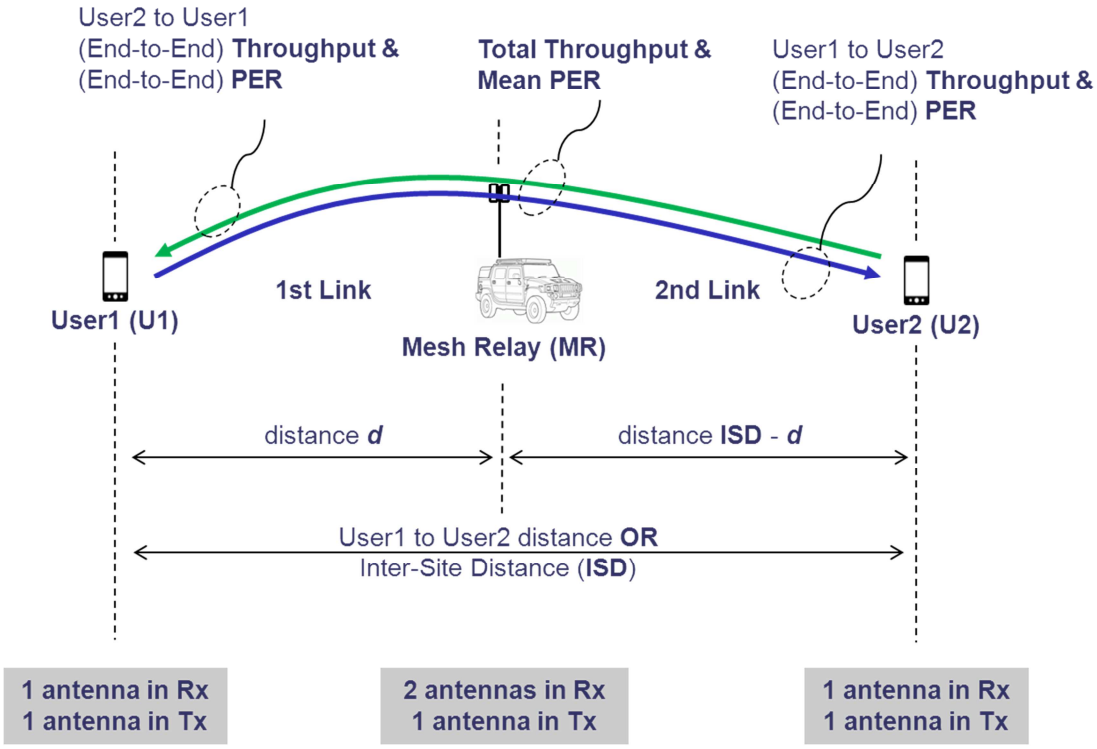

Figure 22: Simplified System Description and KPIs of Interest

5.3.1 Power Allocation for Relaying Schemes

A usually neglected assumption is the power constraint that has to be considered at relay and user level. In this work it is assumed that the power at relay level is bounded by a maximum transmission power and shared between the end-to-end links using the frequency resources at the same time. This effect can be seen as a compromise between the total achievable throughput and the total transmission distance:

1. a smaller-bandwidth MR (e.g. 1.4 MHz) can relay a lower number of connections but for the same maximum transmission power the communication distance is higher.
2. a larger-bandwidth MR (e.g. 5 MHz) can relay a higher number of connections but for the same maximum transmission power the communication distance is lower.

An illustrative example is given in Figure 23. This example is applicable to both TWR and DF schemes previously represented in Figure 21, and shows that there is a maximum transmission power to be transmitted by a user and a maximum transmission power to be transmitted by a MR.

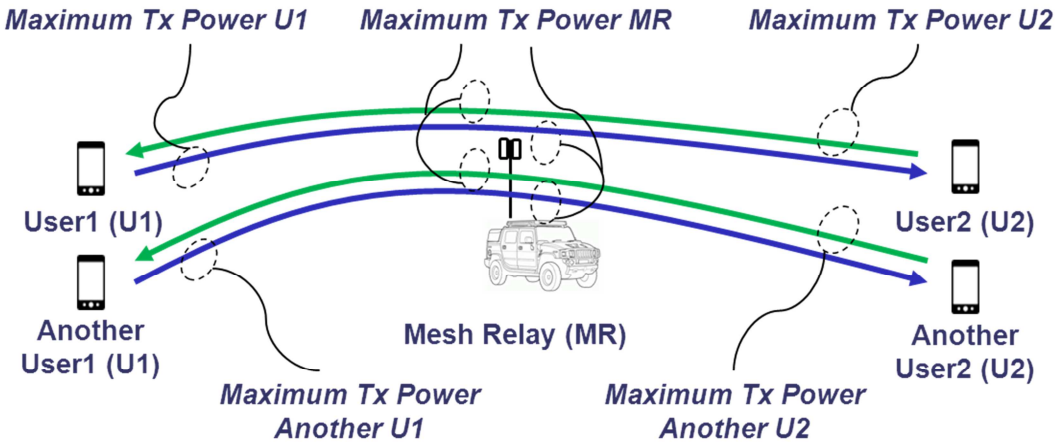

Figure 23: Power Constraint Representation for a Relaying Scheme

No matter if transmission takes place during the first slot or during the second slot, the MR has to support multiple End-to-End transmissions at the same time and therefore the maximum transmission power per link is constrained at MR level with respect to the number of links simultaneously being relayed and the service per each link.

From the point of view of the transmission scheme to be used (DF or TWR) there is no difference with respect to the transmitted power during the first slot or during the second slot per user or per relay. However, in terms of total (global) transmitted power, it is possible that TWR scheme consumes more instantaneous power since during the first slot the users (i.e. U1 & U2) can transmit simultaneously 2 different packets at the same time towards the MR. Similarly, in terms of (global) transmitted average power it is possible that DF scheme consumes more power than TWR since DF uses 2 slots instead of 1 to broadcast information from the MR to end users. In this study we focus only on individual power consumption and power constraints and not on the global (network) power consumption.

As previously mentioned, with respect to the number of resource blocks (RBs) used at the same time, a user or a relay may transmit a certain transmission power which should not be above the maximum allowed transmission power. A few examples with a different RBs allocation schemes (represented in green) are given below in Figure 24 and Figure 25 for a user and a MR respectively. Each RB is represented as a 12 x 7 grid, and each RB is composed from 12 subcarriers (each with 15 kHz) and 7 symbols (when Normal Cyclic Prefix is being used) which are sent in a slot of 0.5 ms duration. Normally the resource allocation is performed on pairs of RBs (corresponding to a Time Transmission Interval of 1ms or a TTI). In Figure 24, the allocation scheme in the middle is not implementable in LTE, except in specific cases like in the PHY UL control channel, and it is given mainly for illustration purpose.

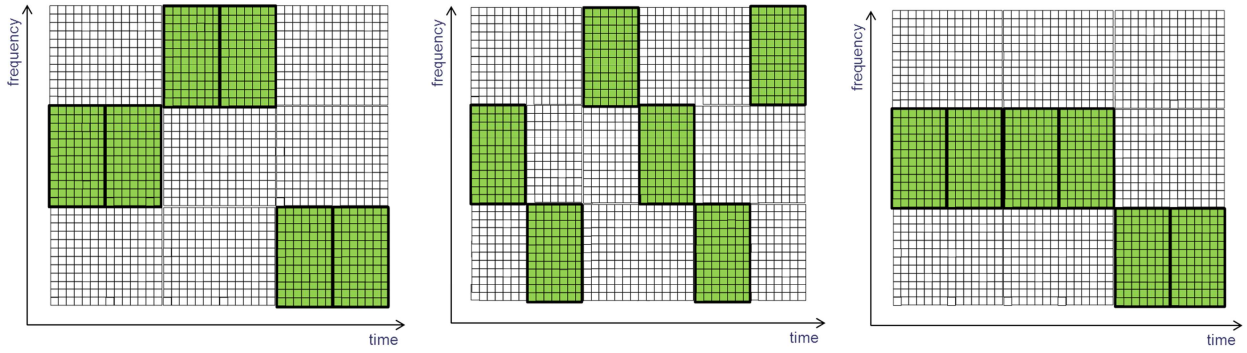

Figure 24: Example of Allocation Schemes for a User

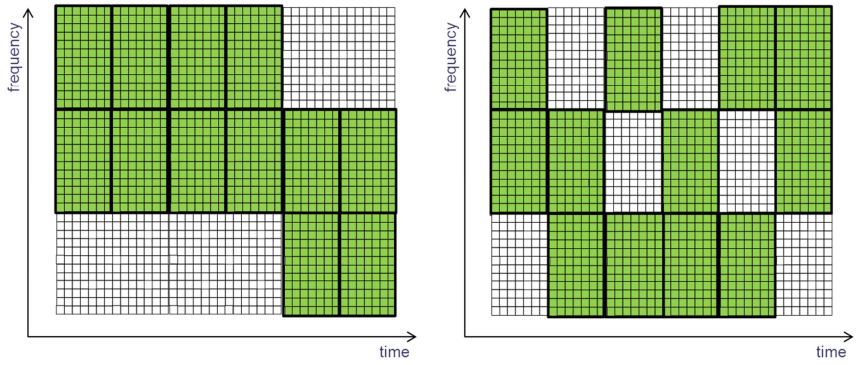

Figure 25: Example of an Allocation Scheme for a MR relaying 2 End-to-End links

The RB allocation can be continuous or discontinuous in time or in frequency domain. However, if the total number of RB transmitted at the same time on the frequency domain increases, the power allocated to each RB block will decrease as a result of the maximum power constraint on all the RB used at the same time. Suppose that the maximum transmission power constraint for a user is 1 W and for a MR is 10 W. As represented in Figure 24, if the user transmits on maximum 1 RB block at the time, then the maximum allowed power per 1 RB is 1 W. However, in the case of a MR represented in Figure 25, if the MR uses 2 RB instead of 1 RB (e.g. because it can simultaneously relay 2 End-to-End links as previously represented in Figure 23), the maximum allowed power per link will be 5 W, meaning that

the MR cannot relay anymore at full power one single link. This would be a disadvantage for the MR in terms of transmission coverage:

1. if the goal is to extend coverage as far as possible, it is better if the MR is not relaying many users at the same time;
2. if the goal is to relay as many users as possible, it is better to use a MR in a scenario with shorter distances between relayed users.

5.4 Results

5.4.1 Simulation Parameters

Physical and MAC layer simulation parameters have been represented in Table 10. The simulation considers a voice service and a SC-FDMA transmission scheme for its reduced PAPR characteristics. The rest of the parameters are LTE compliant.

Table 10: PHY & MAC Simulation Parameters

Parameter	**Value**
Frame Duration	10 ms
Slot Duration	0.5 ms
Voice Transmission Period	20 ms (vocoder parameter)
Coding Scheme	Convolutional coding with 1/3 coding rate
Subcarrier Spacing	15 kHz
Number of Subcarriers	72 (for 1.4 MHz) or 300 (for 5 MHz)
Number of Subcarriers per RB	12
Total # of Simultaneous Transmitted RBs per MR	6 (for 1.4 MHz) or 25 (for 5 MHz)
Total # of Simultaneous Transmitted RBs per UE	1
Number of Symbols per Slot	6 (Extended Cyclic Prefix)
Necessary transmitted information at PHY level (for e.g. voice service type PMR)	e.g. 1 packet of 480 bits each 20 ms
Number of Bits per Symbol	2 bits/symbol (QPSK modulation)
# of RBs necessary to transmit one packet	4 RBs each 20 ms
Total Throughput in Bits/Sec (including pilots)	1.728 Mb/sec or 7.2 Mb/sec
Transmission Scheme	SC-FDMA

Different scenarios have been evaluated as seen in Table 11 with the system parameters. For the simulations, an ITU channel model (ITU-R P.1411-4) designed for computing path loss between two terminals of low height (below roof-top) in urban environments has been used, combined with standard 3GPP Extended Typical Urban (ETU) and Extended Pedestrian A (EPA) channel models. It is also important to mention that the considered ITU model includes both Line-Of-Sight (LOS) and Non-Line-Of-Sight (NLOS) regions and models the rapid decrease in signal level noted at the corner between LOS and NLOS regions.

The used ITU model is based on measurements made in the UHF band with antenna heights between 1.9 and 3.0 m above ground, and transmitter-receiver distances up to 3 000 m. This model is also very well adapted to transmission ranges below 3000 m. The model includes the statistics of location variability in the LOS and NLOS regions, and provides a statistical model for the corner distance between

the LOS and NLOS regions. For all these reasons, the ITU model is very well adapted to our scenarios where the terminals are located below roof-top height and in the Ultra High Frequency (UHF) range (from 300 MHz to 3 GHz). In our simulations results have been obtained for a location variability of 50% and 90% – however the model and the simulator provide different values which can be easily exploited for further work. We have also considered a Noise Figure of 7 dB and a Noise Density of -174 dBm/Hz. Different bandwidths and also different transmission powers have been further considered.

Table 11: System Parameters

System Parameter	**Values**
Inter-Site Distance, ISD (3GPP TR 36.814)	500 m (3GPP Urban) 1732 m (3GPP Rural)
Channel Type	ETU (Extended Typical Urban) EPA (Extended Pedestrian A)
Noise Figure	7 dB
Noise Density	-174 dBm/Hz
Location Variability for ITU Model (ITU-R P.1411-4)	1%, 10%, 50%, 90%, 99% (from LOS to NLOS)
Bandwidth	1.4 MHz or 5 MHz (in the 763-768 MHz band)
Carrier Frequency	763.7 MHz for 1.4 MHz bandwidth 765.5 MHz for 5 MHz bandwidth
# Antennas User	1 Tx, 1 Rx
# Antennas Mesh Relay	1 Tx, 2 Rx
Tx Power User	1 W
Tx Power Mesh Relay	1W - 10 W

5.4.2 Simulation Results

The choice of the simulation scenarios have been carefully taken into account. A first subsection (i.e. Subsection 5.4.2.1) is dedicated to multiple end-to-end transmissions while the second subsection (i.e. Subsection 5.4.2.2) supposes that the MR simultaneously relays only one transmission, which means that in the second subsection the MR can transmit with higher power than in the first subsection (see discussion from Section 5.3.1).

5.4.2.1 Multiple end-to-end transmissions (1.4 MHz and 5 MHz)

This subsection considers mainly two opposite simulation scenarios:

A) A scenario with a smaller frequency bandwidth for MR, a higher ISD and a lower location variability (corresponding to a smaller city for example, with lower number of users and lower roof-top height) – this scenario could be qualified as e.g. suburban or rural;

B) A scenario with a larger frequency bandwidth for MR, a lower ISD and a higher location variability (corresponding to a more populated city for example, with higher number of users and higher roof-top height – predominant NLOS scenario) – this scenario could be qualified as urban.

For the first scenario (i.e. scenario A) we have considered an EPA channel model, a 1.4 MHz MR bandwidth, 50% location variability for ITU model, a Noise Figure NF = 7 dB, a distance between users

of 1732 m (ISD), multiple end-to-end transmissions through the relay (the maximum transmission power at MR level is shared between different end-to-end links), 1 W maximum transmission power for the user, 10 W maximum transmission power for the MR.

For the second scenario (i.e. scenario B) we have considered an EPA channel model, a 5 MHz MR bandwidth, 90% location variability for ITU model, a Noise Figure NF=7 dB, a distance between users of 500 m (ISD), multiple end-to-end transmissions through the relay (the maximum transmission power at MR level is shared between different end-to-end links), 1 W maximum transmission power for the user, 10 W maximum transmission power for the MR.

The End-to-End PER for DF schemes for scenario A and scenario B are shown respectively in Figure 26 and Figure 27. The abscissa represents the distance of the first link as defined in Figure 22. In the first scenario, the MR transmission power of 10 W is divided between 6 simultaneous RBs occupying the 1.4 MHz frequency bandwidth (see Table 10). However, in the second scenario which uses a 5 MHz frequency bandwidth, the MR transmission power of 10 W is divided between 25 simultaneous RBs (see Table 10). In both scenarios we suppose that the frequency bandwidth is completely occupied by simultaneous links. This means that if the communication band is larger, the MR decreases the power allocated per user in order to respect the power constraint. Moreover, the second scenario uses a higher location variability percentage (closer to NLOS model) but a much lower distance between users (only 500 m) and for these reasons the PER is much lower.

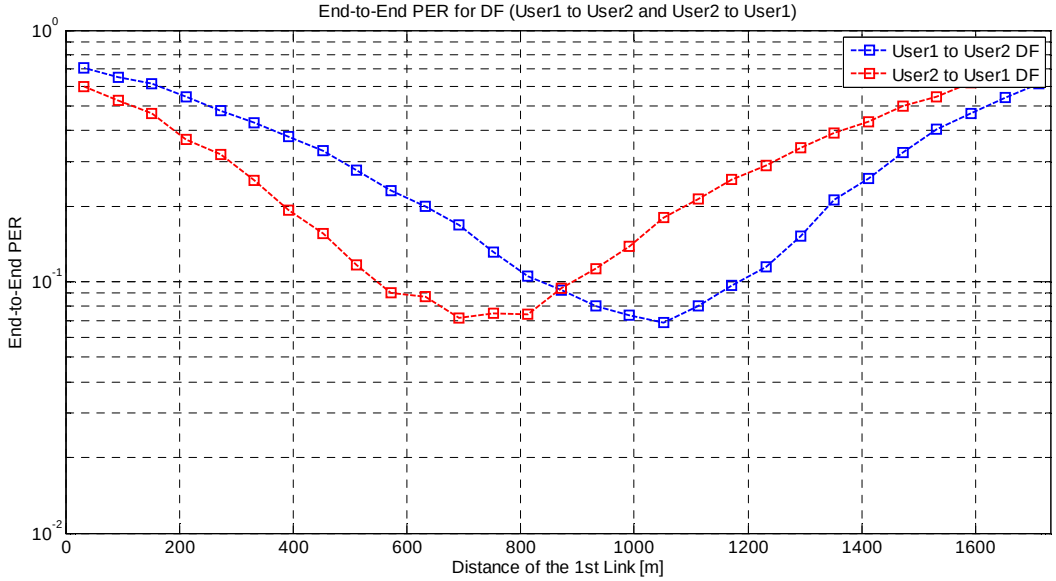

Figure 26: End-to-End PER for DF, Scenario A (EPA, 1.4 MHz, 50% location variability, NF=7 dB, 1732 m ISD, multiple end-to-end transmissions, 1 W maximum Tx power user, 10 W maximum Tx power for Mesh Relay)

It can be also noticed that the minimum PER for the DF scheme represented in Figure 26 is not for a MR located in the middle of the system. Surprisingly the best MR position is at 750 m (when transmitting from U2 to U1) and 1050 m (when transmitting from U1 to U2) for scenario A for 1732 m range between 2 users. This result can be explained because the MR uses two antennas in reception while the users U1 and U2 use only one. This fact creates and asymmetry in the link budgets.

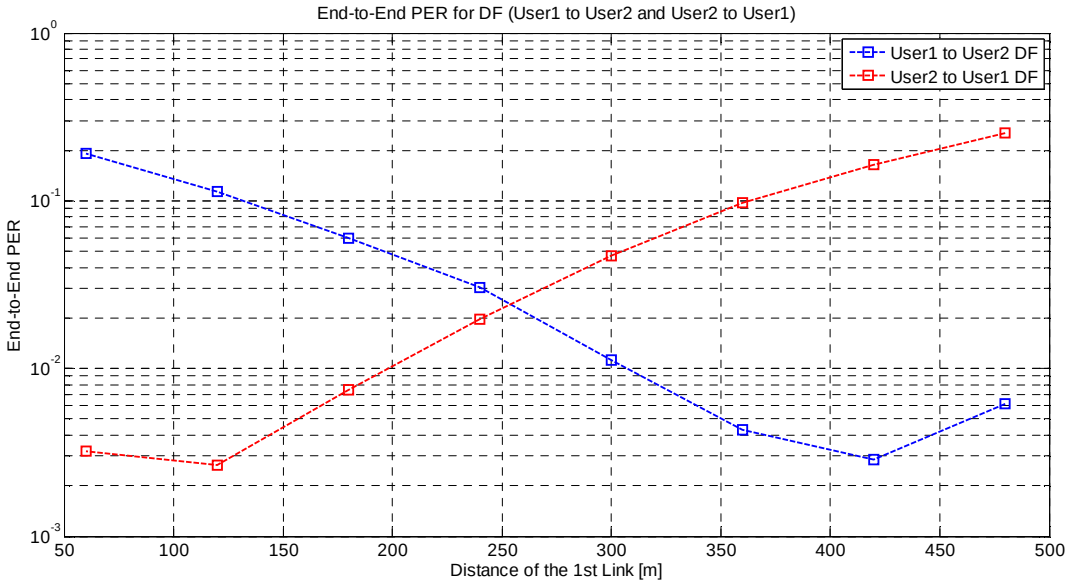

Figure 27: End-to-End PER for DF, scenario B (EPA, 5 MHz, 90% location variability, NF=7 dB, 500 m ISD, multiple end-to-end transmissions, 1 W maximum Tx power user, 10 W maximum Tx power for Mesh Relay)

A similar result as in Figure 26 can be obtained for Figure 27 as well: it can be again noticed that the minimum PER is not for a MR located in the middle of the system. For the scenario B represented in Figure 27, the best MR position is at around 100 m (when transmitting from U2 to U1) and at around 400 m (when transmitting from U1 to U2) – scenario B considers a maximum range between 2 users of 500 m. This result can be explained again because the MR uses two antennas in reception while the users U1 and U2 use only one. For the sake of comparison the algorithm used by MR for DF is a linear MMSE equalizer implemented in frequency domain. In the particular settings used here, each transmission is devoted to one specific user with one transmit antenna. Hence the MR receives with two antennas (standard SIMO system), the implemented equalizer yields a traditional MRC receiver in the frequency domain. For the TWR, a linear MMSE equalizer implemented in frequency domain was used too, but in the virtual MIMO case (multiple transmitters with one antenna) the linear MMSE equalizer is used both to separate the users (with residual interference depending on the specific channel realizations) and to recover spatial receive diversity through MRC.

Even so, in terms of mean PER (among the two end-to-end links), if only one MR is used for both directions (i.e. U1 to U2 and U2 to U1), later figures Figure 34 and Figure 35 show that the minimum mean PER is obtained in the middle of the ISD, i.e. at 866 m and 250 m respectively.

Further, Figure 28 and Figure 29 show a comparison in terms of End-to-End PER for different TWR schemes (i.e. simple TWR and adaptive TWR presented in Figure 10) for scenario A and scenario B respectively. It is further showed that adaptive TWR is better (or equal) than simple TWR for different MR positions.

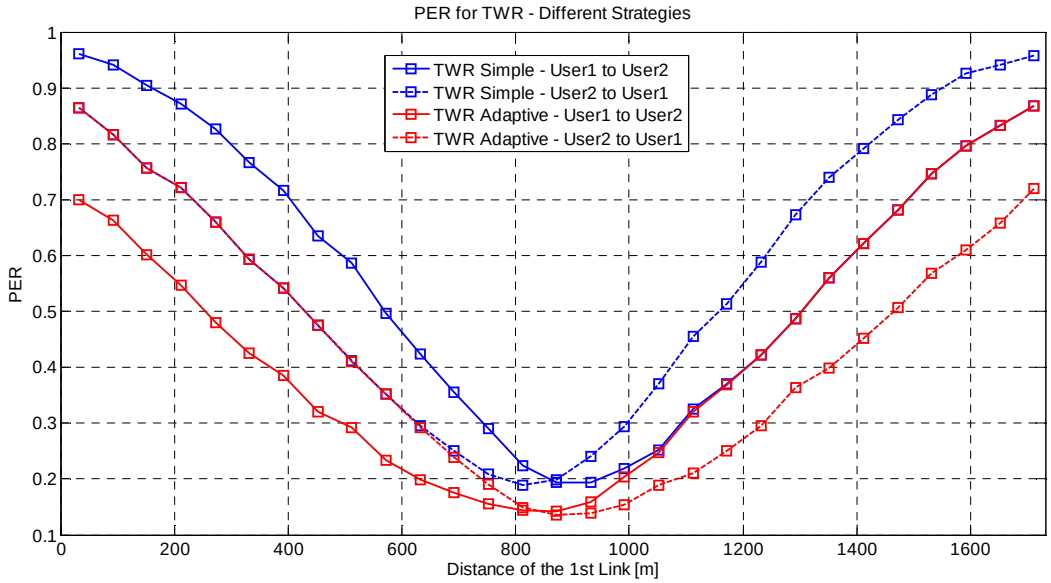

Figure 28: End-to-End PER for TWR, Scenario A

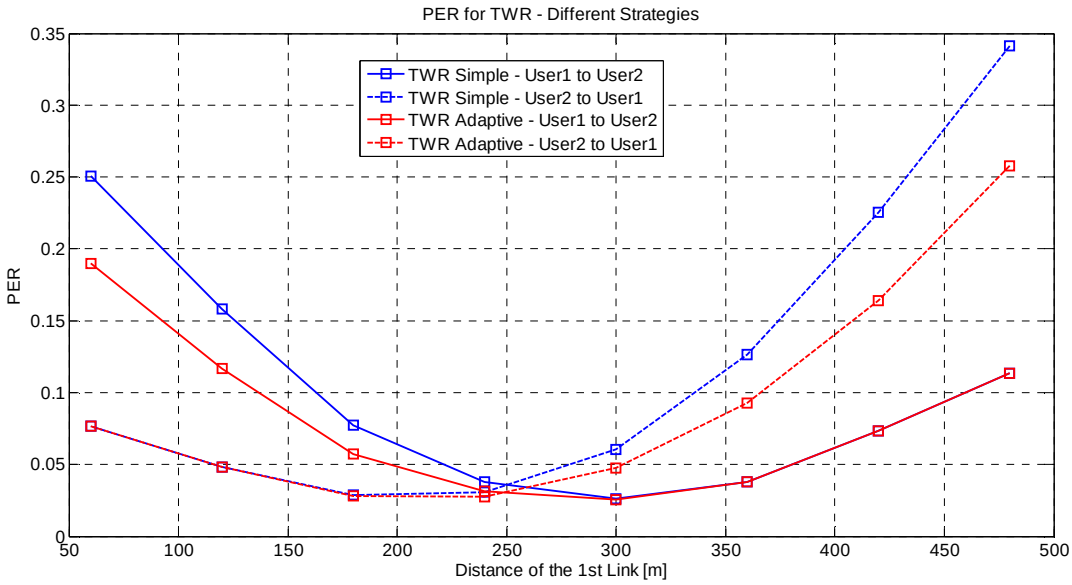

Figure 29: End-to-End PER for TWR, Scenario B

Figure 30 and Figure 31 show U1 to U2 End-to-End PER, as a comparison between TWR and DF schemes. It can be easily noticed that DF outperforms TWR in terms of PER. Moreover, in the case of Figure 31 the gap between TWR and DF is even higher and most probably because in the case of Figure 31 the MR transmits with lower power (since it relays more end-to-end links than in the case of Figure 30, but for the same maximum power of 10 W).

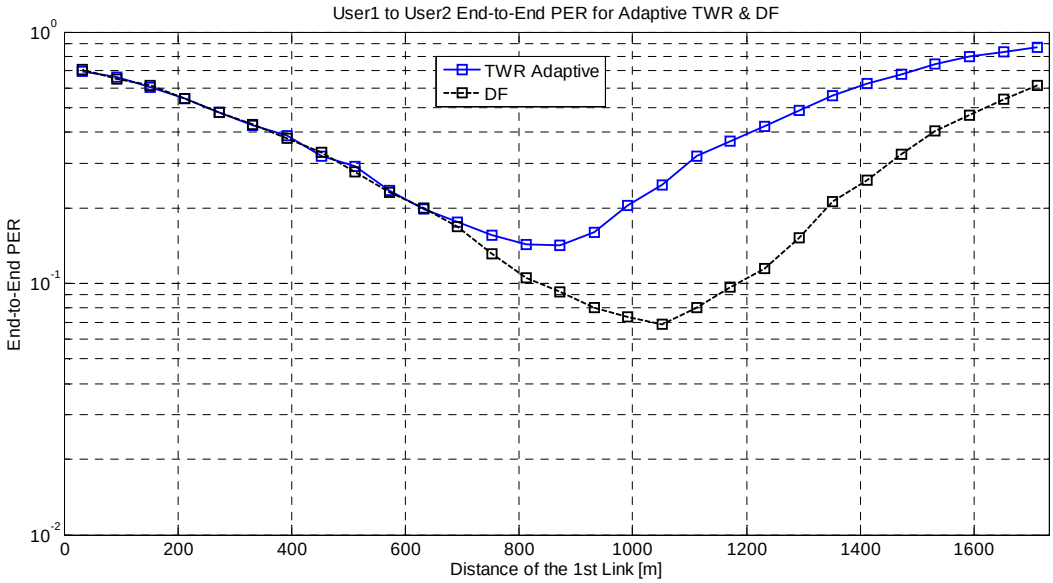

Figure 30: End-to-End PER U1 to U2, comparison between TWR and DF, Scenario A

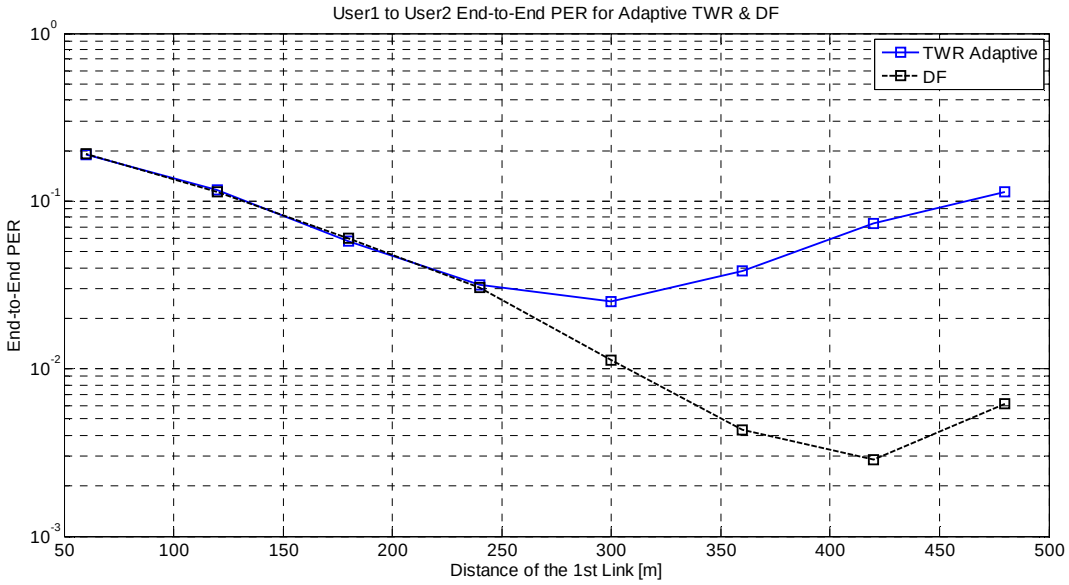

Figure 31: End-to-End PER U1 to U2, comparison between TWR and DF, Scenario B

Similar and symmetric results can be observed when we consider a U2 to U1 transmission represented in Figure 32 for scenario A and in Figure 33 for scenario B.

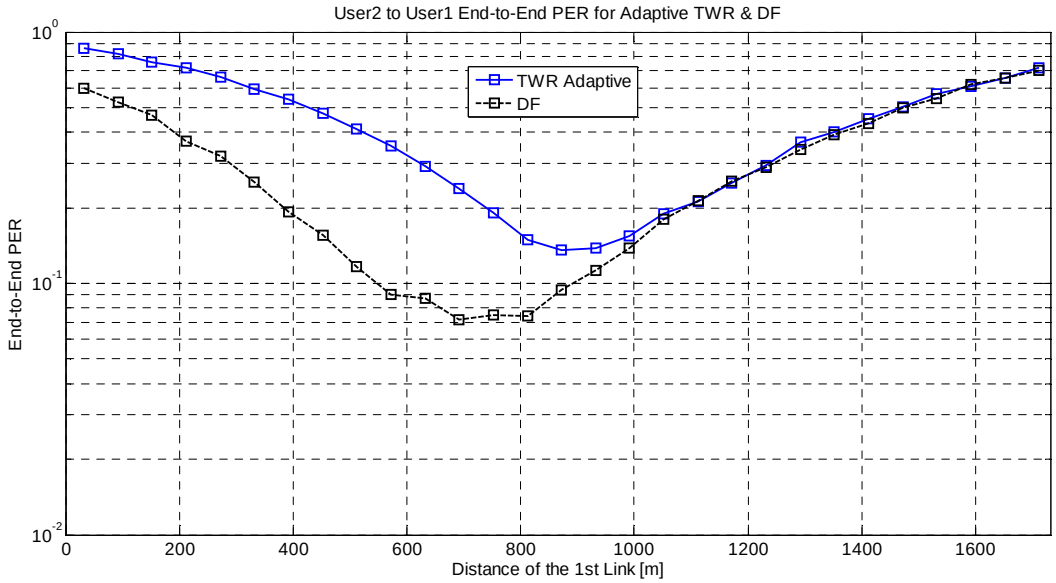

Figure 32: End-to-End PER U2 to U1, comparison between TWR and DF, Scenario A

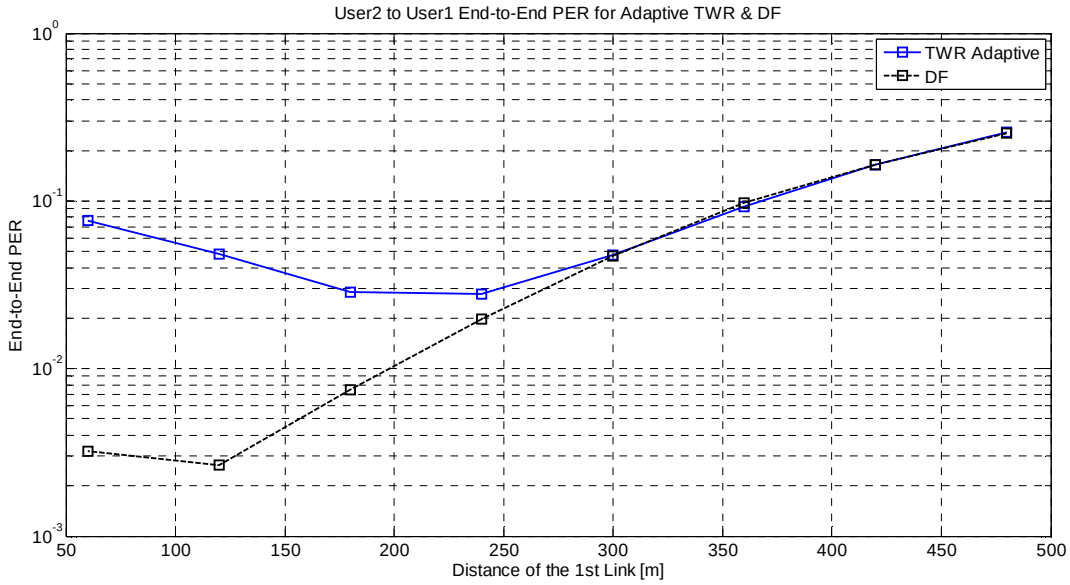

Figure 33: End-to-End PER U2 to U1, comparison between TWR and DF, Scenario B

Overall, as already previously mentioned, DF scheme is better than TWR scheme in terms of mean PER for both scenarios A and B represented in Figure 34 and Figure 35 respectively. As a matter of fact, the results can be explained because in the case of TWR the U1 and U2 are simultaneously transmitting in the first slot interfering with each other and thus increasing PER. However, in the case of DF scheme, U1 and U2 have dedicated transmission slots and therefore their interference at MR level is restricted.

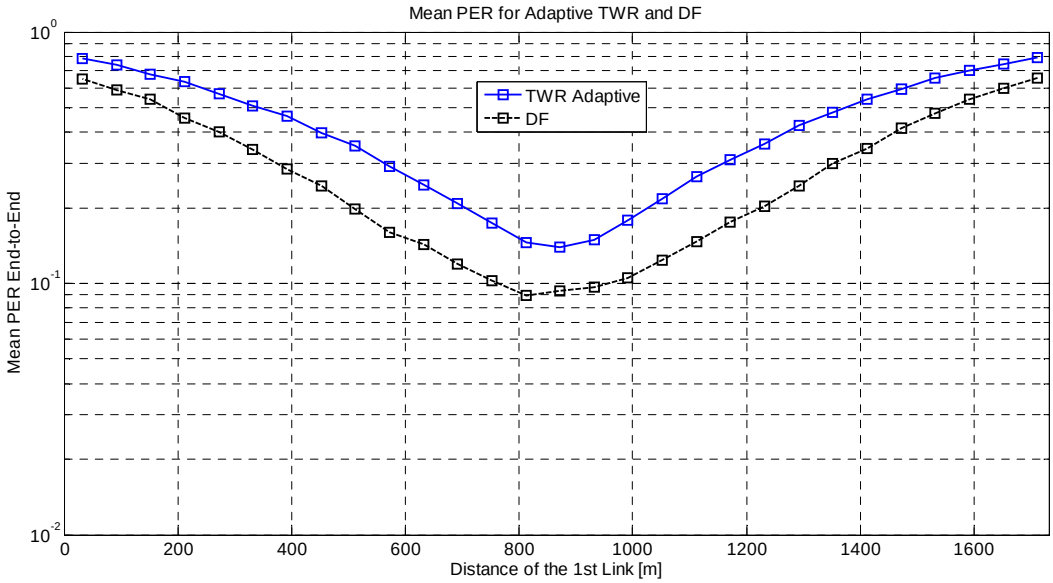

Figure 34: Mean End-to-End PER, comparison between TWR and DF, Scenario A

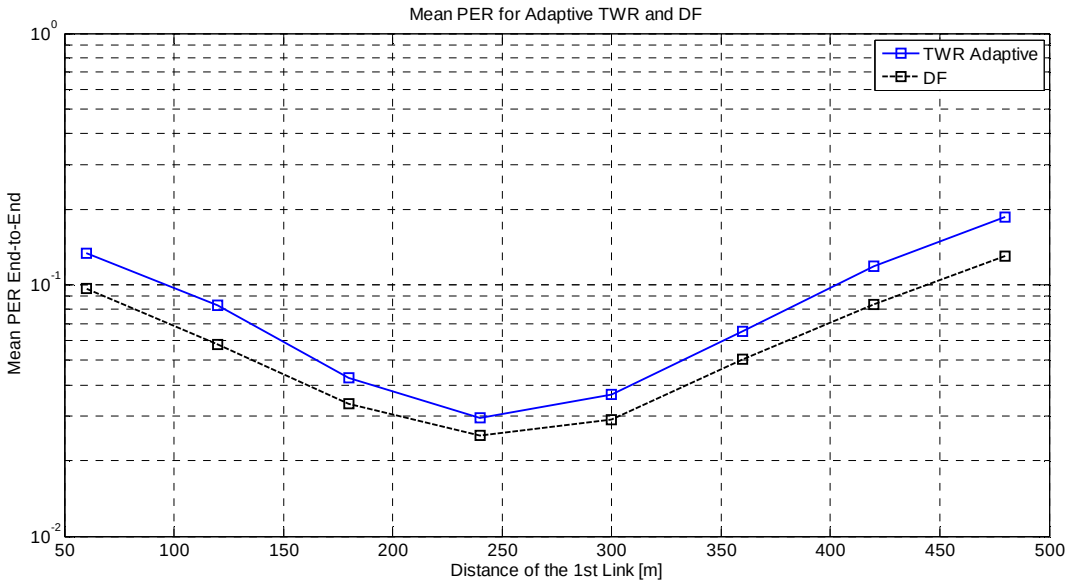

Figure 35: Mean End-to-End PER, comparison between TWR and DF, Scenario B

Another interesting result is in the case of Figure 35, where the PER gap between TWR and DF has been limited. This limitation can be explained because the ISD is much smaller compared to Figure 34, and despite of lower MR transmission power.

Figure 36 and Figure 37 present End-to-End throughput (from U1 to U2 and from U2 to U1) for adaptive TWR and simple TWR, for different MR positions between two users U1 and U2. The maximum throughput is achieved for Figure 36 (with a 1.4 MHz system bandwidth) at approximately 1300 packets/second for a MR located at half of the distance between the two users U1 and U2, and is achieved for Figure 37 (with a 5 MHz system bandwidth) at approximately 6100 packets/second for a MR located at one third of the distance between the two users U1 and U2.

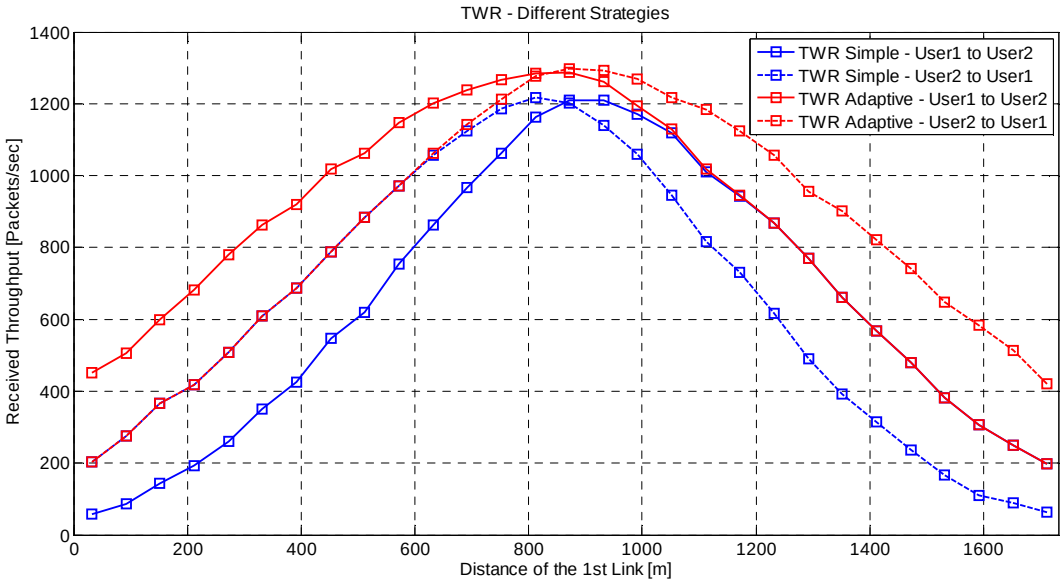

Figure 36. End-to-End Packet Throughput, comparison between Adaptive TWR and Simple TWR, Scenario A

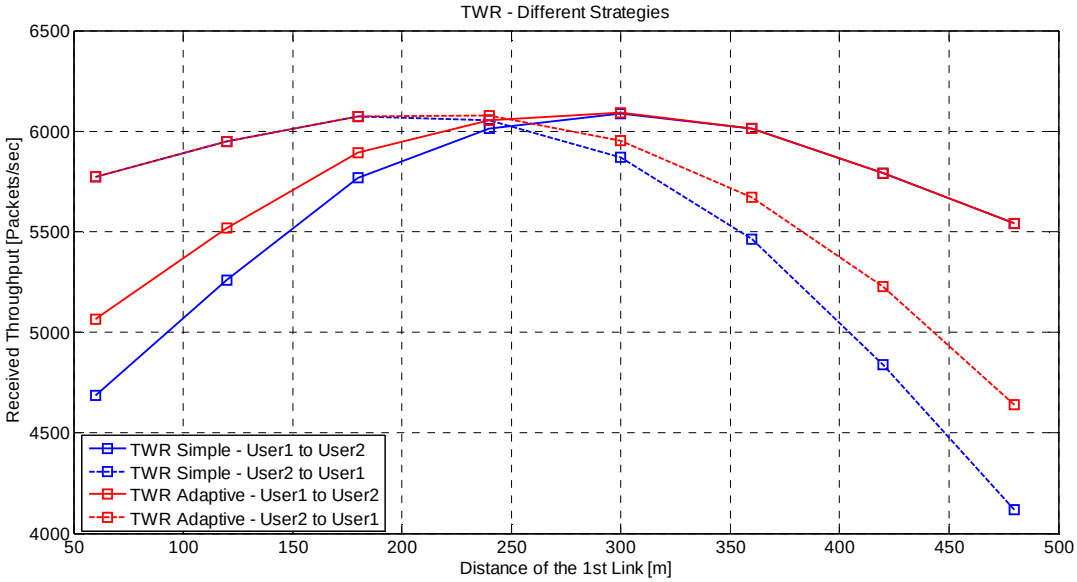

Figure 37: End-to-End Packet Throughput, comparison between Adaptive TWR and Simple TWR, Scenario B

In terms of U2 to U1 received total throughput (Figure 38 and Figure 39), adaptive TWR gives better results than DF in most of the simulation cases. Similar simulation results can be obtained when transmitting from U1 to U2 (as represented in Figure 40 and Figure 41). However, for scenario A, in the case of Figure 38 and Figure 40, when the MR is far away from the transmission source, it seems that DF has a small gain, which is somewhat expected. However, if the distance between U1 and U2 is very small - for scenario B in the case of Figure 39 and Figure 41, the total transmitted throughput is almost double for any MR position between the two users.

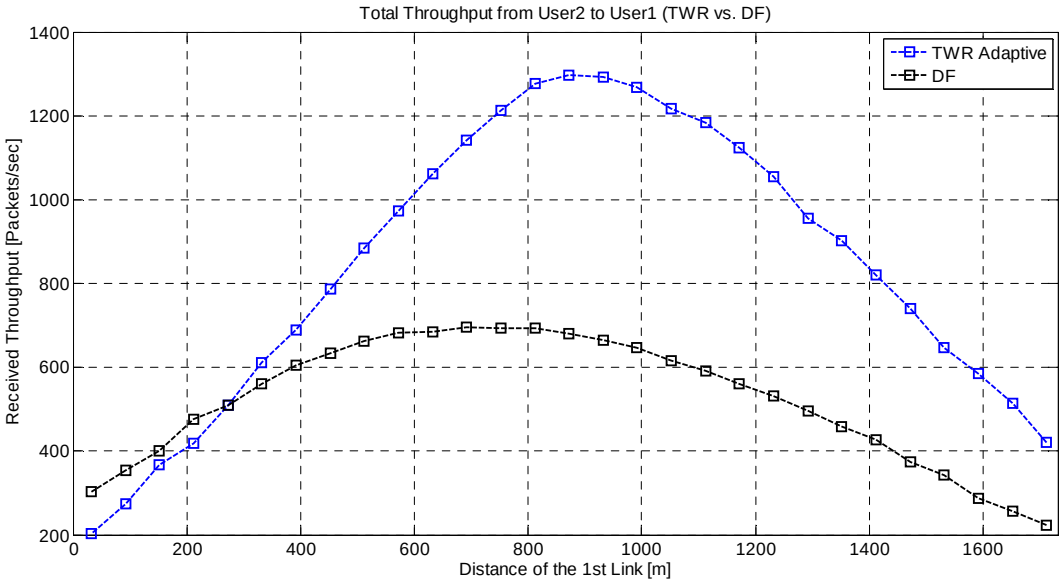

Figure 38: U2 to U1 Packet Throughput, comparison between Adaptive TWR and DF, Scenario A

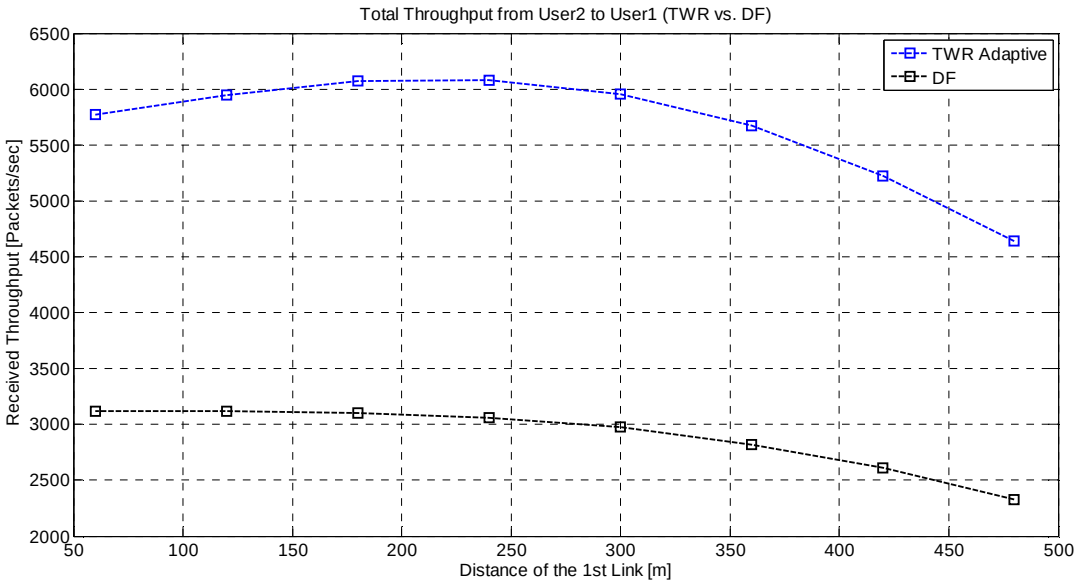

Figure 39: U2 to U1 Packet Throughput, comparison between Adaptive TWR and DF, Scenario B

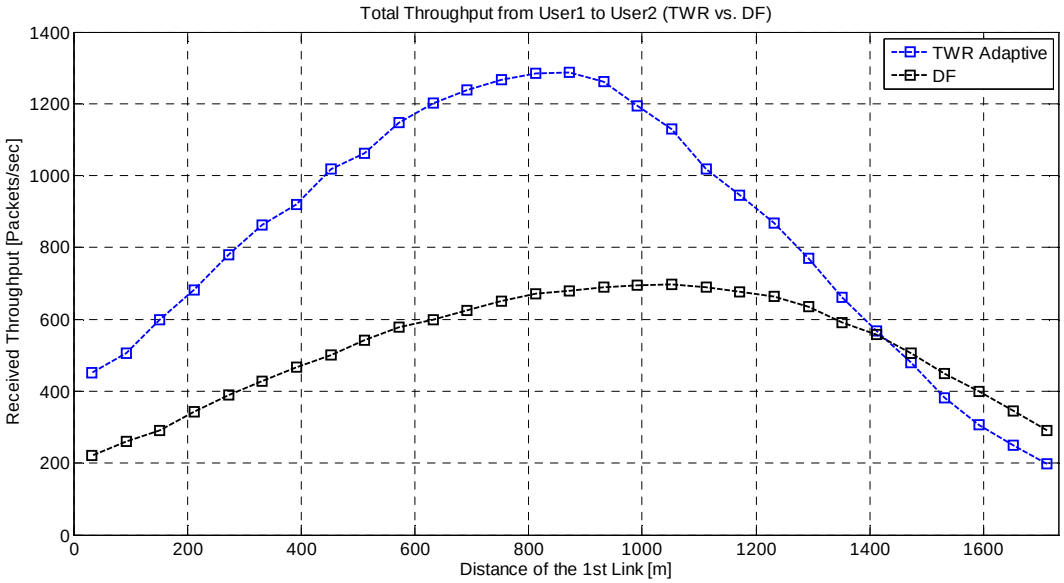

Figure 40: U1 to U2 Packet Throughput, comparison between Adaptive TWR and DF, Scenario A

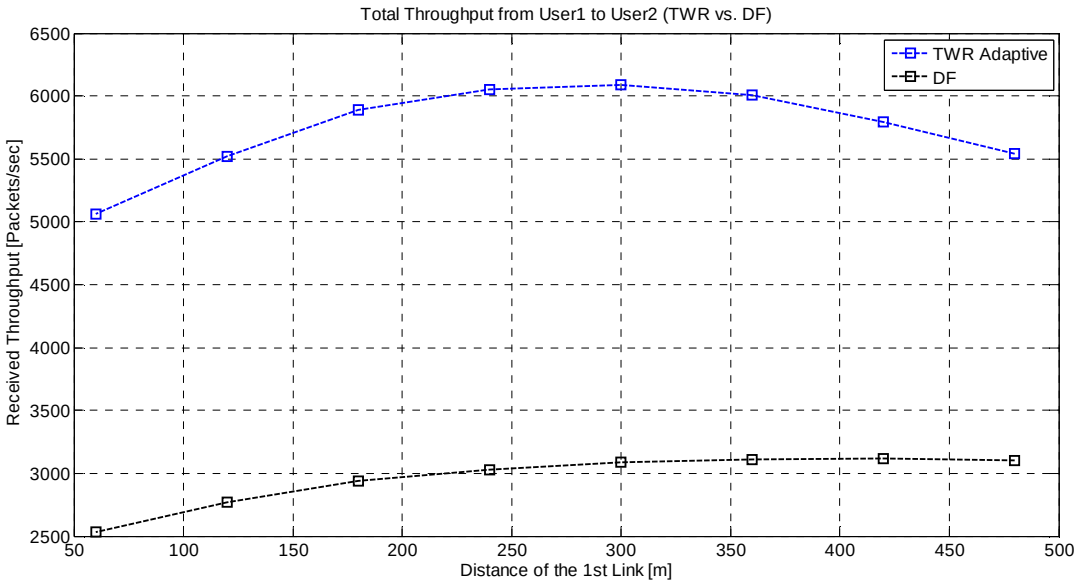

Figure 41: U1 to U2 Packet Throughput, comparison between Adaptive TWR and DF, Scenario B

Finally, if we compute the total transmission throughput (the sum of U1 to U2 throughput and of U2 to U1 throughput) we obtain that overall adaptive TWR gives better results in terms of achievable throughput for any of the scenarios A or B represented in Figure 42 and Figure 43.

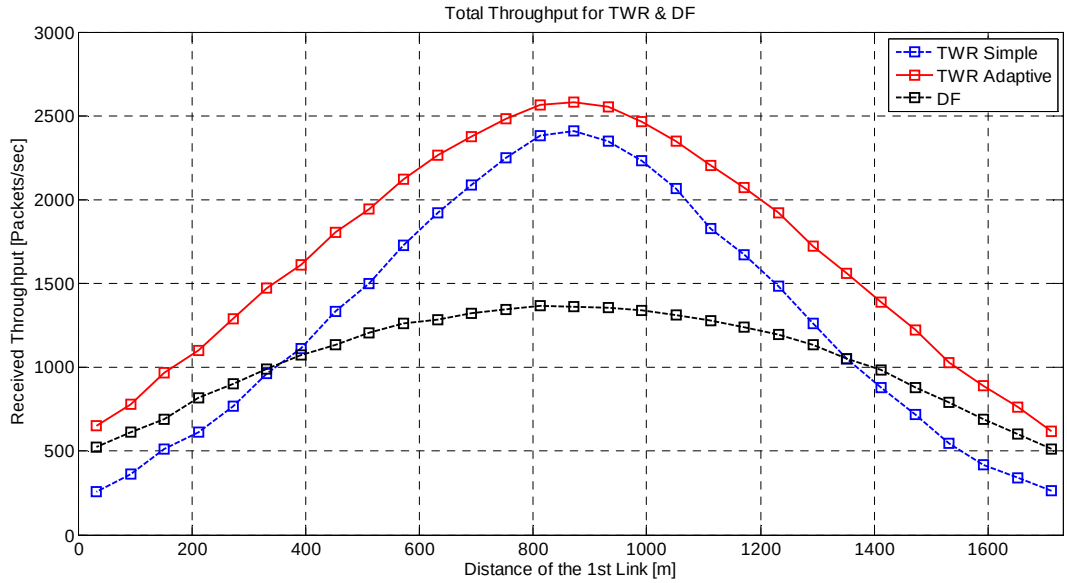

Figure 42: Total Packet Throughput, comparison between Adaptive TWR, Simple TWR & DF, Scenario A

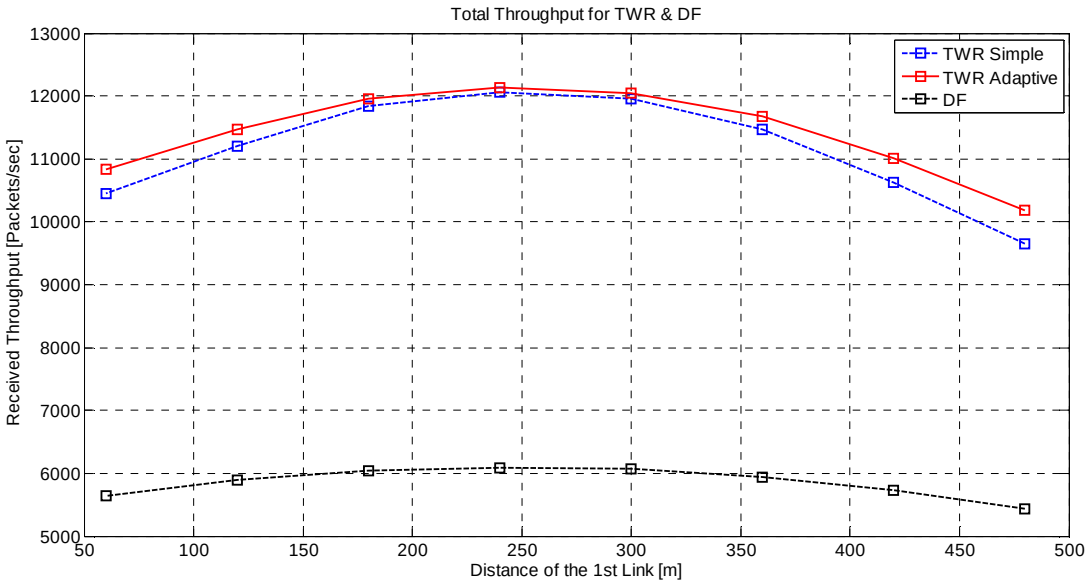

Figure 43: Total Packet Throughput, comparison between Adaptive TWR, Simple TWR & DF, Scenario B

5.4.2.2 Single end-to-end transmissions (best case)

For this scenario we have used an ETU channel model, 1.4 MHz (1.4 MHz or 5 MHz does not matter if there is only one user transmitting in frequency domain using only 1 RB), 1% location variability, a Noise Figure NF = 7 dB, 5000 m ISD - corresponding to a transmitting range larger than in the previous cases, since we want to check the performance in a best case scenario with a single end-to-end transmission relayed by the MR, 1 W maximum transmission power for the user, 10 W maximum transmission power for the MR.

The goal of this short section is to show that if the model is more likely to be LOS (i.e., 1% location variability), and the MR relays only one link at a time – which means that only one RB is actually used per slot (as represented in Figure 24) and not 6 or 25 RBs, the total communication range can be increased.

End-to-End PER results from Figure 44 and Figure 45 show that adaptive TWR can still be used in the above scenario in the case of unidirectional end-to-end transmissions, but the position of the MR is essential. However, results from Figure 46 show that in terms of mean PER (over bi directional

communications), it is no longer acceptable to use adaptive TWR schemes. In such situations - as in the case of very long distances (e.g. up to 5000 m), DF scheme provides better results: DF is more robust to interference as opposed to TWR scheme. This aspect can be easily seen on both directions e.g. on Figure 44 and on Figure 45 respectively, but also on the results obtained in Figure 46 which represents the mean PER as a function of MR position between the 2 users.

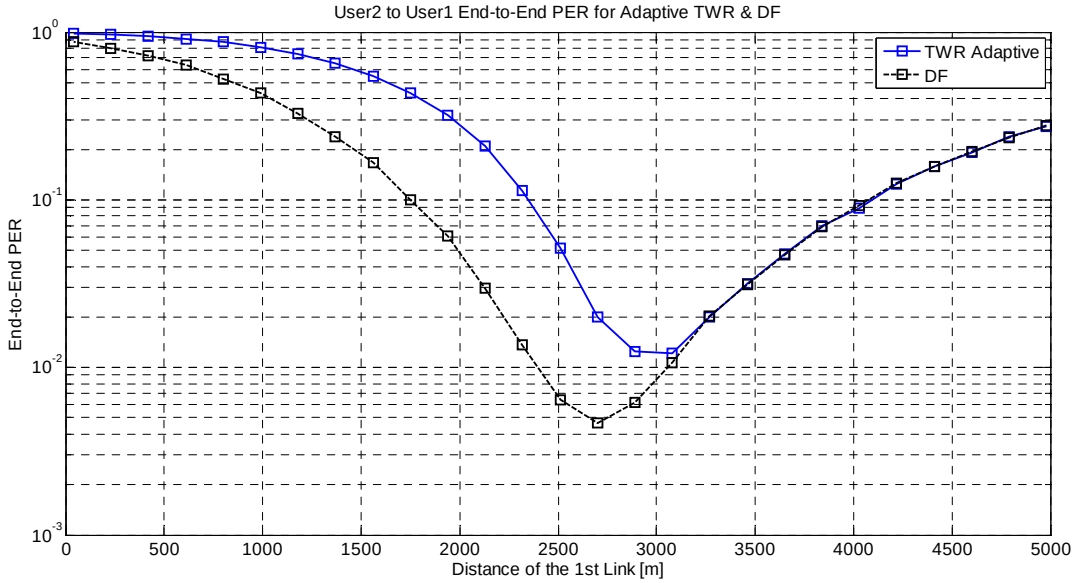

Figure 44: End-to-End PER U2 to U1, ETU, 1% location variability, NF=7 dB, 5000 m between users, single end-to-end transmissions, 1W maximum Tx power for user, 10W maximum Tx power for MR.

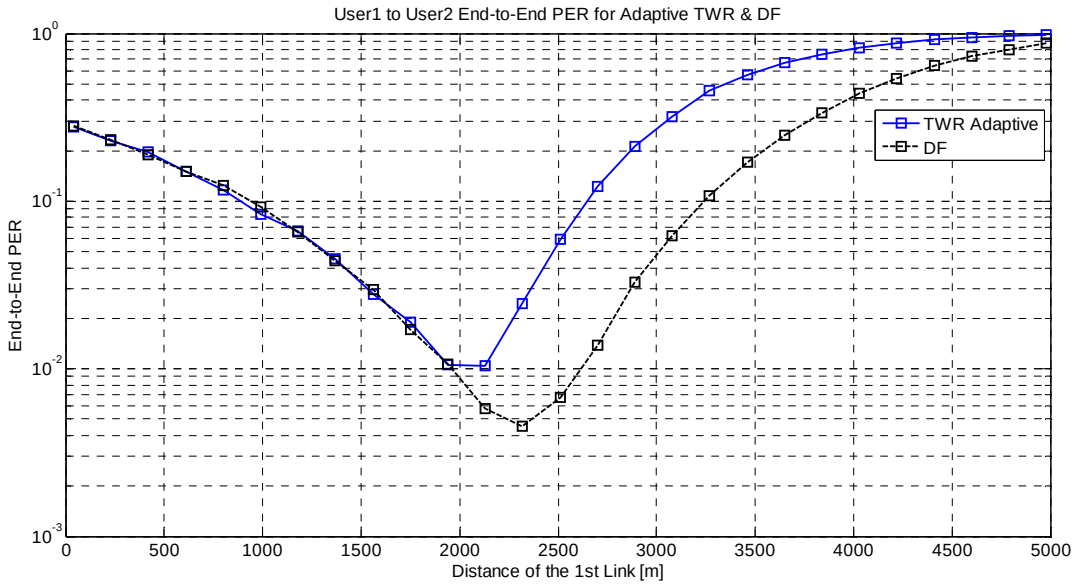

Figure 45: End-to-End PER U1 to U2, ETU, 1% location variability, NF=7 dB, 5000 m between users, single end-to-end transmissions, 1W maximum Tx power for user, 10W maximum Tx power for MR.

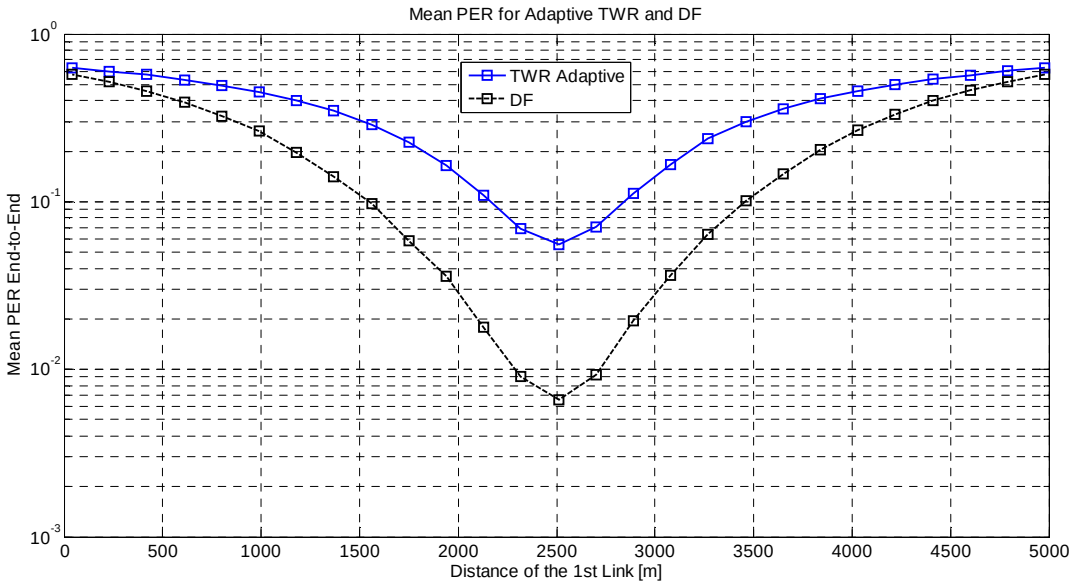

Figure 46: Mean PER, ETU, 1% location variability, NF=7 dB, 5000 m between users, single end-to-end transmissions, 1W maximum Tx power for user, 10W maximum Tx power for MR.

5.5 Discussion and conclusions

The focus of the work was at PHY / MAC layer on relaying strategies for inter-cluster communications, namely for the traffic going through bridging MRs. The bridging relay can be used between multiple users or between different base stations. In wireless mesh networks for fast deployable PMR systems, since the back-bone traffic is going through those MRs, and part of it may be bidirectional, we investigated a two-way relaying technique applied to the bridging MRs. Implementation of Two-Way Relaying (TWR) strategy needs the presence of a bi-directional flow between the CHs of the neighboring clusters. LTE adaptation or design of new signaling and possibly protocols required to share the needed information between CHs will not be investigated in this deliverable.

Two-Way-Relaying has been compared with a traditional Decode-and-Forward strategy for two main deployment scenarios:

A) A scenario with a smaller frequency bandwidth for MR, a larger ISD and a lower location variability (corresponding to a smaller city for example, with lower number of users and lower roof-top height);

B) A scenario with a larger frequency bandwidth for MR, a smaller ISD and a higher location variability (corresponding to a more populated city for example, with higher number of users and higher roof-top height – predominant NLOS scenario).

These categories have been defined by taking into account architecture opportunities and real-deployment situations. Real 3GPP and ITU parameters and system constraints have been also considered: the 700 MHz band was considered for simulations since it is one of the main candidate bands for deployment of the future broadband PMR networks. Scenarios A and B show that TWR provides better throughput than DF, for any possible position of a MR. TWR typically doubles the throughput at the best MR position. In scenario A, TWR achieves significant throughput gains only for certain distances (typically the MR must be placed in between the served nodes). However, for more dense urban deployments like scenario B, throughput gains are weakly sensitive to the MR position, which is a desired feature in rapidly deployable PMR systems. It is also shown that DF is more robust than TWR in terms of end-to-end PER (e.g. DF has better or equal PER than TWR, depending on the MR position).

This section also investigated a best-case scenario for a PMR deployment in the case of voice services. In this case it is showed that for long-distance robust communications (e.g. up to 5 km) where maximum limit for the achievable throughput is not of interest, the DF technique is an interesting approach.

6 Fair resource allocation for multi-hop communications

6.1 Scenario: Clustered wireless mesh networks based on LTE

The aim of this scenario is to study the performance of wireless mesh network (or network extensions) based on LTE. 3GPP is working actively on Private Mobile Radio (PMR) systems, in order to provide LTE solutions to this market. However PMR systems have very often completely different requirements and use cases, with respect to traditional cellular communications. Much more emphasis is given, for instance, to security, reliability and robustness of the communication, rather than throughput.

The scenario focuses on rapidly deployable wireless mesh networks, to be used to cover an area which is not covered by fixed PMR infrastructure. It could be the case after a major natural disaster. Another possible use case is to deploy a wireless network in areas without any infrastructure, or where the main governmental or market actors do not want to invest on a wired infrastructure. A third use case, similar to coverage extension with relays, is when there is a specific and limited area which is not covered by the fixed network, then a wireless extension can be imagined with possibly multiple relays. Here we will focus on the first use case.

In order to reuse as much as possible the LTE structure and protocols, we propose a clustered wireless mesh network meaning that the network is divided in clusters, mapping (or equivalent) to LTE macro (or micro, depending on the available transmit power, type of equipment, etc.) cells. Each cell is controlled by a ClusterHead (CH) which is acting as a 3GPP eNodeB. Mesh Routers (MR) are acting as relays, and inherit relay and UE procedures from LTE. Some MRs, connected to 2 or 3 clusters, are called bridging MRs and allow communications between the clusters. Common bridging MRs between the clusters can cooperate for improving performance (robustness, throughput, latency). Edge MRs are possibly present, if the wireless mesh network is not independent but is linked to other networks via other technologies. A schematic representation of the clustered mesh network is given in the figure below.

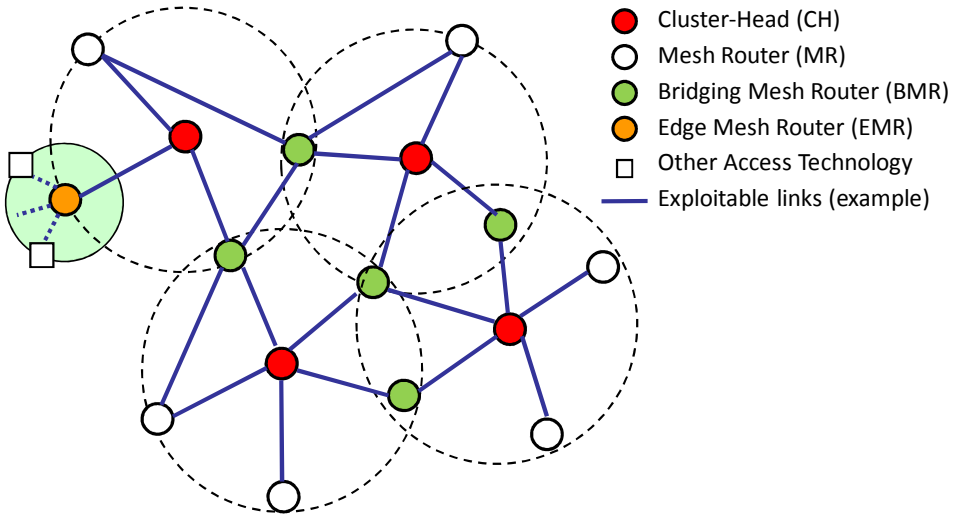

Figure 47: Clustered wireless mesh network

6.2 Challenges

A challenging aspect of this scenario is the design of adequate radio resource strategies that are able to efficiently exploit the benefit brought by the use of cooperative relaying techniques in this networking setting. Scheduling algorithms are of vital importance in today and future wireless communication systems. They are responsible for efficiently sharing scarce and expensive radio spectrum among different users while handling heterogeneous traffic demands and dealing with disparate radio conditions. Another challenge here is that we allow for direct communication inside a given cluster and, possibly, multiple hops inside the same cluster, always under the control of the CH. Please notice that the results described in the following subsections can also be applied to a cell in which direct communications are allowed.

6.3 Innovation: Fair joint scheduling/relaying schemes for multi-hop/mesh communications

We consider efficient and fair opportunistic scheduling of delay tolerant traffics in clustered/cellular environment with dynamic relaying. A wide range of nowadays applications generate this type of traffic, i.e. email, internet browsing, asynchronous file transfer, etc. They are generally classed as requiring a best effort service and give more flexibility to the system to handle them.

Indeed, for traffic presenting such property it has been shown that scheduling at each slot the user undergoing the best radio conditions in fading environment maximizes the overall system throughput in the saturated regime, this is known as the multiuser diversity scheduling (MUDS) [73]. Multiuser diversity comes from the fact that in a wireless communication system the fading channels between the base station and each user undergo independent variations, and then it's likely to always find a user with channel in good radio state. However, the maximization of throughput in MUDS comes at the expense of fairness in the offered throughput as strong users are more often served than weaker ones.

Proportional fair scheduling (PFS) algorithm has been introduced as an attractive solution to the problem since it provides a good compromise between throughput maximization and service fairness [74][75][76]. The idea behind PFS is to ensure more fairness to scheduling by normalizing the instantaneous achievable radio rate by the past average throughput in the cost function of each user. The algorithm is widely used in current cellular systems and exhibits also low implementation complexity which increases its attractiveness, and tends to achieve perfect temporal fairness as the network size increases.

Scheduling algorithms based on the cumulative distribution function (CDF) of users' rates have been introduced in [77][78][79] to better benefit from multiuser diversity while offering perfect temporal fairness even for reduced number of users. Unlike PFS, in cumulative distribution function fair scheduling (CFS), the decision is based on the knowledge of the CDF of users' rates in order to grant channel access to users when they are near their own peaks. These algorithms exhibit good performance in terms of throughput and fairness, their main drawback however is their requirement to have knowledge of the CDF of the users' rates.

Recently, a maximum proportional fair scheduling (MPFS) algorithm has been proposed [80] based on the principle of CFS. The new scheme schedules the users when they are experiencing their best channels compared to their own past channels. Thus the knowledge of the CDF of users' rates is avoided.

In this work we propose to extend the 3 opportunistic schedulers MUDS, PFS, and MPFS to the case of clustered/cellular to consider joint opportunistic scheduling and dynamic relay selection in single channel block fading setting.

6.3.1 System setting

We consider a wireless communication system consisting in a single cluster having K users uniformly distributed around the CH in a circle of radius *R*. We consider a block fading channel of width W (one sub-channel in a multicarrier system) in a time-slotted manner (time division multiple access). We assume that the channel gains are independent but not necessarily identically distributed across the users. We further assume that the channel gains remain constant during each slot but change from one slot to another, and we assume that the scheduler has perfect information of the fading processes of each radio link in the cluster.

Let $h_{u,v}^n$ denotes the state of the radio channel between users u and v at slot n and $r_{u,v}^n = log_2(1+\beta\frac{h_{u,v}^n}{N0})$ the transmission rate between users u and v at slot n, where N_0 is the thermal noise power and $0<\beta<1$ the SNR gap between the considered transmission system and its Shannon capacity limit.

In case where $h_{u,v}^n$ are Rayleigh distributed, the Probability Density Function (PDF) of $h_{u,v}^n$ is given as

$$P\left(h_{u,v}^n = x\right) = \frac{1}{Pr_{u,v}} e^{-\frac{x}{Pr_{u,v}}}$$

Where $Pr_{u,v}$ is the mean received power between u and v

$$Pr_{u,v} = Pt\left[\frac{d0}{d_{u,v}}\right]^{pl}$$

Pt is the transmit power, $d0$ is the minimum distance between any couple of users, and pl is the power loss factor.

We consider that each user has one delay tolerant traffic flow $f_{u,v}$ toward one of the $K-1$ other users. Traffic flows are in saturated traffic regime, i.e., each scheduled user has more data in its queue than the scheduled transmission rate.

6.3.2 Opportunistic schedulers

6.3.2.1 Maximum Multiuser Diversity Scheduling

The long-term average throughput of this system is maximized by scheduling on each slot the user with the best channel gain, exploiting hence fully the multiuser diversity of the system [73]. We call this scheme maximum multiuser diversity scheduling [73]. The winner user w is the one satisfying

$$w = argmax_{u=1,..,K} r_{u,v}^{n}$$

It is well known that the benefit of multiuser diversity, in term of increases of system's spectral efficiency, comes at the expense of poor fairness among the users' scheduling probabilities and achieved throughputs. Indeed, the channel gains of the different users are not equally distributed (due to different distances to base station, scattering environment, mobility, etc.) and the MUDS will advantage the strongest ones.

6.3.2.2 Proportional Fair Scheduling

The Proportional Fair Scheduling was introduced in [74][75][76] in order to take advantage of multiuser diversity while providing good fairness level of channel access among users. The idea behind it is to normalize the score function of each user, i.e. user rate, by its average. Hence, the scheme schedules the user who is experiencing the best fading realization compared to its own past conditions, and not the user with the absolute best instantaneous rate.

The algorithm works as follows:

$$w = argmax_{u=1,..,K} \frac{r_{u,v}^{n}}{RT_{u,v}^{n}}$$

$$Where\ RT_{u,v}^{n} = \begin{cases} \left(1-\frac{1}{Tc}\right) RT_{u,v}^{n-1} + \frac{1}{Tc} r_{u,v}^{n} & if\ link\ (u,v)\ is\ scheduled \\ \left(1-\frac{1}{Tc}\right) RT_{u,v}^{n-1} & otherwise \end{cases}$$

Tc $(\mathrm{Tc} > 1)$ is the length of the moving average window, in normalized units depending on the periodicity of scheduling.

One observes that the normalization is done with respect to the average of past *scheduled* rates and not past *achievable* rates. Indeed, averaging with respect to the average scheduled rate gives to the algorithm the proportional fairness property. Thus, the scheme does not only schedule the user who is near its peak rate as commonly agreed, but also the one who has not been scheduled for sufficiently large time (depending on the value of 'Tc'), losing hence the benefit of multiuser diversity. The loss in throughput may be significant in case where users are scattered across a large cell.

Moreover, even if we normalize by the average past achievable rate we will be far from exploiting sufficiently the multiuser diversity as the scheduler will only choose the user who is near its mean rate and not its peak rate.

6.3.2.3 Maximum Proportional Fair Scheduling

The maximal proportional fair scheduling was introduced in order to well benefit from multiuser diversity while still providing good level of fairness among users [80].

Here, the users compete for the channel by normalizing their instantaneous achievable rate over their past maximal achievable rate.

Unlike the MUDS where the user with the best instantaneous rate is selected, in MPFS the winner is not necessarily the strongest one but the one who is likely experiencing its best radio conditions. And unlike CFS where the empirical distribution of rate is used to select the winner, in MPFS only the maximal value of past rates is used.

The algorithm is defined as follows:

$$w = argmax_{u=1,..,K} \frac{r_{u,v}^{n}}{Rmax_{u,v}^{n}}$$

$$Where\ Rmax_{u,v}^{n} = max_{m=0\dots M-1}\ r_{u,v}^{n-m}$$

$Rmax_{u,v}^{n}$ is a dynamic threshold value around which the user's channel is considered as in its peak region, and M is the depth of moving average window.

6.3.3 Fair joint opportunistic scheduling and dynamic relaying

As opportunistic scheduling tries to exploit multiuser diversity to enhance the transmission efficiency, joint opportunistic scheduling and dynamic relaying is able to exploit also spatial diversity to enhance the overall network multiuser diversity.

In the context of clustered/cellular networks allowing Device to Device (D2D) communications, dynamic relaying will give the scheduler the choice between classical uplink/downlink through CH/BS transmission scheme, direct link transmission scheme, or dynamic one hop relay transmission scheme. Figure 48 describes the different relaying options offered to the scheduler.

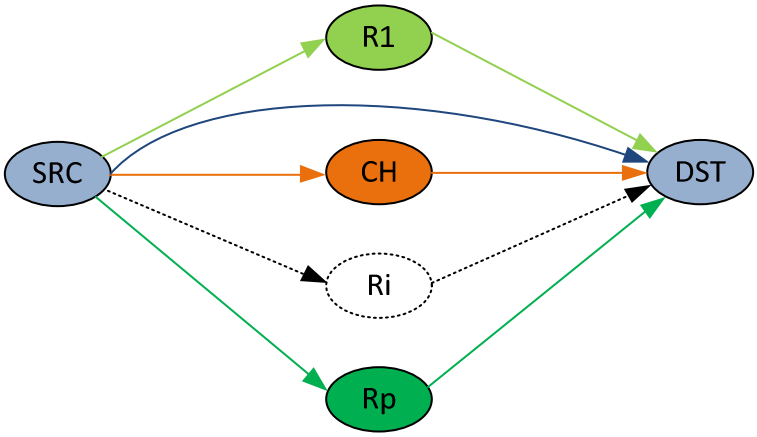

Figure 48: Dynamic relay selection

For each flow $f_{u,v}$ the scheduler compares the different relaying options using a max-min rule as follows

$$SF_{f_{u,v}}^{n} = max\left(Sc_{u,v}^{f_{u,v},n}, min(Sc_{u,R_{n,1}^{u,v}}^{f_{u,v}n}, Sc_{R_{n,1}^{u,v},v}^{f_{u,v}n}), \dots, min(Sc_{u,R_{n,p}^{u,v}}^{f_{u,v}n}, Sc_{R_{n,p}^{u,v},v}^{f_{u,v}n})\right)$$

where

- $\mathrm{Sc}_{a,\mathrm{b}}^{f_{u,v}\mathrm{n}}$ is the score function of the radio link between users a and b at slot n when transporting flow $f_{u,v}$
- $\mathrm{R}_{\mathrm{n,i}}^{\mathrm{u,v}}$; $\mathrm{i} = 1 \dots \mathrm{p}$; are the available relays between users u and v at slot n (the CH is always a candidate relay for any flow).

The scheduler allocates then the channel to the flow achieving the best score

$$w = argmax_{u=1,,K} SF_{f_{u,v}}^{n}$$

Depending on the relaying strategy of the winning flow $f_{u,v}$, the scheduler allocates the channel as follows:

- The channel is allocated during the whole slot to the link if the transmission is not relayed with rate $r_{u,v}^{n}$
- Otherwise, the first half of the slot is allocated to the link between the source and the selected relay and the second half to the link from the selected relay to the destination. We assume no queuing at the relays so the two links are allocated with rate $\min(r_{u,R}^{n} r_{R,v}^{n})$

The score functions of the different opportunistic scheduler are given in the following:

- MUDS

$$Sc_{a,b}^{f_{u,v},n} = r_{a,b}^{n}$$

- PFS

$$Sc_{a,b}^{f_{u,v},n} = \frac{r_{a,b}^{n}}{R_{f_{u,v}}^{n}}$$

$$RT_{f_{u,v}}^{n} = \begin{cases} (1-1/Tc)RT_{u,v}^{n-1} + rs_{f_{u,v}}^{n}/Tc\,,\ if\ f_{u,v}\ \ is\ scheduled\ at\ "n" \\ (1-1/Tc)RT_{u,v}^{n-1},\ Otherwise \end{cases}$$

$$rs_{f_{u,v}}^{n} = \begin{cases} r_{u,v}^{n} \quad , \quad if\ direct\ transmission \\ \dfrac{r_{u,R}^{n} + r_{R,u}^{n}}{2} \quad , \quad if\ relayed\ through\ R \end{cases}$$

- MPFS

$$Sc_{a,b}^{f_{u,v},n} = \frac{r_{a,b}^{n}}{RM_{f_{u,v}}^{n}}$$

$$RM_{f_{u,v}}^{n} = max_{m=n,\dots,n-M+1}\ max\left(r_{u,v}^{m}, min(r_{u,R_{n,1}}^{m}, r_{R_{n,1},v}^{m}), \dots, min(r_{u,R_{n,p}}^{m}, r_{R_{n,p},v}^{m})\right)$$

6.4 Results

We consider users uniformly distributed around the CH within a range of $Dmax = d0.10^{-\frac{\Delta p}{10pl}}$, where Δp is the maximum SNR difference in dB between the strongest user and the weakest user in the network.

For our simulation we consider $\Delta p = 20dB,\ Pt = 10,\ Tc = 500$ and $M = 500$.

Figure 49 depicts the network's spectral efficiency achieved by MUDS, PFS, and MPFS for the 3 considered relaying schemes for different cluster size.

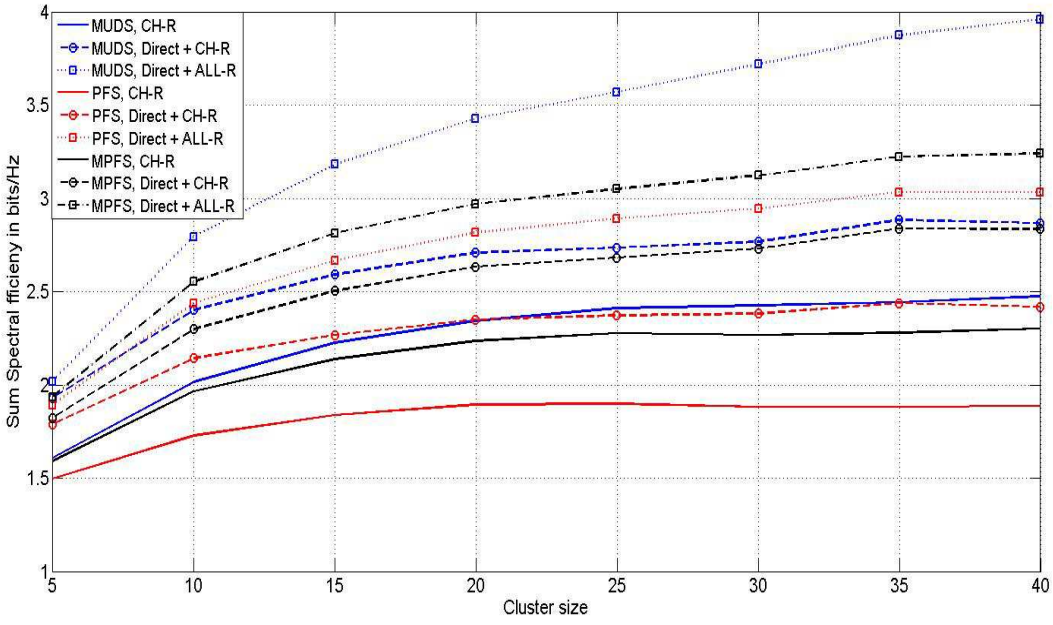

Figure 49: Spectral efficiency, i.e. the average of the network sum rate over simulation time, in saturated regime

We observe then that MUDS outperforms MPFS and largely outperforms PFS when only the CH is relaying ('CH-R' in the legend of the figure). Then we observe that allowing both direct transmission and relaying through the CH ('Direct + CH-R' in the legend of the figure) increases the spectral efficiency of

all schemes and help MPFS to approach the performance of MUDS. Last, we observe that when allowing direct transmission and relaying through any node in the network ('Direct + All-R' in the legend of the figure) the performances of the three schemes are further improved and that MUDS largely outperforms MPFS as it is exploiting now much more multi-user diversity.

The second relaying scheme represents the best trade-off between performance and signalling overhead while the third relaying scheme, despite is very good performance, is much more unrealistic as it requires a huge amount of radio channels statistics feedback. As a matter of fact, when considering direct+CH scheme the source node feedbacks only information about its link to the destination node, assuming channel reciprocity. Only this information is needed by the CH which will then decide if the communication should be direct between the source and destination or should pass through itself. In direct+ALL-R scheme, all nodes needs to feedback information about all their links in order to select the best path.

The gain in throughput brought by efficient opportunistic schedulers comes obviously at the expense of fairness. To evaluate this fairness we use as measure the Jain Fairness Index (JFI) [81][81] defined for a set '$x = \{x_1, .., x_k\}$' of 'N' elements as

$$JFI(x) = \frac{(\sum x_k)^2}{N \sum x_k^2}$$

The index varies between '1/N' in the worst fairness case and '1' in the perfect one. The x-axis is the access probability in saturated regime.

Figure 50 shows the JFI in term of channel's access probability of the three schedulers using the three relaying schemes.

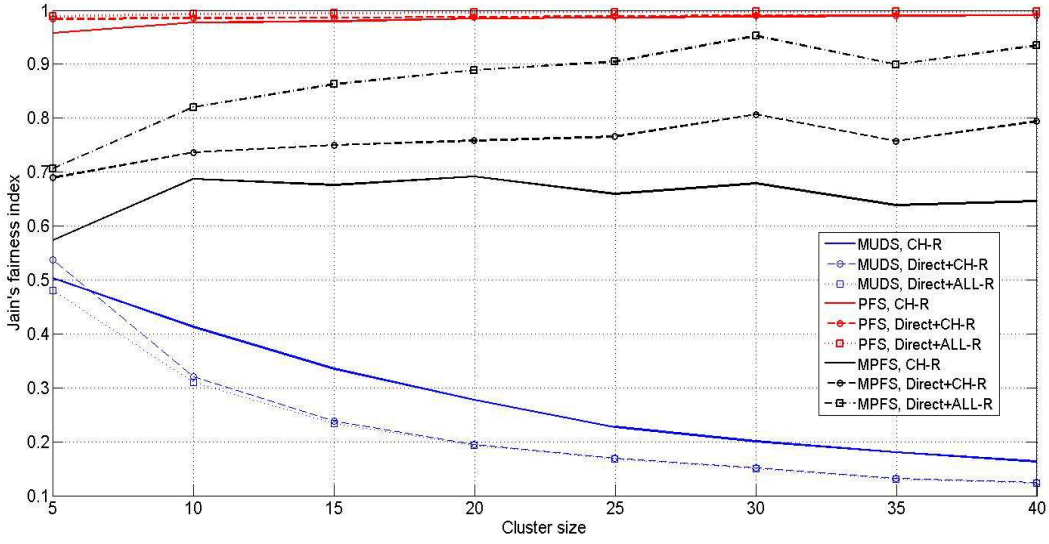

Figure 50: JFI on channel access probability in saturated regime

As expected, MUDS achieves the worst fairness and PFS the best possible one, while MPFS presents a good fairness above 70%. We observe also that increasing the number of possible relays help increasing the fairness of MPFS as pairs of source/destination radio links will share more relays.

6.5 Discussion and conclusion

In this section we provided a new class of joint scheduling/relaying algorithms for delay tolerant traffic.

The joint scheduling and relaying is based on a dynamic max-min decision rule of the best relay for different opportunistic schedulers. The considered opportunistic schedulers are MUDS, PFS, and MPFS.

Simulation results showed that increasing the number of possible relays increases the spectral efficiency of the three schemes and help also enhancing the fairness of PFS and MPFS.

7 Conclusions

This section draws the main conclusions of the document and gives recommendations issued of the studies.

Section 2 was dedicated to the review and investigation of the accuracy of available path loss models for relay deployment. It was pointed out how current models does not have often a clear dependence on the relay station height, which is a parameter influencing in a critical way the results. A measurement campaign was conducted in two locations of Belfort, a typical French medium urban city with 3-5 story buildings. The general recommendations presented here may change with large cities which include large avenues and high-rise buildings. The collected measurements were pre-processed and the resulting data was used to draw intermediate conclusions for each individual link (BS-RS, BS-MS, RS-MS). The final recommendation of the study is that, for the propagation environment of a medium urban city, the ITU [6] models defined for macrocell and microcell environment for LOS and NLOS conditions give the best performance. The recent 3GPP 3-D UMi and Uma models [9] defined for 3-D simulations may also be recommended as they are based on the ITU UMi and Uma [6] models, respectively. Those models shall the preferred ones for system-level simulations with relays in urban environment. Moreover, for the RS-MS link in NLOS conditions, where even the most accurate existing model is not satisfactory at short and long distances, a new general equation of the PL model was derived with an explicit dependence on the RS height. Another conclusion of this study is that the PL models for the RS-MS link (i.e. in microcell environment) depend on the environment that is around the relay, for instance, the presence of vegetation of not. For recommendations on such finer details, the reader can refer to the publications issued from this work and quoted in the section.

Section 3 presents a cooperative coding scheme to communicate efficiently over multiple-relay fading channels with applications to OFDM or narrowband communications. The particularity of the presented approach is to rely on non-binary Low Density Parity Check (NB-LDPC) codes at the source, coupled with non-binary repetition codes at the relays. In the proposed scheme, the source broadcasts a NB-LDPC codeword to the destination and the relays. When the relays successfully decode the received word, extra parity symbols are computed at the relays through optimized non-binary repetition codes, which are then sent to the destination. Part of the work precisely consists in the optimization of the code at the source and of the repetitions at the relays (for non-binary codes, repetition may in fact be different from a simple copy of the bits). The receiver collects the original received word from the source and the non-binary extra symbols from the relays and combines them before the iterative decoding. While for current methods, decoding complexity increases with the number of relays, the proposed scheme has the attractive feature of having a constant iterative decoding complexity in presence or absence of relays. Moreover, schemes in the state of the art show coding gains which become less important when the number of relays increases, while the present approach brings an effective coding gain and maintains a constant gap to the outage probability of the cooperative system, irrespective of the number of relays. As future work, the use of Network-Coding at the relays will be investigated as a means of reducing the traffic load on the relay-to-destination links, while providing the users with significant diversity gain brought by the use of multiple relays.

Section 4 deals with two main scenarios of relay assisted communications in the framework of LTE-A. In the first scenario a wireless network was analyzed where a DeNB communicates with a UE across a Gaussian channel and is assisted by multiple relays operating in half duplex mode. The first part of the work focused on theoretical studies about the capacity of this network which was characterized to within a constant gap, uniformly over all possible choices of channel gains, by using Noisy Network Coding (a generalization of the Compress and Forward strategy) as achievable scheme. For such networks, the capacity achieving scheme must be optimized over a number of possible listen/transmit configurations of the relays, which is exponential in the number of the relays. It was formally proved that the approximately optimal (achieving the cut-set outer bound to within a constant gap) relays schedule (i.e. which relays are active or not) has a number of active states which is equal to the number of relays plus one, thus reducing considerably the complexity of the problem.

The second part of the contribution of this scenario considers the particular case of a single relay network assuming that the UE can receive a signal from the DeNB. Three coding schemes, namely partial decode-and-forward, compress-and-forward and a two-phase three-message strategy were analyzed in terms of gaps to the cut-set upper bound. In particular the last newly proposed strategy achieves the cut-set upper bound on the capacity to within a constant finite gap, uniformly for all channel parameters. It was also pointed out an interesting practical tradeoff between the coding scheme complexity and the gap, with lower gaps for more complex schemes. We discussed both the case of deterministic and random switch at the relays, by showing that, in general, random switch increases the achievable rate at the expense of more complex coding and decoding schemes.

The final contribution of this first scenario consisted in evaluating the two-phase three-message strategy by using codes as in the LTE standard and by running simulations on an LTE test bench (Eurecom's OpenAirInterface). This scheme uses superposition encoding, decode-and-forward relaying and successive interference cancellation in order to send three messages in two time slots from a DeNB to a UE with the help of a relay, which forwards one of the three messages. Comparisons between the theoretical achievable rate with (point-to-point capacity achieving) Gaussian codes and the rate achieved in a practical scenario were provided for a BLER of 10^{-2}. In addition, a baseline scheme was also considered where the DeNB-UE link is absent. The rate performance of this scheme, which mimics the one implemented in today's wireless networks, was shown to be inferior to that of the proposed scheme, implying that physical layer cooperation brings throughput gains. The work done, besides the important theoretical achievements, can also be considered a first important step towards the evaluation of the practical feasibility of these new relay-assisted coding strategies.

The second scenario is a Gaussian relay-aided broadcast channel, a system where a DeNB communicates with multiple users across a Gaussian channel with the help of a full duplex relay, under the assumption full channel state knowledge at all the nodes in the network. First the generalized degree of freedom was derived in closed-form for the case with 2 relays. The generalized degree of freedom is a quantity related to the capacity of the system, namely the pre-logarithmic factor of the sum-capacity, which is an indicator of the throughput at high SNR. Then the set of parameters was identified where the system achieves the same the generalized degree of freedom of the classical relay and broadcast channels. We finally highlighted under which channel conditions the generalized degree of freedom attained by the system is the same as that of a MIMO system with two transmit antennas and two single-antenna UEs, i.e., when the DeNB and the RN create a virtual or distributed MIMO system. In particular, we discussed how the DeNB→RN link should be dimensioned in order to attain the gDoF predicted by MIMO.

Then a more general setting was considered with a number *K* of UEs and it was proved that serving at most 2 UEs (among the *K* possible ones) is gDoF-optimal. This choice was shown to depend on the values of the channel parameters. An interesting connection between information theory and graph theory, namely "the problem of finding the gDoF is equivalent to solving two Maximum Weighted Bipartite Matching problems and taking the minimum among the two solutions", was also shown. This represents the most appealing feature of our scheduling algorithm, since there exist algorithms for solving such a problem in polynomial-time.

Section 5 focuses on clusterized mesh networks for PMR systems. In this context, in the particular case of fast deployable systems e.g. for crisis management, there can be absence of wired back haul between the cells, called here clusters, and hence inter-cluster communications are taken in charge by some relay nodes called bridging mesh routers (MR). Since the back-bone traffic is going through those relay nodes, and part of it may be bidirectional, a two-way relaying technique was investigated and compared to a more traditional decode-and-forward strategy. Results are presented for two main deployment scenarios. The first one, scenario A, has a lower frequency bandwidth for MR, a higher inter-site distance and a lower location variability (corresponding to a smaller city for example, with lower number of users and lower roof-top height). The second one, scenario B, has a higher MR frequency bandwidth, a lower ISD and a higher location variability (corresponding to a more populated city for example, with higher number of users and higher roof-top height – predominant NLOS scenario Real 3GPP and ITU parameters and system constraints have been also considered, for example, the 700 MHz band was considered for simulations since it is one of the main candidate bands for deployment of the future broadband PMR networks. Scenarios A and B show that TWR provides better throughput than DF, for any possible position of a MR. TWR typically doubles the throughput at the best MR position. In scenario A, TWR achieves significant throughput gains only for certain distances (typically the MR must be placed in between the served nodes). However, for more dense urban deployments like scenario B, throughput gains of the TWR strategy are weakly sensitive to the MR position, which is a desired feature in rapidly deployable PMR systems. It is also shown that DF is more robust than TWR in terms of end-to-end PER (e.g. DF has better or equal PER than TWR, depending on the MR position). Finally, a scenario for a PMR deployment in the case of voice services was tested for long-distance robust communications (e.g. up to 5 km). In this case, in which coverage elongation, instead of peak throughput, is of interest, the DF technique remains an interesting approach.

Section 6 deals with resource allocation for multi-hop communications inside a cell or cluster, for applications to PMR context. Scheduling algorithms are of vital importance in today and future wireless communication systems. They are responsible for efficiently sharing scarce and expensive radio spectrum among different users while handling heterogeneous traffic demands and dealing with disparate radio conditions. In PMR systems relaying and direct communications between users are features which are particularly appreciated by the customers since they are included by the legacy PMR standards. In this section a wireless communication system consisting in a single cluster having multiple

users is considered. The study provided a new class of joint scheduling/relaying algorithms for delay tolerant traffic. The work extends three scheduling policies to this new framework; the new proposal is based on a dynamic max-min decision rule of the best relay for different opportunistic schedulers. Three considered opportunistic schedulers are investigated here: multi-user diversity scheduling, proportional fair scheduling, and maximum proportional fair scheduling. In order to differentiate the impact of relaying on performance a comparison is made among the case when all the communications pass mandatorily through the cluster head, which is the traditional configuration, the case in which also direct communications between users are allowed, and finally the case in which any user can be a relay. Simulations were run for increasing number of users inside the cluster under full-buffer assumptions. The maximum proportional fair scheduler achieved the most interesting compromise between the aggregated rate over the cell and the fairness. Also, it was shown that allowing all the users being a relay brings an interesting diversity advantage which however can be exploited only if an additional complexity is accepted in the system. Finally, increasing the number of possible relays increases the spectral efficiency of the three schemes and help also enhancing the fairness of the maximum and traditional proportional fair scheduling.

8 List of Abbreviations, Acronyms, and Definitions

3GPP	3rd Generation Partnership Project
AF	Amplify-and-Forward
BER	Bit Error Rate
BLER	BLock Error Rate
BP	Belief Propagation
BS	Base Station
CB	Circular Buffer
CDF	Cumulative Distribution Function
CF	Compress-and-Forward
CFS	CDF Fair Scheduling
CH	Cluster Head
CRC	Cyclic Redundancy Check
CSI	Channel State Information
D2D	Device-to-Device
DeNB	Donor evolved NodeB
DF	Decode-and-Forward
DL	DownLink
DL-SCH	DownLink Shared CHannel
eNB	Evolved NodeB
EPA	Extended Pedestrian A
ETU	Extended Typical Urban
FD	Full Duplex
FER	Frame Error Rate
FDD	Frequency Division Duplex
FS	Free Space
gDoF	generalized Degree of Freedom
HD	Half Duplex
IMT	International Mobile Communications
IST	Inter-Site Distance
ITU	International Telecommunication Union
ITU-R	International Telecommunication Union-Radio
JFI	Jain Fairness Index
KPI	Key Performance Indicator
LDPC	Low Density Parity Check
LLR	Log-Likelihood Ratio
LOS	Line of Sight
LTE	Long Term Evolution
LTE-A	Long Term Evolution - Advanced
MAC	Medium Access Control

MCS	Modulation and Coding Scheme
MF	Matched Filter
MIMO	Multiple Input Multiple Output
MPFS	Maximum Proportional Fair Scheduling
MR	Mesh Router
MS	Mobile Station
MUDS	Multi User Diversity Scheduling
MWBM	Maximum Weighted Bipartite Matching
NB-LDPC	Non-Binary Low Density Parity Check
NC	Network Coding
NLOS	Non Line of Sight
NNC	Noisy Network Coding
OFDM	Orthogonal Frequency-Division
PD&F	Partial Decode-and-Forward
PDF	Probability Density Function
PDSCH	Physical Downlink Shared CHannel
PER	Packet Error Rate
PFS	Proportional Fair Scheduling
PHY	Physical
PL	Path Loss
PMR	Private Mobile Radio
PPDR	Public Protection and Disaster Relief
PRB	Physical Resource Block
QAM	Quadrature Amplitude Modulation
QPSK	Quadrature Phase Shift Keying
QoS	Quality of Service
RAN	Radio Access Network
RB	Resource Block
RE	Resource Element
RN	Relay Node
RS	Relay Station
RV	Redundancy Version
SDMA	Spatial Division Multiple Access
SIC	Successive Interference Cancellation
SINR	Signal to Interference plus Noise Ratio
SNR	Signal to Noise Ratio
TB	Transport Block
TBS	Transport Block Size
TDD	Time Division Duplex

TTI	Transmission Time Interval
TWR	Two-Way Relaying
UE	User Equipment
UHF	Ultra High Frequency
UL	UpLink
UMTS	Universal Mobile Telecommunications System
XOR	eXclusive OR
WiFi	Wireless Fidelity
WINNER	Wireless World Initiative New Radio
WP	Work Package

9 References

[1] D. Soldani and S. Dixit, ”Wireless Relays for Broadband Access,” Communications Magazine, IEEE, vol. 46, pp. 8, Mar. 2008.

[2] J. Sydir and R. Taori, “An Evolved Cellular System Architecture Incorporating Relay Stations,” Communications Magazine, IEEE, vol 47, pp.115, June 2009.

[3] R. Pabst, B. H. Walke, D. C. Schultz, P. Hernold, H. Yanikomeroglu, S. Mukherjee, H. Viswanthan, M. Loot, W. Zirwass, M. Dohler, H. Aghvami, D. Falconer, G. P. Fettweis, “Relay-Based Deployment Concepts for Wireless and Mobile Broadband Radio,” Communications Magazine, IEEE, vol. 42, pp. 80, Sept. 2004.

[4] 3GPP, "Further advancements for E-UTRA physical layer aspects," http://www.3GPP.org, vol. TR 36.814 V9.0.0, March 2010.

[5] WINNER project, "IST-4-027756 WINNER II D 1.1.2 v1.2, WINNER II Channel Models," 2006.

[6] ITU report, "ITU-R M.2135: Guidelines for evaluation of radio interface technologies for IMT-Advanced," June 2006.

[7] Q. H. Chu, ‘‘A contribution to the multi-link propagation channel modeling for 4G radio mobile relaying systems’’ PH.D Thesis, Paris, 2011.

[8] I. Maaz, J-M. Conrat and J-C. Cousin, ‘‘Path Loss Models in LOS Conditions for Relay Mobile Channels,’’ 8th European Conference on Antennas and Propagation, The Hague, The Netherlands, April 2014.

[9] 3GPP, "Technical Specification Group Radio Access Network Study on 3D Channel Model for LTE," (Release 12) http://www.3GPP.org, vol. TR 36.873 V1.3.0, February 2014.

[10] COST 231, Digital mobile radio towards future generation systems, final report," technical report, European Communities, EUR 18957, 1999.

[11] “CELTIC/CP5-026 WP5 v1, WINNER+ Final Channel Models,” http://projects.celtic-initiative.org/winner+/, 2008.

[12] Q. H. Chu, J. M. Conrat, and J. C. Cousin, "Propagation path loss models for LTE-advanced urban relaying systems," International Symposium on Antennas and Propagation (APS-URSI), Spokane, 2011.

[13] J-M Conrat, Q.H. Chu, I. Maaz, J-C Cousin, “Path Loss Model Comparison for LTE-Advanced Relay Backhaul in Urban Environment, ” 8th European Conference on Antennas and Propagation, The Hague, The Netherlands, April 2014.

[14] TSG-RAN WG1 #75, “Shadow fading modeling for microcell scenarios based on a measurement campaign”, San Francisco, USA, 11th–15th November 2013.

[15] I. Maaz, J-M. Conrat and J-C. Cousin, ‘‘Path Loss Models in NLOS Conditions for Relay Mobile Channels,’’ IEEE 80th Vehicular Technology Conf. (VTC 2014-Fall), Vancouver, Canada, September 2014.

[16] A. Sendonaris, E. Erkip, and B. Aazhang, “User cooperation diversity. Part I. System description,” IEEE Trans. on Communications, vol. 51, no. 11, pp. 1927–1938, 2003.

[17] A. Sendonaris, E. Erkip, and B. Aazhang, “User cooperation diversity. Part II. Implementation aspects and performance analysis,” IEEE Trans. on Communications, vol. 51, no. 11, pp. 1939–1948, 2003.

[18] J.N. Laneman, D.N. Tse, and G.W. Wornell, “Cooperative diversity in wireless networks: efficient protocols and outage behaviour,” IEEE Trans. on Information Theory, vol. 50, no. 12, pp. 3062–3080, 2004.

[19] C.Wang, Y. Fan, J. Thompson, and H. Poor, “A comprehensive study of repetition-coded protocols in multi-user multi-relay networks,” IEEE Trans. on Wireless Comm., vol. 8, no. 8, pp. 4329–4339, 2009.

[20] M.N. Khormuji and E.G. Larsson, “Cooperative transmission based on decode-and-forward relaying with partial repetition coding,” IEEE Trans. on Wireless Comm., vol. 8, no. 4, pp. 1716–1725, 2009.

[21] M. C. Valenti and B. Zhao, “Distributed turbo codes: towards the capacity of the relay channel,” in IEEE Vehicular Technology Conference (VTC), 2003, pp. 322–326.

[22] M. A. Khojastepour, N. Ahmed, and B. Aazhang, “Code design for the relay channel and factor graph decoding,” in Asilomar Conf. On Signals, Systems and Computers, 2004, pp. 2000–2004.

[23] P. Razaghi and W. Yu, “Bilayer LDPC codes for the relay channel,” in IEEE Inter. Conf. on Communications (ICC), 2006, pp. 1574–1579.

[24] P. Razaghi and W. Yu, “Bilayer low-density parity-check codes for decode-and-forward in relay channels,” IEEE Trans. on Information Theory, vol. 53, no. 10, pp. 3723–3739, 2007.

[25] A. Chakrabarti, A. De Baynast, A. Sabharwal, and B. Aazhang, “Lowdensity parity-check codes for the relay channels,” IEEE Journal on Selected Areas in Communications, vol. 25, no. 2, pp. 280–291, 2007.

[26] J. Hu and T. M. Duman, "Low density parity check codes over wireless relay channels," IEEE Trans. on Wireless Communications, vol. 6, no. 9, pp. 3384–3394, 2007.
[27] C. Li, G. Yue, X. Wang, and M.A. Khojastepour, "Ldpc code design for half-duplex cooperative relay," IEEE Trans. on Wireless Communications, vol. 7, no. 11, pp. 4558–4567, 2008.
[28] V. Savin, "Split-extended LDPC codes for coded cooperation," in IEEE Int. Symp. on Inf. Theory and Applications (ISITA), 2010, pp. 151–156.
[29] K. Kasai, D. Declercq, C. Poulliat, and K. Sakaniwa, "Multiplicatively repeated non-binary LDPC codes," IEEE Trans. on Inf. Theory, vol. 57, no. 10, pp. 6788–6795, 2011.
[30] D. Declercq and M. Fossorier, "Decoding algorithms for nonbinary LDPC codes over GF(q)," IEEE Trans. on Communications, vol. 55, no. 4, pp. 633–643, 2007.
[31] M.C. Davey, Error-correction using low-density parity-check codes, Ph.D. thesis, Univ. of Cambridge, 1999.
[32] D. Declercq and M. Fossorier, "Extended min-sum algorithm for decoding LDPC codes over GF(q)," in IEEE Int. Symp. on Information Theory (ISIT), 2005, pp. 464–468.
[33] V. Savin, "Min-Max decoding for non-binary LDPC codes," in IEEE Int. Symp. on Information Theory (ISIT), July 2008, pp. 960–964.
[34] C. Poulliat, M. Fossorier, and D. Declercq, "Design of regular (2; dc)-LDPC codes over GF(q) using their binary images," IEEE Trans. on Communications, vol. 56, no. 10, pp. 1626–1635, 2008.
[35] E. Biglieri, J. Proakis, and S. Shamai, "Fading channels: Information theoretic and Communications aspects," IEEE Trans. on Inf. Theory, vol. 44, no. 6, pp. 2619–2692, 1998.
[36] J.J. Boutros, A. Guillén i Fabregas, E. Biglieri, and G. Zémor, "Design and analysis of Low-Density Parity-Check codes for block-fading channels," in IEEE Inf. Theory and App. Workshop, 2007, pp. 54–62.
[37] Etkin, R.H., Tse, D.N.C., Hua Wang, "Gaussian interference channel capacity to within one bit", IEEE Transactions on Information Theory, vol. 54, no. 12, pp. 5534 – 5562, December 2008.
[38] F. Kaltenberger, "OpenAirInterface Project," Eurecom, February 2014, https://twiki.eurecom.fr/twiki/bin/view/OpenAirInterface. Last accessed on 18 November 2014.
[39] Third Generation Partnership Project, "Multiplexing and channel coding (Release 11)," 3GPP, Tech. Rep. 3GPP TS 36.212 v11.3.0, June 2013.
[40] R. Ghaffar and R. Knopp, "Spatial Interference Cancellation Algorithm," IEEE Wireless Communications and Networking Conference, April 2009.
[41] M. Cardone, D. Tuninetti, R. Knopp, U. Salim, "Gaussian half-duplex relay networks: improved gap and a connection with the assignment problem," IEEE International Information Theory Workshop, September 2013.
[42] M. Cardone, D. Tuninetti, R. Knopp, U. Salim, "Gaussian half-duplex relay networks: improved constant gap and connections with the assignment problem," IEEE Transactions on Information Theory, vol. 60, no. 6, pp. 3559 – 3575, June 2014.
[43] M. Cardone, D. Tuninetti, R. Knopp, U. Salim, "The capacity to within a constant gap of the Gaussian half-duplex relay channel," IEEE International Symposium on Information Theory, July 2013.
[44] M. Cardone, D. Tuninetti, R. Knopp, U. Salim, "Gaussian half-duplex relay channels: generalized degrees of freedom and constant gap result," IEEE International Conference on Communications, June 2013.
[45] M. Cardone, D. Tuninetti, R. Knopp, U. Salim, "On the Gaussian half-duplex relay channel," IEEE Transactions on Information Theory, vol. 60, no. 5, pp. 2542-2562, May 2014.
[46] R. Thomas, M. Cardone, R. Knopp, D. Tuninetti, B.T. Maharaj, "An LTE implementation of a novel strategy for the Gaussian half-duplex relay channel," submitted to IEEE International Conference on Communications, June 2015.
[47] M. Cardone, D. Tuninetti, R. Knopp, "The approximate optimality of simple schedules for half-duplex multi-relay network,'' submitted to IEEE International Information Theory Workshop, April 2015 (available at http://arxiv.org/abs/1410.7174).
[48] M. Cardone, D. Tuninetti, R. Knopp, "On user scheduling for maximum throughput in K-user MISO broadcast channel'', submitted to IEEE International Conference on Communications, June 2015.
[49] F. Bach, "Learning with sub modular functions: a convex optimization perspective", Foundations and Trends in Machine Learning, vol. 6, no. 2-3, oo. 145-373, December 2013.
[50] A. Özgür and S.N. Diggavi, "Approximately achieving Gaussian relay network capacity with lattice-based QMF codes," IEEE Transactions on Information Theory, vol. 59, no. 12, pp. 8275–8294, December 2013.
[51] A. Sendonaris, E. Erkip, and B. Aazhang, "User cooperation diversity. Part I. System description," IEEE Transactions on Communications, vol. 51, no. 11, pp. 1927–1938, 2003.
[52] A. Sendonaris, E. Erkip, and B. Aazhang, "User cooperation diversity. Part II. Implementation aspects and performance analysis," IEEE Transactions on Communications, vol. 51, no. 11, pp. 1939–1948, 2003.

[53] R. Ahlswede, N. Cai, S.-Y. R. Li, and R. W. Yeung, "Network information flow," IEEE Trans. Inform. Theory, vol. 46, no. 4, pp. 1204-1216, Jul. 2000.
[54] P. Razaghi and W. Yu, "Bilayer low-density parity-check codes for decode-and-forward in relay channels," IEEE Trans. on Information Theory, vol. 53, no. 10, pp. 3723–3739, 2007.
[55] A. Chakrabarti, A. De Baynast, A. Sabharwal, and B. Aazhang, "Low density parity-check codes for the relay channels," IEEE Journal on Selected Areas in Communications, vol. 25, no. 2, pp. 280–291, 2007.
[56] J. Hu and T. M. Duman, "Low density parity check codes over wireless relay channels," IEEE Trans. on Wireless Communications, vol. 6, no. 9, pp. 3384–3394, 2007.
[57] C. Li, G. Yue, M. A. Khojastepour, X. Wang, and M. Madihian, "LDPC coded cooperative relay systems: performance analysis and code design," IEEE Trans. on Communications, vol. 56, no. 3, pp. 485–496, 2008.
[58] J. Cances and V. Meghdadi, "Optimized low density parity check codes designs for half duplex relay channels," IEEE Trans. on Wireless Communications, vol. 8, no. 7, pp. 3390–3395, 2009.
[59] T. Tran, T. Nguyen, and B. Bose, "A joint network-channel coding technique for single-hop wireless networks," IEEE Workshop on Network Coding, Theory and Applications (NetCod), 2008, pp. 1–6.
[60] D. Duyck, J. J. Boutros, and M. Moeneclaey, "Low-density parity-check coding for block fading relay channels," in IEEE Inform. Theory Workshop (ITW), 2009, pp. 248–252.
[61] V. Savin, "Split-Extended LDPC codes for coded cooperation", IEEE International Symposium on Information Theory and Applications (ISITA), Taichung, Taiwan, October 2010.
[62] M. Di Renzo, L. Iwaza, M. Kieffer, P. Duhamel, K. Al-Agha, "Robust wireless network coding-an overview," Lecture Notes of the Institute for Computer Sciences, Social Informatics and Telecommunications Engineering, 2010.
[63] Guo, Z., Huang, J., Wang, B., Zhou, S., Cui, J. H., & Willett, P. "A practical joint network-channel coding scheme for reliable communication in wireless networks". Wireless Communications, IEEE Transactions on, 11(6), 2084-2094, June 2012.
[64] Chen, S., Wang, W., & Zhang, X. (2009). "Performance analysis of multiuser diversity in cooperative multi-relay networks under Rayleigh-fading channels". Wireless Communications, IEEE Transactions on, 8(7), 3415-3419, July 2009.
[65] C. Hausl, and P. Dupraz, "Joint network-channel coding for the multiple-access relay channel". In Sensor and Ad Hoc Communications and Networks, 2006. SECON'06. 2006 3rd Annual IEEE Communications Society on (Vol. 3, pp. 817-822).
[66] R. Gallager. Low density parity check codes. IEEE Trans. Inform. Theory, it-8:21-28, 1962.
[67] N. Wiberg. Codes and decoding on general graphs. PhD thesis, Likoping University, Sweden, 1996.
[68] J. Ebrahimi and C. Fragouli, "Vector network coding," EPFL Technical Report, 2010.
[69] T. Doumi, M. F. Dolan, S. Tatesh, A. Casati, G. Tsirtsis, K. Anchan, and D. Flore, "LTE for Public Safety Networks", IEEE Communications Magazine, p: 106 - 112, February 2013.
[70] ICT-LOLA project: Achieving Low Latency in wireless communications: http://www.ict-lola.eu/
[71] Z. Lin, P. Xiao, B. Vucetic, and M. Sellathurai, "Analysis of Receiver Algorithms for LTE SC-FDMA Based Uplink MIMO Systems", IEEE Trans. on Wireless Comm., vol 9, no 1, pp. 60-65, January 2010.
[72] K. Zhou, N. Nikaein, R. Knopp, C. Bonnet, "Contention based access for machine-type communications over LTE," IEEE Vehicular Technologies Conference, May 6-9, 2012, Yokohama, Japan.
[73] R. Knopp and P.A. Humblet, "Information capacity and power control in single-cell multiuser communications", in Proc. IEEE In. Conf. Communications (ICC), Seattle, WA, Jun. 1995, pp. 331-335
[74] P. Bender, P. Black, M. Grob, R. Padovani, N. Sindhushyana, and A. Viterbi, "A bandwidth efficient high speed wireless data service for nomadic users", IEEE Communications Magazine, Jul. 2000.
[75] A. Jalali, R. Padovani, and R. Pankaj, "Data throughput of CDMA HDR: a high efficiency-high data rate personal communication wireless system", in Proc. IEEE Vehicular Technology Conference, May 2000.
[76] P. Viswanath, D. Tse, and R. Laroia, "Opportunistic beamforming using dumb antennas", IEEE Trans. Inform. Theory, vol. 48, pp. 1277-1294, Jun. 2002.
[77] D. park, H. Seo, H. Kwon and B.G. Lee, "Wireless packet Scheduling based on the Cummulative Distribution Function of User Transmission rates", IEEE Trans. Comm., Vol. 53, pp. 1919-1929.
[78] T. Bonald, "A Score-Based Opportunistic Scheduler for Fading Radio Channels", Proc. European Wireless, 2004.
[79] X. Qin and R. Berry, "Opportunistic Splitting Algorithms for Wireless networks with Heterogenous users", Proc. Conf. Inform. Sciences Systems (CISS), March 2004.

[80] H. Anouar "Queue Maximum Proportional Fair Scheduling for Saturated and Non-Saturated Regimes", IEEE WCNC 2014.
[81] R. Jain R, D.M. Chiu and W. Hawe, "A Quantitative Measure of Fairness and Discrimination for Resource Allocation in Shared Computer Systems", DEC Research Report TR-301, 1984.